Spring 7-16-2015

Effects of Wildfire on Mercury, Organic Matter, and Sulfur in Soils and Sediments

Jackson Paul Webster
University of Colorado at Boulder, webster.jacksonpaul@gmail.com

Effects of wildfire on mercury, organic matter, and sulfur in soils and sediments

By

Jackson Paul Webster

B.S., University of Nevada, 2008

M.S., University of Nevada, 2010

A thesis submitted to the Faculty of the

Graduate School of the University of Colorado in partial fulfillment

of the requirements for the degree of

Doctor of Philosophy

Department of Civil, Environmental, and Architectural Engineering

2015

This thesis entitled:

Effects of wildfire on mercury, organic matter, and sulfur in soils and sediments

written by Jackson Paul Webster

has been approved for the Department of Civil, Environmental, and Architectural Engineering

_____

Joseph N. Ryan, committee chair

_____

George R. Aiken

_____

Diane M. McKnight

_____

Fernando L. Rosario-Ortiz

_____

Jeffrey H. Writer

Date _____

The final copy of this thesis has been examined by the signatories, and we find that both the content and the form meet acceptable presentation standards of scholarly work in the above mentioned discipline.

Abstract

Webster, Jackson P. (Ph.D., Civil, Environmental, and Architectural Engineering)

Effects of wildfire on mercury, organic matter, and sulfur in soils and sediments

Thesis directed by Joseph N. Ryan

The transport and deposition of mercury from natural and anthropogenic sources has led to its enrichment in surficial soils on a global scale. In arid climates, such as the western United States, the common occurrence of wildfire mobilizes accumulated mercury. In addition to atmospheric re-emission, wildfire enhances the transport of mercury from forest soils to the sediments of lakes and reservoirs through increased watershed runoff and soil destabilization. Little information is reported on the fate mercury in waters affected by wildfire. To address the knowledge deficit, multiple studies were conducted throughout forested watersheds of Colorado, United States, subjected to historical and recent wildfire to characterize mercury, organic matter, and sulfur oxidation state in soils and sediment. Simulated wildfire heating of soil was conducted using a muffle furnace to observe the influence of heat on sulfur oxidation. Batch experiments were conducted on soils to assess aqueous mercury release from burned, unburned, and laboratory heated soils. To examine the sulfur speciation and mercury behavior following ash-laden sediment deposition in a reservoir, reservoir cores containing these sediments were obtained and analyzed. Additionally, redox transitions occurring during sediment deposition were simulated using microcosms. To measure how oxidizing (heating) and reducing (reservoir deposition) conditions influence sulfur speciation, X-ray absorbance near-edge structure (XANES) spectroscopy was employed. Changes in mercury binding capacity were quantified using a competitive ligand exchange method.

In Mesa Verde National Park, it was found that soils affected by historical wildfires contained about 50 % less organic matter and mercury than unburned soils collected adjacent to the burned samples, which corresponded to mercury release of 19 ± 8.2 g ha^{-1}. In aqueous release experiments from historically burned soils, there was half the amount of carbon and mercury as unburned soils. In contrast, laboratory heating increased the release of organic matter and major ions from soils. Mercury release was linked to organic matter release, though losses from volatilization during heating reduced the total release into solution. Soil subjected to heating contained more oxidized sulfur species and concomitant losses of intermediate oxidation state species, while sulfur oxidation states in ash-laden sediments shifted toward reduced forms following deposition in a reservoir. Laboratory experiments simulating each of these shifts resulted in increased mercury binding capacity. Following heating a 1.5-fold increase in strong mercury binding sites was measured. Following simulated reservoir deposition, there was a 10-fold increase in the number of strong binding sites in the ash-laden sediments. Overall, this study characterizes the underlying processes influencing mercury behavior in soils and sediments following wildfire.

Acknowledgements

First and foremost, I would like to thank Joseph Ryan and George Aiken. It has been a pleasure to have been advised by both and I am very thankful for the inspiration, advice, and support they have given me in this process.

I greatly appreciate the participation of my committee members; Diane McKnight, Fernando Rosario-Ortiz, and Jeffrey Writer, all of whom have contributed to this effort and my experience at University of Colorado, Boulder beyond this committee as well.

There are many co-authors in these chapters and I thank all of them for their contributions and help: Kathryn Nagy, Alain Manceau, Erika Callagon, Brett Poulin, Chris Peltz, Benjamin Kamark, Genevieve Nano, David Vine, and Tyler Kane.

I would like to thank Kenna Butler for her leadership in the Aiken lab.

Many people have contributed there professional expertise and time to various aspects of this project and I would like to acknowledge Deborah Martin with the U.S. Geological Survey, Jill Oropeza with City of Fort Collin's Utilities, John McCutchan with City of Greeley Utilities, George San Miguel with Mesa Verde National Park, and Marcie Bidwell with Mountain Studies Institute.

I thank all of the current and former Joe Ryan Lab Group: Jessica Dehart Rogers, Chase Gerbig, Sanjay Mohanty, Tim Dietrich, and Alison Craven for their contributions to my experience.

I would like to also thank all of the undergrads who have helped over the years: Doug Winter, Crystal Kelly, Chelsea Ottendfeldt, Michelle Hummel, Steven Walton, and Tyler Doughty.

I would like to thank my girlfriend Dorey Chaffee for being loving, patient, and supportive throughout this process.

Finally, I would like to thank my parents Sue Jackson and Jim Webster, who are always my best teachers and advisors. Thank you both for your love and support.

This dissertation was partially funded by the Department of Civil, Environmental, and Architectural Engineering of the University of Colorado Boulder through the Dissertation Completion Fellowship.

Table of Contents

Chapter 1: An Introduction to the Potential Influence of Wildfire on the Fate and Transport of Mercury……1

Chapter 2: Effect of Fire on the Mercury in Soils in Pinion-Juniper Woodland of Mesa Verde National Park
- Abstract 13
- Introduction 14
- Methods 16
- Results 22
- Discussion 31

Chapter 3: Simulated Wildfire Heating of Forest Soil Increases Mercury Affinity and Alters Sulfur Speciation
- Abstract 37
- Introduction 38
- Methods 40
- Results 48
- Discussion 59

Chapter 4: Characterization of Mercury, Sulfur, and Organic Matter in Ash-Laden Stream Bank and Reservoir Sediments
- Abstract 66
- Introduction 67
- Methods 70
- Results 77
- Discussion 85

Chapter 5: Mercury Affinity for Ash-Laden Sediment Increases Following Simulated Reservoir Deposition
Abstract 92
Introduction 93
Methods ..... .96
Results 102
Discussion 108

Chapter 6: Summary and Future Work
Summary 118
Future Work 123

References 125

List of Tables

Table 1.1: Major forms of sulfur……7

Table 2.1: Mesa Verde samples……24

Table 2.2: Emissions estimate (4 cm)……29

Table 2.3: Emissions estimate (2 cm)……30

Table 3.1: Soil characteristics……49

Table 4.1: Hewlett Gulch samples……74

Table 4.2: Hewlett Gulch mercury……82

Table 4.3: Hewlett Gulch elemental analyses……82

Table 4.4: Hewlett Gulch sulfur XANES……84

Table 5.1: Microcosm debris characterization……104

Table 5.2: Competitive ligand exchange data……110

Table 5.3: Microcosm sediment XANES……112

List of Figures

Figure 1.1: Current estimates for global mercury fluxes……..3

Figure 1.2: Ash-laden sediments transported from the High Park Fire (2012)……5

Figure 1.3: Mercury binding coordination……..6

Figure 1.4: Sulfur cycling in sediments……8

Figure 1.5: Sulfur X-ray absorption near edges structure (XANES) spectroscopy ……10

Figure 2.1: Mesa Verde National Park primary land cover types……17

Figure 2.2: Soils of Mesa Verde……18

Figure 2.3: Mercury dependence on organic matter……23

Figure 2.4: Unburned and burned soil profiles ……25

Figure 2.5: Mercury and organic matter released to water……28

Figure 3.1: Samples were collected from two areas near Vallecito Reservoir……41

Figure 3.2: Temperature dependence of soil organic matter and mercury loss……51

Figure 3.3: Dissolved organic carbon and specific ultraviolet absorption ($SUVA_{254}$) as a function of furnace heating temperature……52

Figure 3.4: Mercury released from soil……54

Figure 3.5: Ion release from soil.……55

Figure 3.6: Sulfur XANES spectra in unburned soils (Area B) subjected to increasing duration of heating at 225°C……56

Figure 3.7: Sulfur speciation in unburned soil as a function of exposure to increasing temperature……58

Figure 3.8: Mercury distribution following competitive ligand exchange……60

Figure 3.9: Formation of 2-thiophenethiol……63

Figure 4.1: The Hewlett Gulch study area……71

Figure 4.2: Photo of the study drainage……72

Figure 4.3: Cores collected from reservoir……78

Figure 4.4: Mercury profile in cores……..80

Figure 4.5: Sulfur XANES spectra collected from river bank and reservoir sediments……83

Figure 4.6: Gross oxidation state of sulfur in ash-laden sediment……..86

Figure 5.1: Map of reservoir study area……..97

Figure 5.2: Concentrations of redox-sensitive anions and metals as a function of time in microcosms……105

Figure 5.3: Dissolved organic carbon (DOC) and specific ultraviolet absorption ($SUVA_{254}$) of pore water as a function of time Future work……106

Figure 5.4: Filter-passing and colloidal mercury in microcosm pore water……109

Figure 5.5: Sulfur XANES absorbance spectra obtained from ash-laden sediments……..111

Figure 5.6: Sulfur oxidation states simplified……..114

Chapter 1

An Introduction to the Potential Influence of Wildfire on the Fate and Transport of Mercury

Jackson P. Webster

Department of Civil, Environmental, and Architectural Engineering, University of Colorado Boulder

Mercury contamination of surface waters and subsequent trophic transfer of this mercury into fish has resulted in fish consumption advisories being issued for nearly half of the surface water (on an areal basis) in the United States, far exceeding advisories for other bioaccumulative contaminants (EPA, 2015). The form of mercury responsible for these advisories is methylmercury (CH_3Hg^+), a potent neurotoxin. Methylmercury has a strong tendency for bioaccumulation and biomagnification in aquatic environments which leads to exposure risk among fish consuming organisms, including humans. Concentrations of methylmercury in fish tissues can be 10^6-fold higher than surrounding environmental concentrations (Hsu-Kim *et al*., 2013), thus low very concentrations of mercury in surface waters pose risks to higher trophic feeders (Pirrone *et al.*, 2010; Streets, 2011; Driscoll *et al.*, 2013).

The source of most of the mercury responsible for these advisories is gaseous emissions from anthropogenic activities such as coal burning and mining, and geologic sources such as volcanoes (Driscoll *et al*., 2013; Figure 1.1). Although the sources and effects of mercury contamination are known, the pathways that allow this broadly dispersed contaminant to accumulate in fish are complex. One pathway for increased mercury mobilization into surface water is landscape disturbance such as wildfire. Wildfire occurrence is increasing globally (Westerling *et al.,*2014) and is therefore playing an increasing role in the mobilization and transport of mercury into the aquatic environment. The fate and transport of mercury following wildfire is likely to be closely linked to pre-fire soil accumulation, soil retention mechanisms, mobilization from soil as aqueous Hg-DOM complexes, and interactions with downstream sediments following mobilization. In each of these cases the element sulfur governs mercury behavior through surface interaction, aqueous complex formation and even as an electron acceptor for the organisms responsible for mercury methylation.

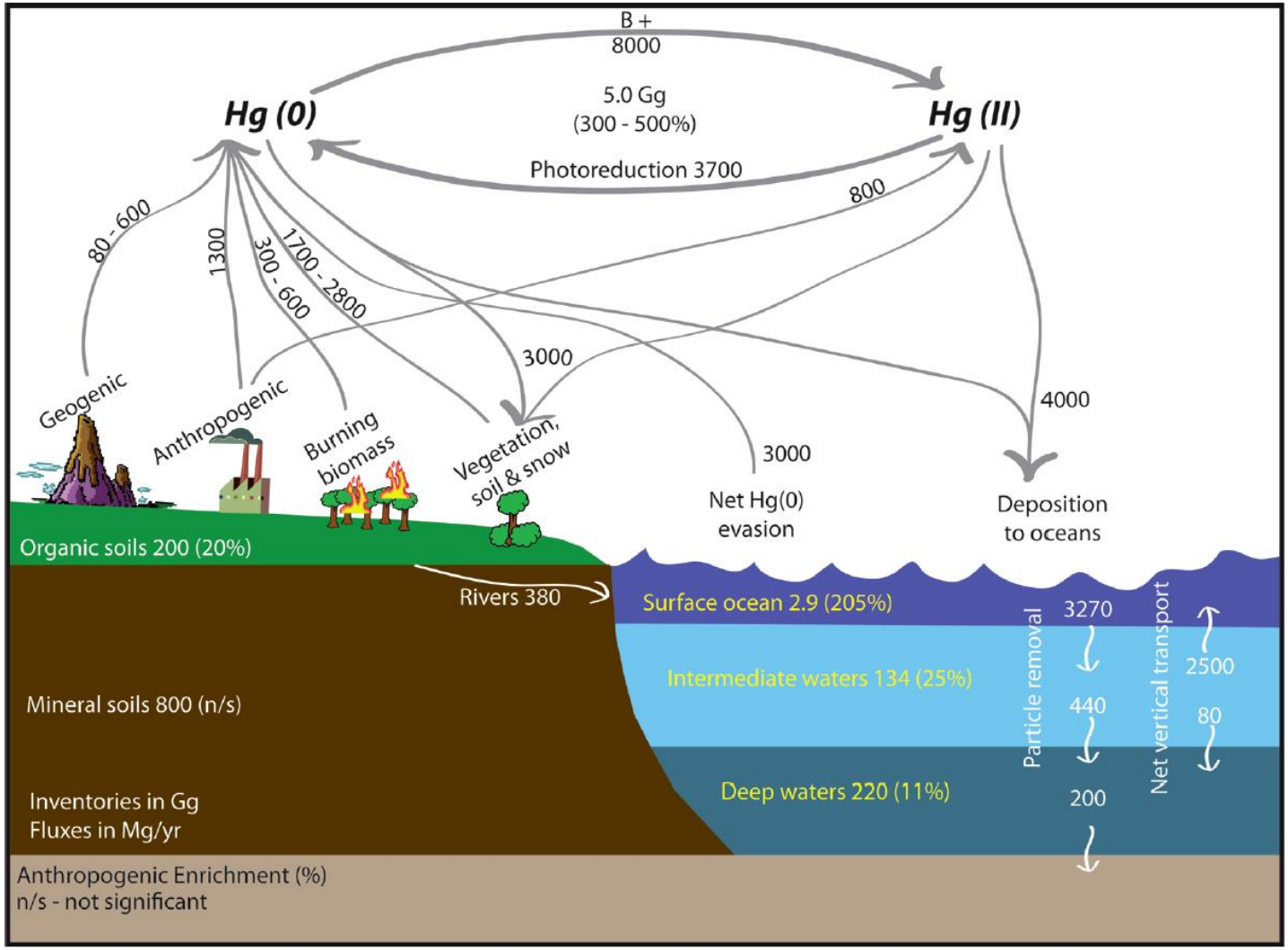

Figure 1.1: Current estimates for global mercury storage and fluxes. Figure from Driscoll *et al.* (2013).

Fire Effects on Soil

Wildfire severity, from a soil perspective, is a function of two components: intensity and duration (Parsons, 2003). The intensity of a wildfire is the specific temperature that is achieved, and the duration is the length of time that the fire persists. Soil temperatures resulting from wildfire vary depending on available fuel, ambient temperature, relative humidity, and other local factors. In general, fire temperatures at the soil surface do not reflect the degree of soil heating. For instance, a fire burning at 850°C on the ground surface will generally not raise the subsurface temperature beyond 150°C below 5 cm (DeBano, 2000), producing a steep thermal gradient. Soils containing moisture will not rise above 95-100°C due to the latent heat of vaporization, but following the loss of water, soil temperatures may climb to 200 - 300°C in the first few centimeters of soil (Gonzalez-Perez *et al.,* 2004; Certini, 2005). As soil temperatures reach 100 - 200°C, the loss of easily vaporized organic carbon and the incomplete combustion of organic material (charring) begins between 130 - 200°C (Gonzalez-Perez *et al.,* 2004; Certini, 2005). It is around these temperatures that organic acid losses and addition of hydroxyl groups begin to occur (Fernandez *et al.,* 1997). At temperatures above 460°C, there is combustion woody materials (Riscassi and Scanlon, 2011).

Fire Effects on Watershed Hydrology

Wildfire commonly results in increased surface flow and sediment transport from watersheds (Figure 1.2). Increases in flow can be primarily attributed to loss of intercepting foliage and the development of a hydrophobic layer in the soil, which leads to mobilization of burnt soils, ash, and charcoals down slope and toward waterways.

Following erosional events, the transport of ash-laden sediments in downstream rivers, lakes, and reservoirs can lead to changes in environmental conditions. In particular, redox transitions may greatly influence the fate of mercury in ash-laden sediments. Little information is reported in the

literature regarding diagenesis of fire debris in lakes and reservoirs, particularly in regard to effects on mercury binding and release; however, sulfur is likely an important control on mercury speciation and availability in these lake and reservoir sediments (Di Toro *et al.,* 1990; Lee *et al.,* 2000).

Figure 1.2: Ash-laden sediments transported from the High Park Fire (2012) line the banks of the Cache la Poudre River near Fort Collins, Colorado, USA.

Mercury Accumulation in Soils

`The amount of mercury available for remobilization through the occurrence of wildfire is a function to the amount present prior to burning. This mercury derives from globally dispersed atmospheric that has been deposited on terrestrial surfaces. Deposition occurs when gaseous mercury (Hg^0) is oxidized into ionic mercury (Hg^{2+}), which can then be associated with either wet or dry

deposition on the landscape. Atmospheric mercury deposited in terrestrial environments collects on leaves, branches, and other organic materials (Obrist *et al.,* 2011; Pokharel and Obrist, 2011). Mercury associated with forest material is transferred into the soil column through decomposition of parent material (Selin, 2009; Obrist *et al.,* 2011), where it forms strong associations with soil organic matter (Grigal, 2003; Engle *et al.,* 2006; Biswas *et al.,* 2007; Obrist *et al.,* 2011). The strong binding of mercury in soil organic matter is due to the presence of reduced organic sulfur moieties within the soil (Figure 1.2; Skyllberg *et al*., 2000; Khwaja *et al.,* 2006; Skyllberg *et al*., 2006). Forest soils retain atmospherically deposited mercury and this has led to a 15 - 20 % increase in global soil-mercury concentrations in the last century (Selin, 2009; Driscoll *et al.,* 2013).

Aquatic Transport of Mercury

Following wildfire, increases in watershed runoff could influence mercury transport. The aqueous transport of mercury is closely linked to carbon release from soils. Mercury is transported from soil into surface water through complexation by mobilized dissolved organic matter (DOM) and specifically, reduced organic sulfur moieties associated with DOM (Xia *et al*., 1999; Skyllberg *et al*., 2000; Benoit *et al*., 2001; Haitzer *et al*., 2003; Hsu-Kim and Sedlak, 2005). Dissolved organic matter can transport mercury to oxygen limited waters, such as wetlands or stratified reservoirs. Mercury is methylated in oxygen-limited environments by sulfate-reducing bacteria (Benoit *et al*., 2001; Ranchou-Peyruse *et al*., 2009; Gilmour *et al.*, 2011, 2013).

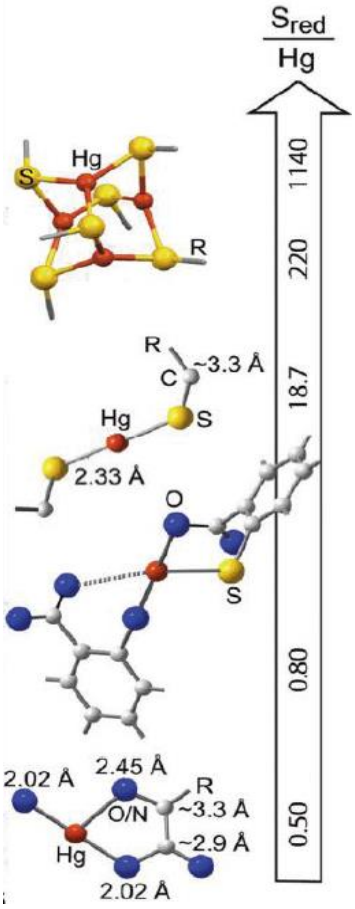

Figure 1.3: Mercury binding coordination dependents on the ratio of reduced sulfur to mercury (S_{red}/Hg). Figure from Nagy *et al.* (2011).

Furthermore, the generation of sulfide in anoxic environments can lead to the formation of inorganic mercury sulfide species and precipitation of metacinnabar (β-HgS(s)) (Benoit *et al*., 2001; Skyllberg, 2008; Gerbig *et al*., 2011). Recent studies have demonstrated that newly-formed mercuric sulfide clusters or nanocolloids are stabilized by strong interactions with DOM. Gerbig *et al*. (2011) demonstrated that nanocolloidal mercuric sulfide associated with DOM formed under environmentally relevant conditions (low mercury:DOM concentration ratio). Subsequent studies have demonstrated the role of nanocolloidal phases of mercuric sulfide in the methylation of mercury by sulfate-reducing bacteria, a previously unrecognized source of bioavailable mercury (Graham *et al*., 2012; Zhang *et al*., 2012).

Sulfur

Wildfire likely affects soil sulfur speciation. Previous studies characterizing sulfur oxidation states in variety of environmental matrices have found that sulfur oxidation states are dynamic and that shifts in oxidation state may occur through landscape disturbance (Solomon *et al.,* 2003; Schroth *et al.,* 2007). Sulfur exists in a variety of forms in the environment, with oxidation states ranging from -II to +VI (Table 1.1). In soils, most sulfur (>80%) is found in an organic form (Solomon *et al.,* 2003; Schroth *et al.*, 2007). Organic forms of sulfur are generally divided

Table 1.1. Major forms of sulfur in the environment and their oxidations states. Table from Werne *et al.* (2004).

Compound	Formula	Oxidation State of Sulfur
Sulfate	SO_4^{2-}	+6
Sulfite	SO_3^{2-}	+4
Tetrathionate	$S_4O_6^{-}$	+2.5
Thiosulfate	$S_2O_3^{2-}$	+2
Elemental sulfur	S_8, S^0	0
Polysulfides	HS_x^-, S_x^{2-}	-0.5
Organic sulfur	R-S-S-R	-1
Pyrite	FeS_2	-1
Iron monosulfide	FeS	-2
Organic sulfur	R-SH	-2
Bisulfide	HS^-	-2
Hydrogen sulfide	H_2S	-2

into three classes: reduced (thiols, mono, di-, and polysulfides, thiophenes), partially oxidized (sulfoxides), and highly oxidized (sulfonates, sulfones, and ester sulfates). Reduced organic sulfur is responsible for mercury binding, but this also appear to be the form of sulfur most affected by disturbance (Solomon *et al*., 2003).

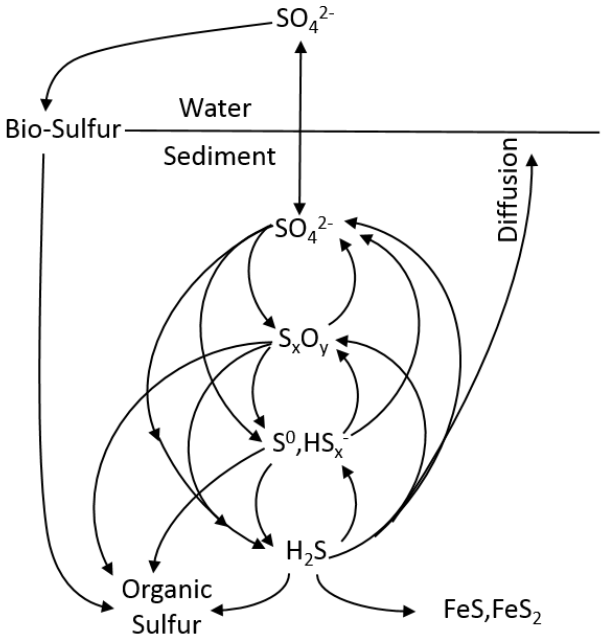

Figure 1.4: Sulfur accumulation in sediment can involve multiple pathways and intermediate steps. Figure from Werne *et al.* (2004).

The export of sulfate from recently burned watersheds likely influences sulfur cycling in sediments. Under anoxic conditions, sulfate may be reduced to inorganic sulfide. Sulfide produced in sediments and anoxic waters may be permanently incorporated into sediments or re-oxidized into sulfate (Figure 1.6). Incorporation into organic matter is due to the strong nucleophilic tendencies of sulfide, which reacts with organic carbon moieties (Perlinger *et al*., 2006). When a sulfide is added across an unsaturated bond, an organic sulfide bond is formed. Disulfide bonds can be formed when two bisulfide molecules oxidize a carbon bond or when inorganic polysulfides are incorporated into organic matter (Vairavamurthy *et al.,* 1997). Thus, the export of sulfate from recently burned watershed likely results in an increase in organic sulfur from the overlying water column in downstream anoxic sediments.

Summary, Hypotheses, and Approach

Summary

Wildfire has been increasing in occurrence and severity in many parts of the world. The occurrence of wildfire mobilizes mercury that is otherwise sequestered in soil organic matter into the atmosphere. In addition to atmospheric emissions, recently burned watersheds may initially export more total mercury and methylmercury (Caldwell *et al*., 2000; Kelly *et al*., 2006). Increased mercury export may be due to loss or changes to soil organic matter responsible for retaining mercury. Mercury is strongly bound to organic matter in soil due to reduced organic sulfur moieties. Landscape disturbance can result in the oxidation of reduced sulfur; however, the effect of fire on reduced organic sulfur in forest soil is unclear and little is known about mercury binding by organic matter in fire-affected soils.

In addition to the potential for increased release of mercury from soils following wildfire, increased surface flow and erosion may transport ash-laden sediments into surface waters and reservoirs. Sulfur transformations ash-laden sediments, particularly the formation of reduced organic sulfur during deposition and subsequent burial, may control the fate of the mercury associated with the mobilized sediments.

Hypotheses

To investigate the effects of wildfire on mercury, organic matter and sulfur in soil sand sediment the two broad hypotheses were tested. First, it was hypothesized that thermal oxidation of organic matter would decrease mercury binding capacity in organic matter. Specifically, that strong metal binding attributed to reduced sulfur functional groups in the soil organic matter will be diminished as reduced sulfur is oxidized. Secondly, it was hypothesized that that following deposition and burial of transported sediments, diagenesis of sediments under anoxic conditions would result in more reduced

sulfur and increase mercury binding. Specifically, sulfide incorporation into anoxic pore water would result in incorporation of sulfide to form organic sulfur and re-establish strong mercury binding sites.

Approach

To examine the effect of fire on mercury in forest soils subjected to heavy mercury deposition, we collected soil samples from Mesa Verde National Park and surrounding terrain in southwestern Colorado, USA. The soils were sampled from areas burned by eight wildfires and one prescribed burn from 1934 to 2012 and intervening unburned areas. Soil organic matter content and total mercury concentrations were measured in the upper 4 cm of soil, in 1 cm and 2 cm intervals. A subset of soils were evaluated for aqueous release of mercury and organic matter through a series of batch experiments.

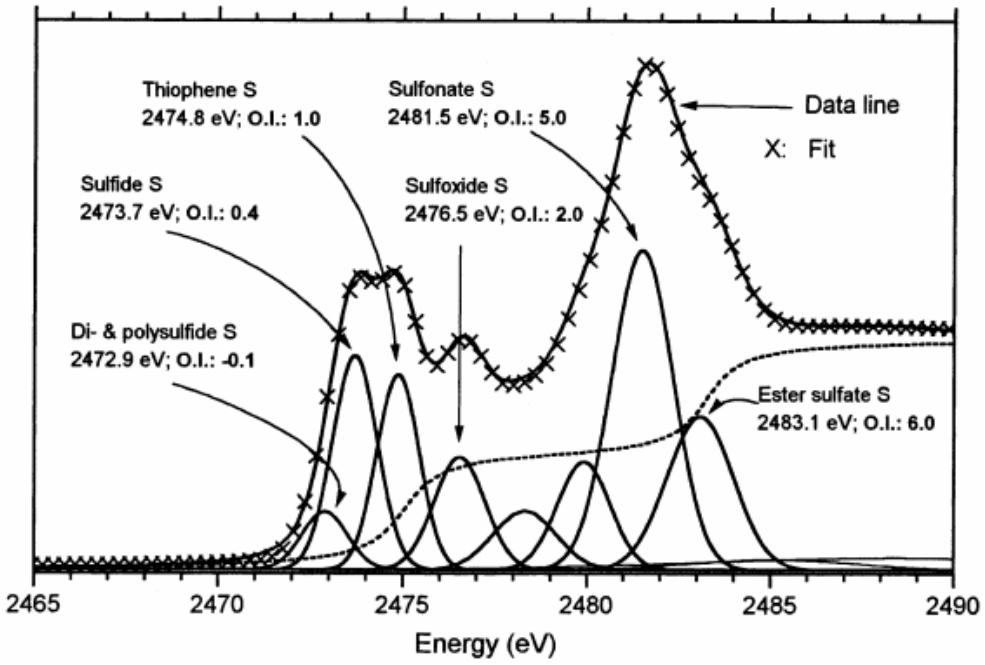

Figure 1.5: Sulfur X-ray absorption near edge structure (XANES) spectra is de-convoluted using linear fitting of Gaussian curves centered at the absorption energy of a particular oxidation state. Reduced species occupy the low-energy range (< 2476 eV) and oxidized species occupy the high-energy range (> 2479 eV). Figure from Vairavamurthy (1998).

To understand the behavior of mercury in forest soils subjected to fire, the effect of heat on mercury binding to soils from Vallecito Reservoir (La Plata county Colorado, USA) watershed was examined. Forest soils were heated in a furnace at temperatures from 25°C (control) to 250°C, ranging from 20 minutes to 240 minutes, which is representative of wildfire. Sulfur XANES spectroscopy was used to assess changes in sulfur speciation due to heating (Figure 1.5). Heated soils were then subjected to leaching experiments in aqueous suspensions. The release of mercury, organic matter, and major ions were measured following 24 h. The heated forest soils were compared with unheated soils in competitive ligand exchange experiments to assess changes in the capacity for mercury adsorption.

To investigate the geochemical processes leading to enhanced methylation, ash-laden sediments and native (underlying) reservoir sediments were collected from a watershed-reservoir system burned in the Hewlett Gulch Fire, 2012, near Fort Collins, Colorado, USA. Sediments from the banks and reservoir were characterized for organic matter content, total mercury, methylmercury, and major elements. The deposited ash-laden sediments were analyzed for total sulfur and sulfur oxidation state in summer, fall, and spring following the fire.

To investigate the influence of reducing conditions and sulfur incorporation on mercury binding capacity of ash-laden sediment, we simulated conditions at the bottom of a reservoir. Ash-laden sediment was incubated under an argon atmosphere and pore water was sampled over 33 d to monitor mercury, dissolved organic matter, and major ions throughout the redox transition. Sediments representing initial conditions, pre- and post-sulfate reduction, and final conditions were analyzed using sulfur X-ray absorption near-edge structure spectroscopy to characterize changes in sulfur oxidation states throughout microcosm incubation. Competitive ligand exchange experiments were employed to quantify changes in mercury binding capacity of the sediment.

Chapter 2

Effect of Fire on the Mercury in Soils in Pinion-Juniper Woodland of Mesa Verde National Park

Jackson P. Webster[a], George R. Aiken[b], and Joseph N. Ryan[a]

[a] Department of Civil, Environmental, and Architectural Engineering, University of Colorado Boulder

[b] U.S. Geological Survey

Manuscript to be submitted to *Science of the Total Environment*

Abstract

Current climate trends favor increases in wildfire occurrence and severity in many parts of the world. Wildfire is known to cause mercury remobilization into the atmosphere and may also affect mercury retention in soils. To examine the effect of fire on mercury in forest soils subjected to heavy mercury deposition from local coal fired power plants, we collected soil samples from Mesa Verde National Park and surrounding terrain in southwestern Colorado, USA. The soils were sampled from areas burned by eight wildfires and one prescribed burn from 1934 to 2012 and intervening unburned areas. Soil organic matter content and total mercury concentrations were measured in the upper 4 cm of soil. A subset of soils were evaluated for release of mercury and organic matter into water through a series of batch experiments. Wildfire depleted soil of 50% of the initial organic matter and 50 - 72 % mercury to 4 cm depth. Our mercury release estimates averaged 19 ± 8.2 g ha^{-1}. In aqueous release experiments, burned soil released half the amount of carbon and mercury as unburned soils. We compared soil mercury content between two historical fires, the Bircher Fire (2000) and the Weber Fire (1934), and determined an average Hg accumulation rate of0 0.06 ±0 0.03 g ha^{-1} y^{-1}. This deposition rate was similar to average wet deposition rates reported by the Mercury Deposition Network for the Park over the previous decade (0.063 g ha^{-1} y^{-1}). These results indicate that mercury was depleted through wildfire heating and release was governed by soil organic matter losses during wildfire. Soils affected by historical wildfire contained less total mercury and this decreased the amount of mercury available for aqueous release.

Introduction

Mercury contamination of terrestrial and aquatic environments is a burden to human and ecological health on a global scale. Primary sources of mercury mainly include coal combustion, mining, and volcanoes (Pirrone *et al.*, 2010; Streets, 2011; Driscoll *et al.*, 2013). In addition to primary sources, re-emission of natural and anthropogenic mercury through land disturbance, such as biomass burning, is a major distributed source of atmospheric mercury (Wiedinmyer and Friedli, 2007; Friedli *et al*., 2009; Pirrone *et al.*, 2010). Wildfires are prevalent across much of the sub-polar climates and the occurrence and severity of wildfires is increasing globally (Westerling *et al.*, 2006; McCoy and Burn, 2005; Kasischke *et al.*, 2010; Westerling *et al*., 2014). Due to diversity of landscape, fire characteristics, and difficulty in obtaining pre-wildfire samples, wildfire emissions remain as one of the least constrained major sources of atmospheric mercury (Wiedinmyer and Friedli, 2007; Driscoll *et al.,* 2013; Smith-Downey *et al.*, 2010).

The amount of mercury available for mobilization during wildfire depends on pre-fire accumulation in forest soils. Accumulation of mercury in terrestrial landscapes is driven by wet and dry deposition processes. In the case of wet deposition, precipitation scavenges mercury from the atmosphere and causes deposition on terrestrial surfaces such as grasses, leaves, needles, branches, and soil (Grigal, 2003). Rainfall may also increase mercury accumulation in soil by causing mercury deposited on leaves and needles to transfer into the soil column (Obrist *et al.*, 2011). In addition to wet deposition, mercury may be deposited through dry deposition. Dry deposition involves transfer of mercury from air parcels to surfaces, such as foliage and litter layers, or from deposition of mercury associated with particles (Selin *et al.*, 2007; Hynes *et al.*, 2009; Amos *et al.*, 2012). Deposition of mercury associated with particles is likely to occur near primary combustion sources because particles have atmospheric residence times of hours to days, whereas gaseous elemental mercury may stay in the atmosphere for y (Sherman *et al.*, 2012; Amos *et al.*, 2012).

In soils, mercury cycling closely follows the carbon cycle through leaf and needle fall, litter accumulation, and microbial degradation of litter in forest soils (Grigal, 2003; Obrist *et al.*, 2011; Pokharel and Obrist, 2011; Demers *et al*., 2013). Fallen leaves, twigs, and bark (litter) typically have mercury concentrations similar to the mercury concentrations in attached leaves (Obrist *et al.,* 2011). The organic matter-rich O-horizons containing degraded plant materials (duff) have mercury concentrations higher than those of the recently deposited materials (litter) (Obrist *et al*., 2011). Below the O-horizon, mercury concentrations decrease to the natural background concentration with depth (Obrist *et al.*, 2011). The correlation between mercury and organic matter concentrations observed in soils is driven by strong binding between mercury and reduced sulfur moieties in the soil organic matter (Skyllberg *et al.*, 2000; Khwaja *et al*., 2006; Skyllberg *et al*., 2006).

In southwestern Colorado, multiple coal-fired power stations contribute to elevated mercury deposition and regional mercury contamination. Elevated mercury deposition in this area is evidenced by mercury concentrations as high as 126 ng L^{-1} in rainfall collected at Mesa Verde National Park, which is among the highest in the country (National atmospheric deposition program, 2006). The effects of mercury deposition are also observed among the region's major reservoirs – McPhee, Narraguinnep, Navajo, Totten, and Vallecito – all of which are listed on the state's fish consumption advisory list due to mercury in predatory fish (CDPHE, 2015). For the Narraguinnep Reservoir, Gray *et al.* (2005) investigated the distribution of mercury in ^{137}Cs-dated sediment cores and found increases in mercury consistent with local coal power plant operation and expansion in the region. Recently, Gray *et al*. (2014) identified coal ash particles in the sediments of Narraguinnep Reservoir, which provides further evidence that the nearby coal-burning power plants are the main source of mercury to the reservoir.

Potentially compounding the mercury transport issue in southwestern Colorado is frequent and widespread wildfire. For example, within the 21,000 ha of Mesa Verde National Park, five wildfires burned nearly 15,000 ha between 1996 and 2003. Floyd *et al.* (2004) suggested that the fires that burned in early 2000's burned an area ten times larger than that which burned within Mesa Verde National Park for the preceding 150 y, and possibly for the preceding 300 y. Considering climate-fire relationships (Westerling *et al*., 2006; Little *et al*., 2009, Westerling *et al*., 2014) and the current outlook for increased wildfire activity (Yue *et al*., 2013), wildfire will persist as a major source of mercury re-emission for the foreseeable future. The effects of wildfire heating on the ability of soil organic matter to bind mercury are relatively unknown. It is clear that biomass combustion and heat transferred to the underlying soil during wildfire liberates mercury (Friedli *et al*., 2001; Friedli *et al*., 2003; Obrist *et al*., 2007; Engle *et al*., 2006; Biswas *et al*., 2007; Biswas *et al*., 2008; Woodruff and Cannon, 2010; Mitchel *et al*., 2012).

To quantify wildfire-induced changes to mercury content in forest soils and predict mobilization to the atmosphere and aquatic environments soil samples were collected from areas burned by eight wildfires and one prescribed burn from 1934 to 2012 and the intervening unburned areas. We evaluated the samples for mercury and organic matter content as well as aqueous release of these soil components. Using soil mercury concentration, we calculated the emission of mercury from historical fires. We hypothesized that wildfire would reduce mercury binding by soil and result in greater release to water due to loss of organic matter.

Methods

Site description

Mesa Verde National Park is located in southwestern Colorado, in the Four Corners region of the United States, on a south-facing cuesta. The Park's northern boundary has a maximum elevation of

2,600 m and at its southern boundary the elevation ranges from 2000 - 2100 m. North-south drainages, nearly 300 m deep, cut into the low-angle cuesta and flow into the Mancos River, which runs along the southern boundary of the Park. The incising of sedimentary rock has exposed layers of shale and sandstone bedrock (Figure 2.1). The soil of Mesa Verde National Park consists of (1) unconsolidated colluvium distributed throughout the Park and (2) loess found mainly on the mesa tops (Figure 2.2) (Carrara, 2012). The soils of Mesa Verde do not generally have a deep layer of degraded plant litter (duff).

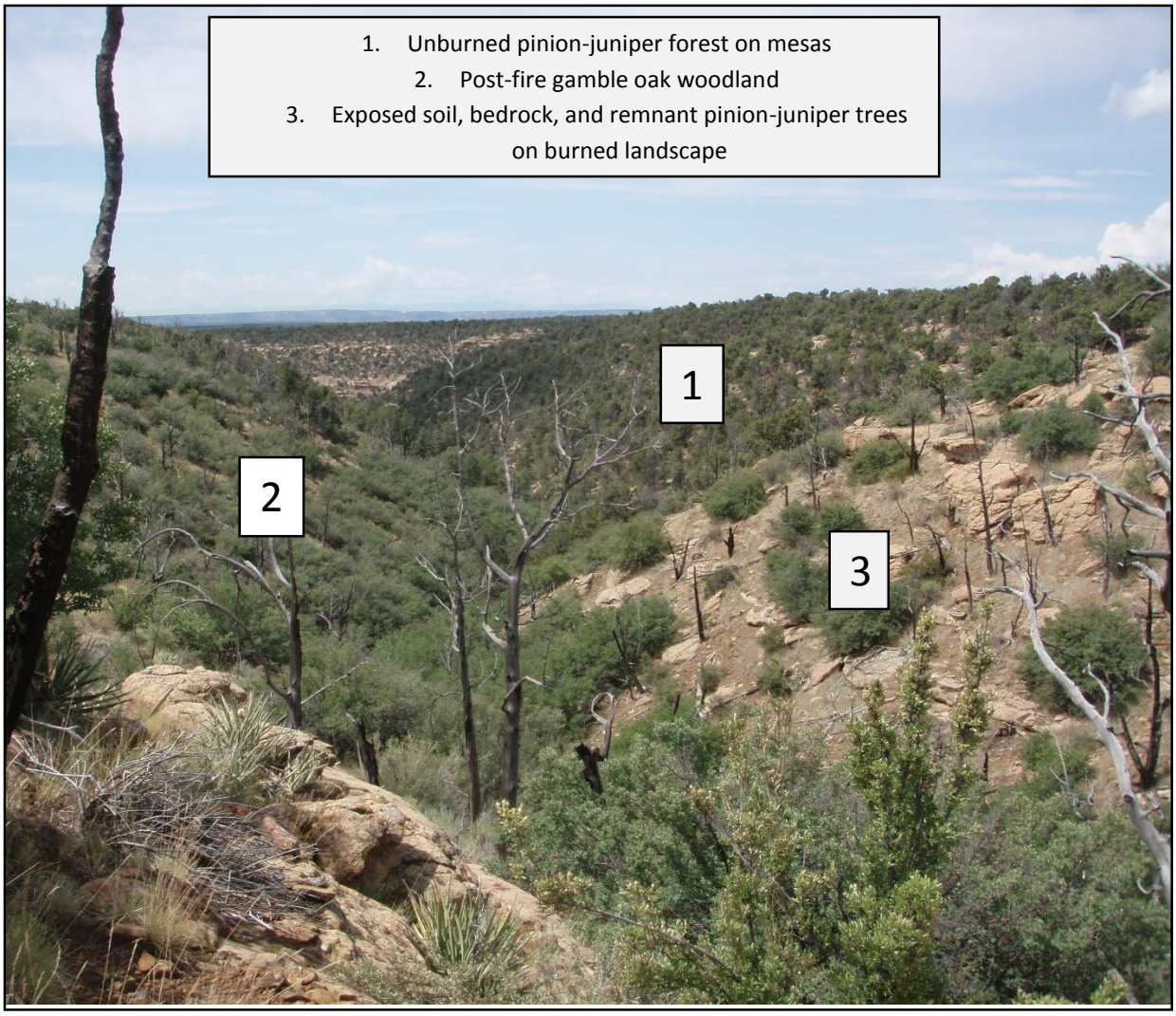

Figure 2.1: The primary land cover types of Mesa Verde National Park are (1) pinion-juniper forest and (2) scrub-oak woodland. The landscape contains many stages of post-fire succession, including (3) remnants of pinion and juniper trees.

Pinion-juniper woodland is the prevalent forest type on the unburned mesas, accounting for 18 % of the Park's land cover (Thomas *et al*., 2009). Much of the previously burned area of the Park has transitioned through post-fire succession into gamble oak and post-fire herb cover-types, which account for approximately 48 % of the land cover (Thomas *et al.*, 2009). The landscape is in various states of post-fire succession. Fire plays a major role in the distribution of vegetation throughout Mesa Verde National Park.

Figure 2.2: Profiles of unconsolidated colluvium (left) and loess soil (right). The left profile is typical of oak and grass covers of northern Mesa Verde soils and the right profile is typical of unburned soils in the pinion-juniper forest. The depth of the litter material (right) is typical for unburned needle mats in the pinion-juniper forest.

Fire-managed land is minimal within the Park. Prescribed burning is limited to two areas: (1) adjacent to the Long View Visitor Station and (2) an area of the Chapin Mesa near the Park management headquarters. These sites undergo annual fuel reduction using burning combined with mechanical thinning to provide "safe zones" in the event of a major wildfire threatening Park employees.

Cleaning procedures

To reduce the risk of sample contamination, all sampling items were cleaned prior to contact with samples. Soil core barrels were cleaned with a bottle-brush and triple-rinsed in ultrapure (18.2 MΩ cm) water. Soil cores were transferred into new Thermo Scientific® I-chem® glass vials with polytetrafluoroethene (PTFE) lids (Fisher Scientific, USA). Vials are pre-cleaned and certified to contain negligible leachable mercury from the manufacturer. All reused glass used in the release experiments were rinsed for 24 h on an end-over-end turn bar (10 rpm) in a 10 % HCl acid and 10 % HNO_3 acid solution. Vials were then rinsed with three vessel volumes of ultrapure water. A new disposable BD Luer-Lok® tip plastic syringe affixed with a new Supor® (hydrophilic polyethersulfone) membrane in an Acrodisc® modified acrylic housing filtering apparatus was rinsed with ultrapure water in the amount of three sample volumes prior to filtering.

Sampling location and procedures

Sampling locations were selected by laying an 800-meter point grid on a Mesa Verde National Park map and choosing individual points based on burn status (unburned, burned by wildfire, burned by prescribed burn), accessibility, and Park management recommendations. Once a sampling location was determined, burn history was established based on National Park Service fire history mapping (NPS, 2008). Following the Weber fire (June 2012), additional soil samples were collected (May 2013) in naturally burned and unburned areas located east of the Park. These samples were collected to characterize a recently-burned pinion-juniper woodland in greater detail. Soils collected in the vicinity

of the Weber Fire were representative of the unconsolidated colluvium found in Mesa Verde National Park.

We sampled a total of 96 locations in the course of this study, which included 34 unburned locations, 57 locations with previous wildfire spanning 1934 to 2012, and 5 prescribed-burn locations with ongoing treatment. At each sampling location, triplicate soil cores of 10 cm depth were collected using polyvinylchloride core barrels of 5 cm diameter. The triplicate cores were collected from specific locations representing the sampling site as best as possible. For instance, if the location had bare soil, a shrub covered area, and a pinion needle mat, a core would be collected from each to represent the landscape heterogeneity. The soil litter layer, defined by the presence of non-degraded sticks, leaves, and needles, was removed and core barrels were pressed in by hammer. The soil cores were placed in double re-sealable plastic bags, stored on ice for transport, and then stored in a laboratory freezer. We did not characterize the layers of each soil core; instead, we examined each core by depth interval. Soils were extruded from core barrels in depth intervals of four intervals of 1 cm each to obtain detailed mercury and organic matter depth profiles. Due to the large number of sampling locations, we only used 1 cm intervals for 25 samples and then switched to intervals of0-2 and 2-4 cm for the remainder of the sampling locations. From the triplicate soil cores collected at each sampling location, a single composite sample was created. Composite samples were placed in I-Chem™ vials (40 mL) and freeze-dried for 1 week. Following freeze-drying, rocks, sticks, and large roots were removed with a 2 mm stainless steel sieve, and then soils were ground using a mortar and pestle.

Soil samples were characterized for organic matter content gravimetrically by loss on ignition (LOI) for 2 h at 550°C. Freeze-dried soil samples were weighed out to 1 g in pre-weighed ceramic boats. Samples were then heated for 2 h, cooled in a desiccator, and re-weighed to determine mass loss. Total mercury was measured using thermal decomposition / catalytic reduction / atomic absorption spectroscopy (DMA-80 analyzer, Milestone, Shelton CT, USA). Freeze-dried soil (0.1 g) was transferred

to pre-weighed sample boats using a stainless steel scoop. All mercury measurements were calibrated using standards certified by the National Institute of Standards and Technology (NIST) and National Research Council of Canada (NRCC). Target concentrations of reference standards were confirmed to be within 10 % for each analytical group run. Additionally, all samples were accompanied by analytical blanks to assess instrument carry-over and baseline.

We analyzed a total of 35 samples in duplicate to determine analytical variability. For environmental samples with considerable heterogeneity we considered that a difference of 35 % or less was acceptable. Within these samples, 25 of the 35 duplicates were within this range, but the additional ten duplicates contained a greater percent difference. The samples responsible for this large percent difference tended to be soils with low mercury concentrations (< 20 ng).

Release of Soil Mercury to Water

Release of mercury from the soil samples was tested by adding 400 mg of soil to 40 mL of ultrapure 18.2 MΩ water (Millipore Milli-Q®) water in ground glass-stoppered vials. The soil suspensions were equilibrated for 24 h on an end-over-end rotating wheel at 10 rpm. After 24 h of rotation, the suspensions were transferred to Teflon® Oak Ridge round-bottom 50 mL centrifuge tubes and centrifuged at 14,000 rpm for 15 min (Sorvall RC2-B centrifuge, SS-34 angle head rotor). Samples were filtered into new glass vials (40 mL) and capped with PTFE lids. The filtrate was divided into two separate samples for future analyses: one for DOC analysis and the other for determination of total mercury content.

Dissolved organic carbon was measured within 14 d using a total organic carbon analyzer (OI 700, Oceanography International) and persulfate oxidation (Aiken, 1992). Samples for total mercury analysis were immediately preserved by the addition of 1 % bromine monochloride (BrCl; Bloom *et al.*, 2003), and subsequently analyzed by cold vapor atomic fluorescence spectroscopy (CVAFS; Tekran 2600) following EPA Method 1631.

Data and Statistical Analysis

The mass of mercury emitted from soils during fires was determined as the difference between the burned and unburned mercury concentrations in the soil:

$$M_{Hg} = \left([\mathrm{Hg}]_{soil}^{unburned} - [\mathrm{Hg}]_{soil}^{burned} \right) d_{soil} \rho_{soil}^{b} \quad (1.1)$$

M_{Hg} is the mass of mercury emitted on an areal basis (ng cm^{-2}), $[\mathrm{Hg}]_{soil}^{unburned}$ and $[\mathrm{Hg}]_{soil}^{burned}$ are the mercury concentrations of unburned and burned soil (ng g^{-1}), d_{soil} is the depth of the soil sample (cm), and ρ_{soil}^{b} is the bulk density of the soil (g cm^{-3}). The bulk density of the soil was not directly measured; instead, an arbitrary value of 1.2 ± 0.2 g cm^{-3} was used as an estimate for dry bulk soil.

Differences between soil intervals of the same condition (burned, unburned) were compared using one-tailed *t*-test to determine statistical difference between burned and unburned soil profile increments. The *t*-tests evaluated the hypothesis that burned soil contained less mercury or organic matter than the unburned soil at each increment tested. Sample populations were assumed to have unequal variance and statistical significance was considered at the 5 % level.

Results

The average organic matter and mercury content at each depth interval, the release of mercury and organic matter from soil into aqueous solution are presented in Table 2.1.

Soil Organic Matter

The depth profiles of soil organic matter content revealed that unburned soils contained more organic matter than burned soils at each interval in samples collected from within the Park (Figure 2.3). In unburned soils, the mean organic matter content decreased with depth ($p < 0.05$, *t*-test). In the burned, organic matter content did not vary with depth ($p > 0.05$, *t*-test) (Figure 2.3).

Organic matter content in the 0-2 cm interval averaged 20 ± 11 % in unburned soils and 9 ± 4 % in wildfire burned soils. There was an increase in the organic matter content of wildfire-burned soils that varied with time since the last fire. For instance, the average soil organic matter content (0-2 cm) was 7 ± 1 % in soils collected from the Long Mesa Fire (2002), and 14 ± 6 % in soils collected from the Wildhorse Fire (1934). Soil samples collected from areas that underwent prescribed burning were found to contain 8 ± 1 % (n = 5) organic matter content.

In the unburned soils collected adjacent to the Weber Fire, the organic matter content was lower than the unburned soils in the Park (Figure 2.3). Similar to Mesa Verde National Park, burned soil contained less organic matter than unburned soil. Organic matter content in burned and unburned soils were not statistically different ($p > 0.05$) from one another beyond 1 cm depth, but was statistically different at the 10 % confidence interval at the 2 cm depth interval.

Duplicate analysis of soil resulted in differences that ranged from 0-117 %. Only two of the 15 duplicates were greater than 20 %. The difference of 20 % might be considered high; however, these samples represent a heterogeneous mixture of soil and some differences were expected.

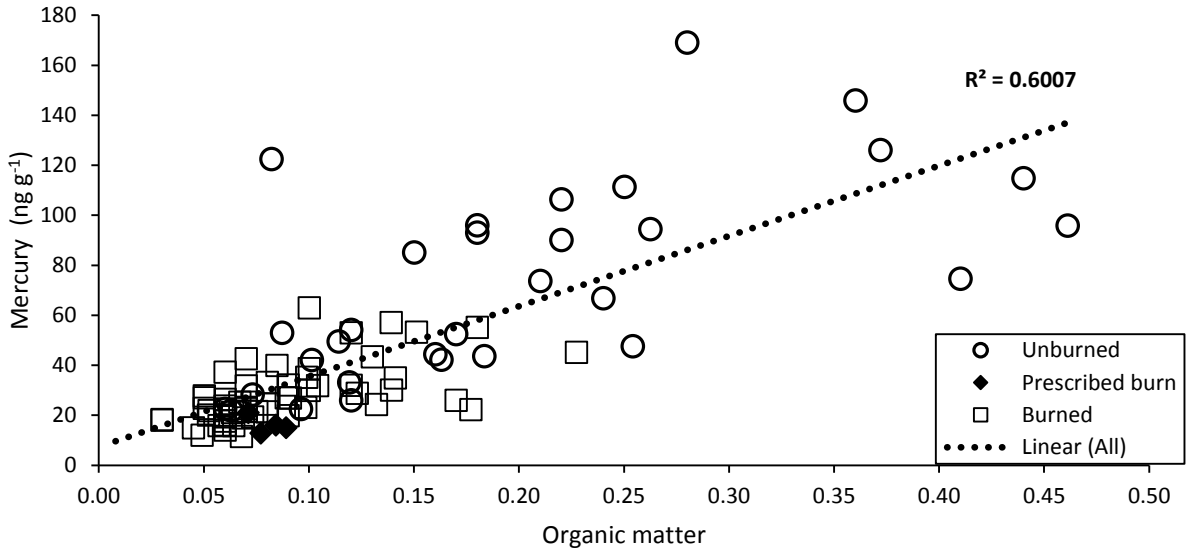

Figure 2.3: Mercury concentration plotted against soil organic matter content in the 0-2 cm depth of soils across the Mesa Verde National Park.

Table 2.1: Mercury (Hg) and organic matter (OM) content in soil profiles and release experiments from unburned areas and within burn perimeters. Samples are listed by fire, depth interval (int.) and the number of samples measured (#). The average (ave.) standard deviation (std .dev.) and difference for duplicate analyses (dup) are shown. Samples marked with "*" include average values from combining the 1 cm intervals.

Sample	Y	Int. (cm)	# (Hg/OM)	Ave. OM ($g\ g^{-1}$)	OM std. dev ($g\ g^{-1}$)	Ave. Hg ($ng\ g^{-1}$)	Hg std. dev ($ng\ g^{-1}$)	Aqueous release	Hg dup diff (%)	OM Dup diff (%)	Released Hg dup diff (%)
Unburned	N/A	0-1 1-2 2-3 3-4 0-2 2-4	13/12 13/12 13/12 13/12 15/31* 15/31*	0.21 0.17 0.17 0.14 0.20 -	0.10 0.06 0.07 0.06 0.11 -	84 73 63 56 70 38	39 30 25 23 37 25	(n=15) Hg ($ng\ L^{-1}$) 9.7±6.8 DOC ($mg\ L^{-1}$) 16±16.6	(n=11) 4, 23, 8, 71, 57, 14, 49, 33, 19, 4, 28, 6, 4	(n=4) 20, 5, 117, 15,16	(n=3) 12, 33, 80
Unburned, Adjacent to Weber Fire	N/A	0-1 1-2 2-3 3-4 4-5 5-6 6-7 7-8	3/3 3/3 3/3 3/3 3/3 3/3 3/3 3/3	0.10 0.09 0.08 0.07 0.06 0.06 0.05 0.08	0.02 0.02 0.01 0.01 0.01 0.01 0.01 0.03	35 35 34 32 30 29 32 30	1.3 1.3 1.5 4.0 2.3 2.5 8.2 6.6	-	-	-	-
Wildhorse Fire	1934	0-2 2-4	5/5 5/-	0.14 -	0.06 -	48 24	23 6.1	(n=4) Hg ($ng\ L^{-1}$) 6.5±2.0 DOC ($mg\ L^{-1}$) 16.8±17.1	(n=4) 0, 27, 69, 27	(n=1) 0	(n=1) 38
Long Mesa Fire	1989	0-2 2-4	4/5 4/-	0.11 -	0.05 -	24 20	2.6 3.7	(n=2) Hg ($ng\ L^{-1}$) 3.4 DOC ($mg\ L^{-1}$) 3.4	(n=2) 24, 26	(n=1) 16	-
Chapin Fire	1996	0-1 1-2 2-3 3-4 0-2 2-4	2/2 2/2 2/2 2/2 1/3* 1/1	0.10 0.08 0.10 0.09 0.10 -	- - - - 0.04 -	38 25 31 27 23 16	- - - - - -	(n=1) Hg ($ng\ L^{-1}$) 5.8 DOC ($mg\ L^{-1}$) -	-	-	(n=1) 65
Pony Fire	2000	0-1 1-2 2-3 3-4 0-2 2-4	3/3 3/3 3/3 3/3 4/5* 4/4	0.09 0.09 0.08 0.09 0.09 -	0.03 0.03 0.01 0.01 0.02 -	27 25 27 26 25 17	5.9 5.9 3.4 5.6 7.2 7.3	(n=2) Hg ($ng\ L^{-1}$) 3.4±1.0 DOC ($mg\ L^{-1}$) 7.7±3.2	(n=4) 23, 3, 31, 51	(n=3) 50, 13, 16	(n=1) 0
Bircher Fire	2000	0-1 1-2 2-3 3-4 0-2 2-4	6/5 6/5 6/5 6/5 24/24 24/24	0.09 0.10 0.07 0.08 0.07 0.07	0.05 0.05 0.04 0.02 0.03 0.03	29 32 31 29 30 25	13 13 12 11 13 9.3	(n=16) Hg ($ng\ L^{-1}$) 4.4±2.2 DOC ($mg\ L^{-1}$) 5.1±1.7	(n=5) 48, 22, 70, 8, 42	(n=3) 11, 3, 12	(n=3) 4, 7, 89
Long Mesa Fire	2002	0-2 2-4	6/6 6/-	0.07 -	0.01 -	21 12	5.1 1.9	(n=4) Hg ($ng\ L^{-1}$) 7.6±6.0 DOC ($mg\ L^{-1}$) 6.2±1.9	(n=5) 24, 26, 62, 71 29	(n=1) 9	-
Weber Fire	2012	0-1 1-2 2-3 3-4 4-5 5-6 6-7 7-8	5/5 5/5 5/5 5/5 5/5 5/5 5/5 5/5	0.06 0.06 0.06 0.06 0.07 0.07 0.07 0.07	0.01 0.01 0.01 0.01 0.02 0.03 0.02 0.02	10 14 16 17 21 25 26 25	2.0 4.5 4.9 2.0 7.5 7.6 6.5 9.0	-	-	-	-
Prescribed Fire	2010	0-2 2-4	5/5 -	0.08 -	0.01 -	17 -	3.5 -	(n=5) Hg ($ng\ L^{-1}$) 5.2±1.1 DOC ($mg\ L^{-1}$) 6.4±0.9	(n=2) 1, 18	-	(n=1) 33

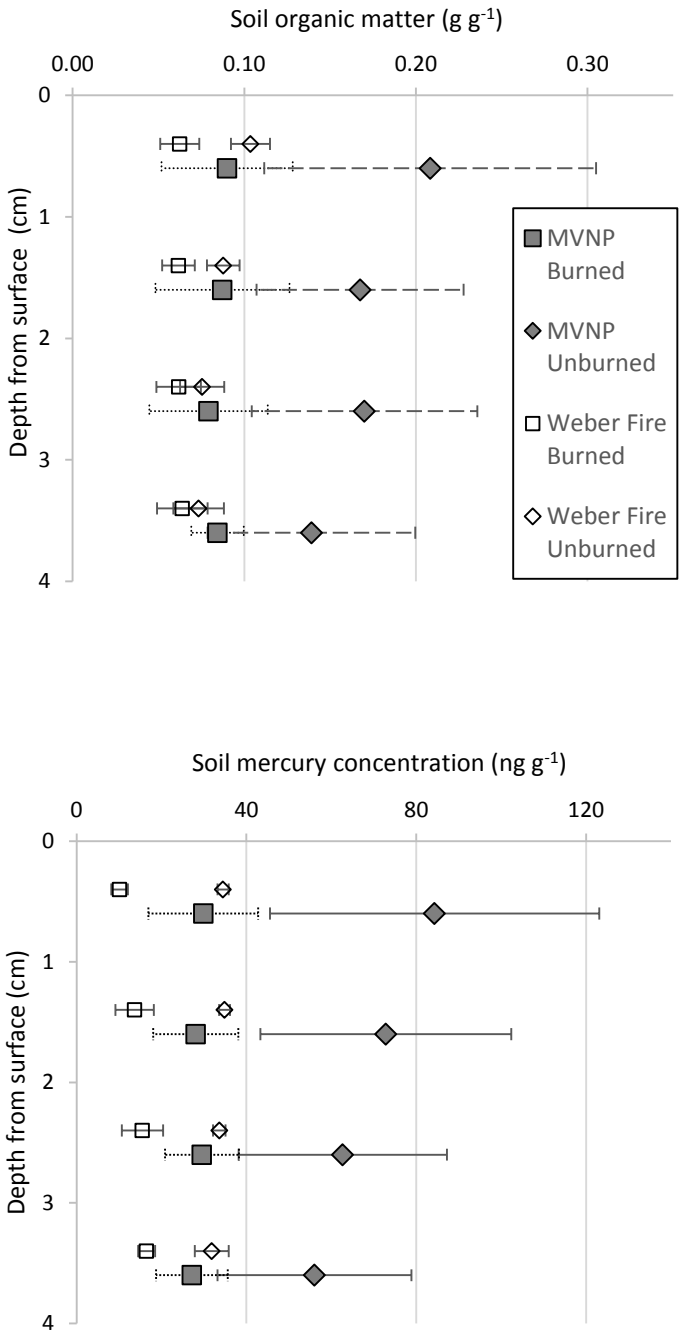

Figure 2.4: (top) Unburned (12 samples) and burned (11 samples) soil organic matter content profiles and (bottom) unburned (13 samples) and burned (12 samples) soil mercury concentration profiles in soils of Mesa Verde National Park (MVNP). The open symbols represent the Weber Fire samples (2012). All error bars represent the stadard deveation of the measurements.

Soil Mercury

Total mercury concentrations in the depth profiles of Mesa Verde National Park soils were significantly greater in unburned soils than in burned soils at each depth interval measured (Figure 2.3). Results from the one-way *t*-test revealed that mercury concentrations in burned and unburned soil were significantly lower in burned soils than in unburned soils at each depth ($p < 0.05$). Mercury concentrations of the unburned Park soils decreased significantly with depth (*t*-test, $p < 0.05$), while mercury profiles in burned soils remained unchanged with depth (Figure 2.3). Soils subjected to prescribe burning contained less mercury (17 ± 3.5 ng g^{-1}) than wildfire burned soils (Table 2.1).

Soils collected adjacent to the Weber Fire contained less total mercury throughout the depth collected than most unburned soils from within the Park. Mercury concentrations in unburned soils collected adjacent to the Weber Fire contained 35 ± 1.3 ng g^{-1} at the surface and reached the lowest concentration (30 ± 2.3 ng g^{-1}) at 5 cm. Conversely, the average burned soil collected nearby contained less mercury at the surface (10 ± 2 ng g^{-1}) and concentrations increased with depth (21 ± 7 ng g^{-1}; Figure 2.3). Weber Fire soil below 4 cm did not reveal a significant difference in mercury content between unburned and burned.

The soils of Long Mesa Fire (2002), Bircher Fire (2000), Pony Fire (2000), Chapin Fire (1996), and Long Mesa Fire, (1989) did not vary with time between burns spanning 1989 to 2002. The mercury content in Wildhorse Fire (1934) soils contained significantly greater mercury content (48 ± 23 ng g^{-1}) than the soils spanning from 1989 to 2012.

Organic Matter and Mercury Release to Water

In general, soils from unburned locations released a greater amount of organic matter (measured as DOC) than soil from burned areas or prescribed burn locations (Figure 2.4); however, release of organic matter from soils into water was variable within burned and unburned soils. Both

burned and unburned soils released a wide range (unburned, 4.7-65 $mg_C\ L^{-1}$; burned, 1.9 -43 $mg_C\ L^{-1}$) of organic matter into solution. The wide range of release resulted in 100 % standard deviation among both burned and unburned soils (Table 2.1). The exclusion of values from the Wildhorse Fire (1934) greatly reduced the range of organic matter released from burned soils (1.9-11 $mg_C\ L^{-1}$). Soil from the prescribed burns released the same amount of organic matter into solution as the burned soils (Table .1).

Mercury release into water followed the pattern of organic matter release. Unburned soils tended to release more mercury into water than burned soils (Table 2.1). The range of mercury release was greater in unburned soils (4.3-31 ng L^{-1}) than in burned (1.9-17 ng L^{-1}) or prescribed burn (4.3-6.8 ng L^{-1}) soils. Mercury release from prescribed burn soils were not statistically different than those of wildfire-burned soil. The release of mercury from unburned soil corresponded to 2 ± 1.4 % of the initial soil mercury. In burned soils, the release of mercury corresponded to 1.9 ± 1.4 % of the initial soil mercury.

Estimated Mercury Emissions

Mercury emission estimates were generated for each major fire with four-interval samples (Table 2.2) and two-interval samples (Table 2.3) using in Eqn. 1. The combined average of Mesa Verde National Park samples with 1 cm intervals resulted in atmospheric release estimates (19 ± 8.2 g ha^{-1}) greater than the 2 cm interval estimate (13 ± 3.3 g ha^{-1}). The Weber Fire (1 cm) released half (9.5 ± 1.8 g ha^{-1}) that of the 1 cm Park soils. We did not generate an estimate for prescribed burns because losses would be based on repeated events such as mechanical thinning and repeated burning over a number of years.

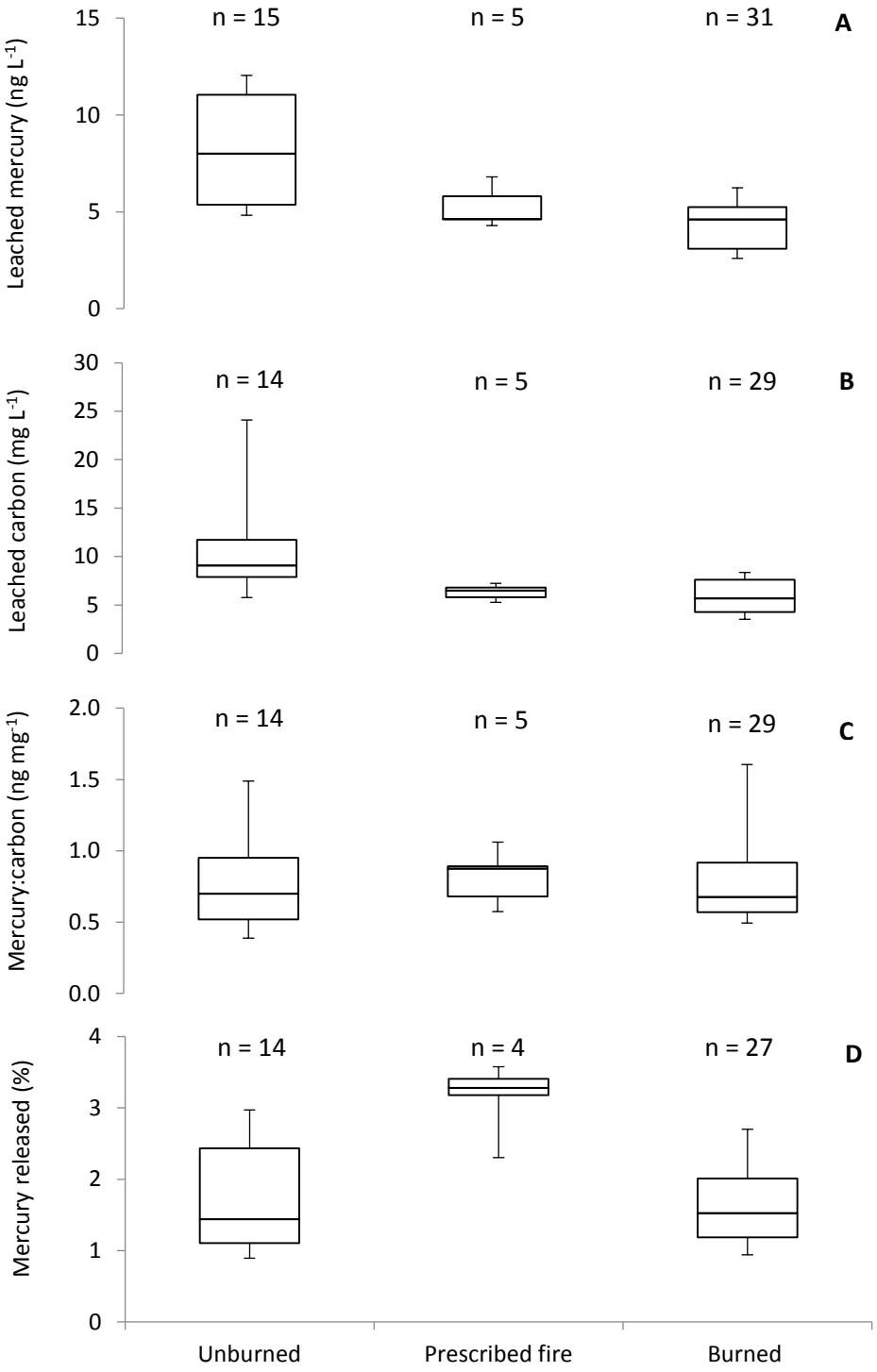

Figure 2.5: (A) Mercury and (B) organic matter (reported as dissolved organic carbon) released to water, (C) the ratio between two, and (D) fractional release of mercury are represented as the 10th and 90th percentile; box boundaries are the 1st, 2nd (median), and 3rd quartiles.

Table 2.2: Soil mercury content is given for burned and unburned soils that were sectioned into 1 cm intervals to 4 cm depth. The difference is the unburned soils mercury content minus the burned soil mercury content.

	Weber Unburned (3 samples)	Mesa Verde Unburned (13 samples)	Weber 2012 (5 samples)	Pony 2000 (3 samples)	Bircher 2000 (6 samples)	Chapin 1996 (1 sample)	All Mesa Verde Average (14 samples)
	Average ± Standard Deviation (g ha^{-1})						
0-1 cm	4.1 ± 0.7	10 ± 5.0	1.2 ± 0.7	3.2 ± 0.9	3.5 ± 1.7	4.6	3.6 ± 1.7
1-2 cm	4.2 ± 0.7	8.8 ± 3.9	1.6 ± 0.7	3.0 ± 0.9	3.8 ± 1.7	3.0	3.4 ± 1.3
2-3 cm	4.0 ± 0.7	7.6 ± 3.3	1.9 ± 0.7	3.2 ± 0.7	3.7 ± 1.6	3.7	3.6 ± 1.2
3-4 cm	3.8 ± 0.7	6.7 ± 3.0	2.0 ± 0.7	3.1 ± 0.8	3.5 ± 1.4	3.2	3.2 ± 1.1
Sum	16 ± 0.7	33 ± 7.7	6.7 ± 1.0	13 ± 1.7	15 ± 3.2	15	14 ± 2.7
Difference			**9.5 ± 1.8**	**21 ± 7.9**	**19 ± 8.3**	**19**	**19 ± 8.2**
Estimated loss			59 %	66 %	60 %	60 %	58 %

Table 2.3: Soil mercury content is given for unburned soils that were sectioned into 2 cm intervals to 4 cm depth. The difference is the unburned soils mercury content minus the burned soil mercury content.

	Mesa Verde Unburned (15 samples)	Long Mesa 2002 (6 samples)	Pony 2000 (4 samples)	Bircher 2000 (24 samples)	Long Mesa 1989 (4 samples)	Wildhorse 1934 (5 samples)	Mesa Verde Average (44 samples)
	Average ± Standard Deviation (g ha^{-1})						
0-2 cm	17 ± 2.2	5.0 ± 0.7	6.0 ± 1.0	7.2 ± 2.2	5.8 ± 0.7	12 ± 2.9	7.2 ± 1.8
2-4 cm	9.1 ± 1.3	2.9 ± 0.3	4.1 ± 0.9	6.0 ± 2.2	4.8 ± 0.5	5.8 ± 0.9	5.3 ± 1.2
Sum	26 ± 2.6	7.9 ± 0.8	10 ± 1.4	13 ± 2.2	11 ± 0.7	17 ± 3.0	13 ± 2.1
Difference		**18 ± 2.7**	**16 ± 2.9**	**13 ± 1.2**	**15 ± 0.5**	**8.6 ± 3.9**	**13 ± 3.3**
Estimated loss		72 %	64 %	53 %	63 %	52 %	50 %

Discussion

Consideration of Fire Severity and Soil Depth Loss

Fire severity, from a soil perspective, is a function of two components: the temperature achieved (intensity) and the duration of burning. Both of these components influence the amount of energy transferred into soil. From a forestry perspective, fire severity may be qualitatively described by observations of fire behavior. These observations are often based on the degree of burning and combustion within a forest stand (Parsons, 2003). In Mesa Verde National Park, he areas studied contained no visual indication of variable burn severity. All areas burned in stand replacing fires and there was no indication that certain areas of forest burned with different behavior than others.

From the observation that pinion-juniper forests in the park all burned in stand replacing fire, wildfire in pinion-juniper forests could be defined, from a forestry perspective, as high severity (complete canopy destruction). The soils of pinion-juniper forests tend to have more variation in severity because needle mats and combustion of above ground fuels (pinion-juniper canopy) results in localized soil heating below the trees (Madsen *et al*., 2011). Our composite sampling method should have accounted for localized heating and we assumed that our samples represent the average burning effects on the landscape.

Mercury concentrations in burned soils were not adjusted for soil depth loss or change in soil density due to loss of organic matter. In previous studies quantifying mercury emissions from soil, there has been an attempt to account for additional mercury losses from the consumed soil horizon (Engle *et al*, 2006; Biswas *et al*., 2007). The soils collected in Mesa Verde National Park contained very shallow organic layers, if any (Figure 2.2). Often sites had a high degree of barren soil, even in unburned locations, and it was unreasonable to quantify a change in depth. We did not calculate a change in soil

density, as there is no reliable means to do so. The large deviation (20 %) in soil density that was assumed for all calculations accounts for minor density changes that may have occurred during wildfire.

Soil Organic Matter and Heat Penetration during Wildfire

Soil organic matter losses from soils affected by wildfire provide an indication of the heat transfer into the soil. In Mesa Verde National Park soils, wildfire depleted organic matter throughout the sampled depth of 4 cm (Figure 2.3). In the Weber Fire locations, where soil was samples to 8 cm depth, there was no indication that heating or organic matter losses extended beyond 4 cm. The depth of soil heating in this arid landscape is likely a function of minimal soil moisture during the summer and a thin degraded organic soil (duff) layer. The presence of either would insulate soils during wildfire (Certini, 2005, Stoof *et al.*, 2013). During wildfire, temperatures above ground surface can be over 850°C; however, temperatures generally diminished to less than 300°C in the first 1 to 3 cm due to insulating properties of soil (Certini, 2005). Loss of soil organic matter during heating begins near 100°C and combustion occurs at 460°C (Gonzalez-Perez *et al*., 2004; Certini, 2005). In soils of Mesa Verde National Park, losses were measured to 4 cm and therefore 100°C temperatures were likely at this depth. Because there is still organic matter remaining in the soil at burned locations, temperatures likely did not exceed 460°C below the soil surface.

Soil Mercury Loss during Wildfire

Sites affected by wildfire contained between 52 and 72 % less mercury to a depth of 4 cm than soils at unburned locations. Temperatures that cause mercury release from humic acids (200-300°C; Biester and Scholz, 1996) are within the range responsible for organic matter loss (100-460°C). The result that soil heating caused organic matter and mercury losses from depths of 4 cm is in contrast to previous studies comparing unburned and burned sites. For instance, Engle *et al.* (2006) reported that mercury emissions were not detected at depths of 0-10 cm below the litter layer in a ponderosa forest.

Similarly, Mitchell *et al.* (2012) found fire did not result in mercury loss at depths of 0-10 cm below the litter layer in a jack pine forest. However, our data is consistent with the findings of Biswas *et al.* (2007; 2008) and Woodruff and Cannon (2010). Biswas *et al.* (2007; 2008) reported mercury losses as high as 94 % to depths of 8 cm in a mixed lodgepole, spruce, and Douglas fir forest. Woodruff and Cannon (2010) reported losses in a soil A-horizon (below the litter layer) of a mixed conifer forest, but no depths were reported. The differences in mercury losses from mineral soils are likely caused by differences in fire intensity, forest type, and the abundance of insulating organic material at specific sampling locations. It is also possible the bulk soil-horizon measurements caused a dilution effect, which would make determination of mercury losses difficult.

Soil Mercury Emission Estimates

Areal emission estimates generated from the average of wildfire-burned soils in the 0-2 and 2-4 cm intervals (13 ± 3.3 g ha^{-1}) and in the 0-1, 1-2, 2-3, and 3-4 cm depths of Mesa Verde National Park soils resulted in different release estimates (19 ± 8.2 g ha^{-1}). The difference between the two estimates is a result of greater resolution in the 1 cm interval depth profiles. Comparing the four-interval depth profiles between the Weber Fire (9.5 ± 1.2 g ha^{-1}) and those in Mesa Verde soils revealed that half as much mercury was lost in the Weber soil. This result follows the total soil mercury content in the unburned soil (16 ± 1.5 g ha^{-1}), which was half that of total soil mercury in Mesa Verde National Park (33 ± 7.7 g ha^{-1}). Clearly, the initial mercury content of soil was large influence on the amount released during wildfire.

Our estimates for areal emissions of mercury (9.5 ± 1.2 g ha^{-1} to 21 ± 7.9 g ha^{-1}) are similar to the 25 g ha^{-1} reported for high severity wildfire in conifer forests (Biswas *et al*., 2007). Biswas *et al.* (2007) reported 76 % and 87 % loss of mercury in 8 cm soil cores containing 32 ± 27 ng g^{-1} to 208 ± 263 ng g^{-1}. However, there was no comment on the how well their unburned reference site represented the two burned locations (triplicate soil cores) sampled. Our estimates are substantially greater than that of

Engle *et al.* (2006), who reported 2.0-5.1 g ha^{-1} of mercury released from a ponderosa pine forest. Engle *et al*., (2006) reported mercury concentrations of 91 ± 32 ng g^{-1} in unburned litter material, but only 8.8 ng g^{-1} in the 0-10 cm soil depth. Engle *et al*. (2006) was unable to detect a change in soil mercury content below the litter layer and assumed that mercury was only released from litter and the first 5 mm of underlying soils. Similarly, estimates made by Mitchell *et al.* (2012) for jack pine forest (4.2 g ha^{-1}) were also based on litter layer losses only, as wildfire did not liberate mercury from below the organic layer (no depth given) due to low severity burning. The losses reported by Mitchell *et al.* (2012) were based on forest litter concentrations of approximately 150 ± 75 ng g^{-1}. A comparison of our results with these studies demonstrate that in addition to mercury concentrations in fuel and soil, the severity of burning plays a large role on the amount of mercury released during wildfire.

Mercury release from soil to water

We hypothesized that release of mercury from the Mesa Verde soils would be enhanced in burned soils due to oxidation and loss of organic matter; however, we did not find evidence to support hypothesis. Both burned and unburned soil released the same average fraction of mercury initially present in the soil to water (1.9 ± 1.3 and 2.0 ± 1.4, respectively). Burned soil tended to release less net organic matter and soil mercury due to the lower initial content. A similar result was observed on a watershed scale by Amirbahman *et al.* (2004). In examination of a pair of watersheds (one burned and one unburned), Amirbahman *et al.* (2004) found the burned watershed exported less carbon and mercury than the unburned watershed 50 y after wildfire.

Mercury Accumulation on Burned Landscapes

Following wildfire, mercury accumulation on the landscape appeared limited due to the loss of organic material responsible for mercury binding. We compared the observed overall change in mercury concentration from soil obtained from the Bircher Fire (2000; 13 ± 1.2 g ha^{-1}), which was the

most robust single fire data set, with soil mercury concentrations of the Wildhorse Fire (1934; 17 ± 3.0 g ha^{-1}). Based on this comparison, the average rate of mercury accumulation over the 66 y time period is 0.061 g ha^{-1} y^{-1}. The Mercury Deposition Network (National Atmospheric Deposition Program, 2012) reported an average annual wet deposition of 0.063 g ha^{-1} y^{-1} for the time period 2002-2011 at the measuring station in Mesa Verde National Park (National Atmospheric Deposition Program, 2012). We acknowledge that this estimate varies depending on the fires chosen and does not account for changes in mercury deposition across the time scale presented, which has increased greatly since 1934 and 2000. However, the similarity between wet deposition measurements and measured mercury accumulation on burned landscapes suggests that wet deposition is a reasonable predictor for mercury accumulation in these soils.

Summary

This study was the first to investigate losses of mercury from pinion-juniper forests during wildfire. The study demonstrates the loss of organic matter and mercury from soil depths below a combusted layer during wildfire. We found that in areas affected by wildfire, soil organic matter depletion and mercury release occurred to a depth of 4 cm. Within this depth, initial mercury content was depleted by 52-72 %. Mercury loss from soil corresponded to emissions ranging from 9.5 ± 1.8 g ha^{-1} to 21 ± 7.9 g ha^{-1}. In addition to atmospheric emissions, we evaluated aqueous release of soil mercury from burned and unburned soils. Results showed that unburned soils release a greater amount of organic matter and mercury than the burned soil, while releasing the same fractional percentage of initial soil mercury. These results indicate that mercury retention by soils is not greatly altered by these historical wildfires. Comparing measured soil mercury content among two historical fires, the Bircher Fire (2000) and the Weber Fire (1934), resulted in an average accumulation rate of 0.06 g ha^{-1} y^{-1} that was similar to wet deposition rates measured in the Park over the previous decade (0.063 g ha^{-1} y^{-1};National Atmospheric Deposition Program, 2012).

Chapter 3

Simulated Wildfire Heating of Forest Soil Increases Mercury Affinity and Alters Sulfur Speciation

Jackson P. Webster *[a], Benjamin Kamark [a], Genevieve Nano [b], Kathryn Nagy [b], Alain Manceau [c], George R. Aiken [d], and Joseph N. Ryan [a]

[a] Department of Civil, Environmental, and Architectural Engineering, University of Colorado, Boulder

[b] Department of Earth and Environmental Sciences University of Illinois at Chicago

[c] ISTerre, CNRS Universite de Grenoble, Grenoble, France,

[d] US Geological Survey, Boulder, Colorado

To be submitted to *Environmental Science & Technology*

Abstract

Mercury transport and accumulation threatens human and ecological health on a global scale. Wildfire is a major land disturbance that remobilizes mercury from soil. In addition to atmospheric re-emission through volatilization during heating, wildfire in forested watersheds enhances the transport of mercury from forest soils to the sediments of lakes and reservoirs. To understand the behavior of mercury in forest soils subjected to fire, the effect of heat on mercury binding to soils was examined. Soil samples were collected from the Vallecito Reservoir watershed In La Plata County, Colorado, in May 2009. Forest soils were heated in a furnace at temperatures from 25°C (control) to 250°C and over times of 20 to 240 min, representative of wildfire. Sulfur x-ray absorption near edge structure spectroscopy was used to assess changes in sulfur speciation due to heating. Heated soils were then subjected to release experiments in aqueous suspensions. The release of mercury, organic matter, and major ions were measured following 24 h. The heated forest soils were compared with unheated soils and used in competitive ligand exchange experiments to assess changes in capacity of mercury adsorption by the soils.

X-ray absorption near edge structure spectroscopy reveals that soils subjected to heating contained more oxidized sulfur species and concomitant losses of intermediate oxidation state species. The content on reduced heterocyclic sulfur, such as thiophenes, was not greatly changes by heating. Heated soils released greater amounts of organic matter and major ions from soils. The fraction of initial soil mercury released into aqueous solution was increased following heating, though losses from volatilization during heating reduced the total release into solution. Comparison of mercury phase distribution between heated and unheated soils in the presence of a competing ligand revealed that mercury had increased affinity for heated soils. We observed a 5 % increase in mercury association with organic matter following heating, which corresponds to a 54 % increase in strong mercury binding sites.

Introduction

Mercury accumulation in soil, sediment, and biota poses a serious risk to human and ecological health. Re-mobilization of mercury from soil is a major contributor to the global mercury cycle and wildfire is a major land disturbance causing this re-mobilization. While wildfire is a well-documented pathway for atmospheric mercury re-mobilization from forest soil, there is little information regarding post-fire mobilization of mercury into surface water. Wildfire occurrence and severity are increasing through the sub-polar latitudes (Westerling *et al*., 2006; McCoy and Burn, 2005; Kasischke *et al.,* 2010; Westerling *et al*., 2014) and this warrants investigation into mobilization mechanisms facilitating increased mercury transport in recently burned watersheds and affected surface waters.

Studies investigating post-wildfire mobilization of mercury into aquatic environments demonstrate increased mercury transport and methylation. Caldwell *et al*. (2000) reported two-fold increases of total Hg, and 14-fold increases of methylmercury (CH_3Hg^+) in lake sediments following fire-induced debris transport from a forested watershed into a reservoir in New Mexico. Similarly, Kelly *et al.* (2006) reported increased mercury transport from a forested watershed and subsequent increases in food-web mercury in a mountain lake following wildfire. Kelly *et al*. (2006) suggested that soil heating may have altered the soil organic matter in a manner that increased mercury export and caused elevated dissolved mercury in surface water. In addition to increased transport, wildfire appears to increase mercury methylation rates in sediment affected by wildfire (Caldwell *et al*., 2000; Krabbenhoft and Fink, 2001; Gilmour *et al*., 2004). One reason for increased methylation may be increased mercury availability to methylating organisms combined with elevated sulfate, labile carbon, and reducing conditions (Krabbenhoft and Fink, 2001), which are often present following wildfire (Smith *et al*., 2011).

It is likely that changes in mercury mobility and increases in the concentration of mercury species, which can be converted to methylmercury, are closely related to the specific binding environment of mercury. In forest soils, surface waters, and sediments, mercury is bound to organic matter, and binding is directly related to the coordination of mercury with reduced sulfur moieties (Xia

et al., 1999; Skyllberg *et al*., 2000; Hesterberg *et al*., 2001; Drexel *et al*., 2002; Haitzer *et al*., 2003; Wolfenden *et al*., 2005; Khwaja *et al*., 2006;, Skyllberg *et al*., 2006; Nagy *et al*., 2011). Reduced organic sulfur functional groups are responsible for the strong binding capacity of mercury by organic matter, although not all reduced organic sulfur participates in binding. For instance, by comparing sulfur abundance from X-ray absorbance near-edge structure spectroscopy (XANES) analysis and mercury titrations of dissolved organic matter, Haitzer *et al*. (2003) determined that only 1.6 % of reduced organic sulfur was available for strong mercury binding.

Mercury-organic matter stability constants are primarily reported for complexes of dissolved organic matter and mercury, whereas measurements of whole-soil mercury organic matter stability constants are few. Measurements that have been reported are in agreement with values reported for dissolved phase complexes. For example, Skyllberg *et al*. (2000) reported stability constants between K of $10^{31.6}$ to $10^{32.2}$ $M_{reduced\ sulfur}^{-1}$ for whole soil complexes of organic matter and mercury by employing a competitive bromide-ligand exchange method. It has since been noted that the presence of a soil-associated bromide-mercury complex may have artificially increased the reported stability constants (Khwaja *et al*., 2006). Considering a lower stability constant, their results agree with measurements of Drexel *et al*. (2002) who reported value of $K = 10^{27.2}$ $M_{reduced\ sulfur}^{-1}$ derived from modelling of mercury-peat adsorption isotherms. Both results are similar to reported dissolved organic matter binding constants (Haitzer *et al*., 2003; Hsu-Kim and Sedlak, 2003; Gasper *et al*., 2007).

Studies using sulfur-XANES spectroscopy have demonstrated that sulfur oxidation states are dynamic, and shifts in oxidation state may occur through landscape alteration (Solomon *et al.,* 2003; Schroth *et al*., 2007). Sulfur exists in a variety of forms in the environment corresponding to oxidation states ranging from -II to +VI. In soils, most sulfur (>80%) is found in an organic form (Solomon *et al.,* 2003; Prietzel *et al*., 2003; Schroth *et al*., 2007; Prietzel *et al*., 2009). Organic forms of sulfur can be divided into three classes: reduced (thiols, mono, di-, and polysulfides, thiophenes), partially-oxidized

(sulfoxides), and highly-oxidized (sulfonates, sulfones, and ester sulfates). Shifts in sulfur oxidation state often affect the reduced fraction of sulfur, which appears to be the most reactive pool of organic sulfur (Solomon *et al.,* 2003; Scroth *et al*., 2007).

The influence of wildfire on organic sulfur speciation is unknown. Smith *et al*. (2011) cited studies reporting elevated levels of sulfate in surface waters from catchments affected by wildfire. The source of this sulfate is not clear, but it is possible that it was generated through soil heating. Conversely, Czimczik *et al.* (2003) found decreases in C:S ratios in burned soils, which suggests retention of organic sulfur relative to carbon in soil affected by wildfire. In either case, the influence of post-wildfire sulfur speciation is likely to affect mercury binding in soil. Therefore, we hypothesized that heating would result in loss of reduced sulfur functional groups and subsequently decrease the mercury binding capacity of organic matter. To test this hypothesis, we quantified sulfur transformations that occurred during laboratory simulated wildfire heating of forest soils and applied a competitive ligand exchange technique to measure changes in mercury binding capacity of whole soils following heating.

Methods

Sampling Location

Soil samples were collected from the Vallecito Reservoir watershed in La Plata County, CO, in May, 2009 (Figure 3.1). Soils were collected from two areas of the watershed, a south-east facing slope on the west side of Vallecito Reservoir (Area A), and the west facing east side of Vallecito Reservoir (Area B). Soils were collected from unburned, moderately burned, and severely burned locations within the perimeter of the Missionary Ridge Fire (2002). Burn intensities were defined by visual indices

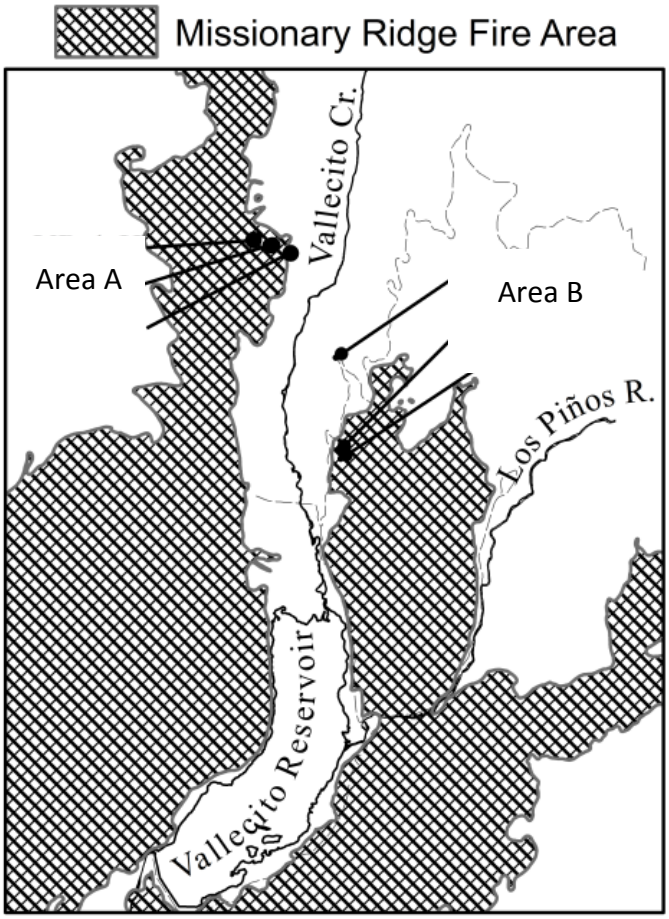

Figure 3.1: Samples were collected from two areas near Vallecito Reservoir: (A) the west side of the Reservoir, and (B) the east side of the Reservoir. The samples were collected in unburned, moderately-burned, and severely-burned locations.

outlined by the Baer classification scheme (Parsons, 2003). Unburned areas were defined based on visual evidence of no recent fires and global positioning system (GPS) coordinates that verified the locations were outside the burn perimeter. Sample sites included aspen, spruce, fir, and ponderosa pine and elevations ranged from 2470-2650 m.

Soil Sampling and Preparation

Soil cores of 7 cm depth were collected with polyvinylchloride (PVC) pipe of 5 cm diameter at each sample site. The core barrels were hammered into the soil until the top of the core barrel was flush with the soil surface. Soil was transferred into new trace-metal clean glass jars with polytetrafluoroethene (PTFE)-lined caps (250 mL; I-Chem™, Fisher, USA). Soil samples were placed in a freezer within 48 h of sampling. Within two weeks soils were freeze-dried, homogenized using a mortar and pestle to break up soil pieces, and sieved (25 mesh).

Experimental Procedures

To simulate the effect of wildfire heating, the soil samples were heated in a muffle furnace over a range of times (0.25-6 h) and temperatures (100-625°C) chosen to be representative of predicted conditions during wildfire (Gonzalez-Perez *et al*., 2004; Certini, 2005). Soil was weighed to 10 g, placed into ceramic crucibles, and placed evenly in a pre-heated muffle furnace for the specified temperature and duration.

Soil release experiments were performed using unheated soils and using soils heated at 225°C for 2 h. Soil suspensions containing 1 g soil and 40 mL of ultrapure water (18.2 MΩ cm at 25°C) were mixed on an end-over-end mixer for 24 h in pre-cleaned (24 h rinse with 10 % HCl and 10 % HNO_3 solution) Pyrex® centrifuge tubes with ground glass stoppers (50 mL). Following mixing, solutions were transferred to PTFE tubes and centrifuged for 20 min at 24,000 relative centrifugal force (RCF).

After centrifugation, the supernatant solution was filtered through a polyethersulfone membrane (0.45 µm pore; 32 mm diameter; Pall Corporation, Supor®) in a polypropylene filter cartridge (Pall Corporation; Acrodisc®) into 40 mL glass vials for mercury, dissolved organic matter, and major ion analyses. Samples for mercury analyses were preserved using a bromine monochloride (BrCl) as outlined by Telliard and Gomez-Taylor (2002). The presence of excess oxidant in sample vials was confirmed prior to mercury analysis. Samples analyzed for dissolved organic carbon (DOC) and ultra-violet absorbance at 254 nm were transferred to new amber glass vials with PTFE lids, preserved using refrigeration, and analyzed within two weeks. Major ion samples were preserved with refrigeration and analyzed within 2-weeks.

Competitive Ligand Exchange Experiments

Mercury exchange between sediment and a competing ligand was used to determine the change in soil binding capacity caused by heating. Soils were prepared by fine grinding using a mortar and pestle. Stock solutions were made in an argon filled glove box. A 0.01 M stock solution of *meso*-2, 3-dimercaptosuccinic acid (DMSA; Sigma Aldrich, 98 % purity) ligand solution was made prior to each experiment. Ultrapure water was de-aired by sparging with high-purity nitrogen prior to use, which minimizes the potential for oxidation of thiol functional groups on DMSA molecules. DMSA is sparingly soluble; therefore 2 mL of 0.1 M NaOH was added to the stock solution to raise the pH to a circumneutral value to dissolve the acid. Stock ligand solution was stored in a refrigerator overnight to ensure dissolution. A stock solution of sodium acetate buffer was made with glacial acetic acid and sodium acetate measured to 1 M.

Competitive ligand exchange experiments were prepared in an argon filled glove box and conducted in triplicate. Mercury addition to the dried and ground sediment was carried out in an argon filled glove box where 0.1 g solid, 5 mL of de-aerated ultrapure water, and 40 µL of stock solution

containing 1 mg L^{-1} $Hg(NO_3)_2$ in 1% nitric acid solution were combined in glass vials (40 mL, I-Chem™, Fisher Scientific, USA). We added 0.03 M sodium azide to the vessels to inhibit microbial activity in the experiments. Soil-water-mercury solutions were mixed at 10 rpm for 7 d using an end-over-end mixer to allow mercury to associate with strong binding sites in soil (Khwaja *et al.*, 2006).

Following mercury association with soil, DMSA (2 mL of the 0.01 M stock solution) was added to the vials at 0.5 mM to compete with the soil organic matter binding sites. Acetate buffer was added to the vials in the amount of 0.4 mL of 1 M to achieve a 0.01 M buffer and 1.33 mL of 3 M sodium perchlorate was added to achieve 0.1 M electrolyte. Vials were brought to 40 mL total volume with ultrapure water and then mixed at 10 RPM for 14 d.

After mixing, soil and aqueous phases were separated. Samples were transferred into pre-cleaned (24 h rinse with 10 % HCl and 10 % HNO_3 solution) PTFE centrifuge tubes (50 mL, Nalgene, Oak Ridge), centrifuged for 15 min at 24, 000 RCF, decanted into BD Luer-Lok® disposable syringes, and filtered through a 32 mm Acrodisc® filter cartridge containing a 0.45 µm polyethersulfone membrane (Supor®, Pall Corporation, USA). Syringes and filter cartridges were rinsed with three syringe volumes of ultrapure water three times prior to use. Filtrate was collected in their original glass I-Chem™ vials with PTFE lined lids (Fisher Scientific, USA). From the experimental vials containing filtrate, 5 mL was pipetted into 40 mL amber glass I-Chem™ vials and diluted 8-fold using ultrapure water for future dissolved organic carbon measurements. The remaining filtrate in the experimental vials was preserved for future mercury analysis by adding BrCl (Telliard and Gomez-Taylor, 2002). Sediment remaining in the centrifuge tube following decanting was rinsed using 20 mL of 0.1 M sodium perchlorate in the PTFE centrifuge tube, shaken, and centrifuged for 15 min at 24,000 RCF to remove any remaining ligand-bound mercury from the solid. Ultrapure water in the amount of 5 mL was added to sediments, which was then poured into polystyrene weigh boats and placed in positive-pressure flow hood equipped with a high efficiency particulate arrestance (HEPA) filter.

The competitive ligand exchange (CLE) experiments were conducted in triplicate and were accompanied by experimental blanks to evaluate mercury, carbon losses, and recovery in the vials. Blanks were treated as CLE samples and run with chemical additions identical to those with solids and mercury. Mercury spikes were conducted with and without soils to evaluate recovery. Recoveries were calculated for each of the individual CLE vials based on mercury addition and native mercury. Dissolved organic matter blanks were prepared to verify recovery of ligand and buffer additions and to ensure that sodium azide additions prevented microbial degradation of ligand or acetate buffer during equilibration. Blanks were also used to determine the release of dissolved organic carbon from the soil by measuring and comparing independent samples containing buffer, ligand, and no soil.

To quantify the observed results, mercury binding with an active strong binding site in organic matter was modeled as

$$RSHg^{+} \Leftrightarrow Hg^{2+} + RS^{-} \tag{3.1}$$

$$K_{RSHg} = \frac{[Hg^{2+}][RS^{-}]}{[RSHg^{+}]} \tag{3.2}$$

where Hg^{2+} was mercury in the experimental vial, RS^{-} was the concentration of strong binding thiol site, and $RSHg^{+}$ was the measured sulfur-bound mercury in the soil (Drexel *et al.*, 2002). The conditional stability constant, K_{RSHg}, is for mercury adsorption with strong sites in soil. Aqueous-phase mercury complexation was modeled as:

$$2\ Hg^{2+} + 2\ H_2DMSA^{2-} \Leftrightarrow Hg_2DMSA_2^{4-} \tag{3.3}$$

$$K_{Hg2DMSA2} = \frac{[Hg_2DMSA_2^{4-}]}{[Hg^{2+}]^2[H_2DMSA^{2-}]^2} \tag{3.4}$$

where H_2DMSA^{2-} was the ligand species in solution and $Hg_2DMSA_2^{4-}$ was the mercury ligand complex in solution measured as filterable mercury (George *et al.*, 2004). The stability constant, $K_{Hg2DMSA2}$, is for the

mercury ligand complex. Adjusting for stoichiometry and combining these equations generated the following equilibrium expressions:

$$K_{RSHg}^2 = \frac{[Hg^{2+}]^2[RS^-]^2}{[RSHg^+]^2} \quad (3.5)$$

$$K_{Hg2DMSA2} = \frac{[Hg_2DMSA_2^{4-}]}{[Hg^{2+}]^2[H_2DMSA^{2-}]^2} \quad (3.6)$$

$$[RS^-] = K_{RSHg}^2 K_{Hg2DMSA2} \frac{[RSHg^+][H_2DMSA^{2-}]}{[Hg_2DMSA_2^{4-}]^{1/2}} \quad (3.7)$$

$$\Delta[RS^-]\ (\%) = 100 \times \frac{[RS^-]_{final} - [RS^-]_{initial}}{[RS^-]_{initial}} \quad (3.8)$$

where $\Delta[RS^-]$ is the fractional change in strong binding sites based on the change in equilibrium distribution of mercury between the soil and the ligand. We are not directly determining $[RS^-]$, just the change in $[RS^-]$.

Analytical Procedures

The organic matter content of the soils was determined gravimetrically by loss on ignition (LOI) for 2 h at 550 °C. Freeze-dried soil samples were weighed out to 1 g in pre-weighed and cleaned ceramic boats. Samples were then heated for 2 h, cooled in a desiccator, and re-weighed to determine mass loss. Total mercury concentrations were measured using thermal decomposition / catalytic reduction / atomic absorption spectroscopy (DMA-80 analyzer, Milestone, Shelton CT, USA). Approximately 0.1 g of freeze dried soil was transferred to pre-weighed sample boats using a stainless steel scoop. All solid phase mercury measurements were calibrated using National Institute of Standards and Technology (NIST) and National Research Council of Canada (NRCC) certified standards. Target concentrations of reference standards were confirmed to be within 10 % for each analytical group run. Additionally, all samples were accompanied by analytical blanks to assess instrument carryover and instrument baseline. Total sulfur concentration in the soil samples was measured at

Huffman Laboratories (Golden, Colorado) employing perchlorate acid digestion and ICP-OES following the methods of Huffman and Stuber (1985) for which the stated limit of detection is 0.01 % by sample weight.

Aqueous mercury concentrations were measured on a Tekran 2600 (Tekran) mercury analyzers using stannous chloride reduction and cold vapor atomic fluorescence spectroscopy (Telliard and Gomez-Taylor, 2002). Calibration standards were made using the National institute of standard and technology (NIST) 3133 mercury standard. Reference materials (USGS standards Hg-45, Hg-51, and Hg-52) were measured to confirm analytical accuracy and to test quantification limits. Dissolved organic carbon in solution was measured with a total organic carbon analyzer (OI Corp., model 700) that employs platinum-catalyzed, heated persulfate oxidation (Aiken, 1992). Ultraviolet absorption at a wavelength of 254 nm (UVA_{254}) was measured using an ultraviolet-visible spectrophotometer (Agilent, model UV-Vis 8453) with a 1 cm path length. All DOC measurements were made within two weeks of experiments. Major ions were measured by ion chromatography (Dionex DX-120).

Alkalinity and pH were measured following filtration using an automatic titrator (Radiometer Analytical TIM900 TitraLab). Select samples were analyzed for manganese and iron after preservation with 1 % nitric acid.

Experimental blanks averaged 0.2 ng L^{-1} mercury, averages of each standard were within each expected range (all less than 10 % relative standard deviation, RSD), and spike recoveries averaged 91 % to 109 % for unheated and heated soils, respectively. The RSD of duplicate mercury analyses was less than 15 % in all but one Area A sample (moderately burned soil, heated at 175 °C, relative standard deviation= 40 %).

Sulfur Oxidation State Measurements

Sulfur X-ray adsorption near-edge structure (XANES) spectra were measured by fluorescence detection at the Advanced Light Source (ALS, Berkeley) on the microfocus beamline 10.3.2, with a top-off current of 500 MA. A two-crystal Si (111) monochromator was used to focus X-rays into He-N_2 gas-filled ionization chamber and fluorescence signals were recorded with a seven-element Ge detector (Canberra; Meriden CT). The estimated uncertainty in energy is 0.1 eV (Manceau and Nagy, 2012). Energy was calibrated by setting the $CaSO_4$ peak to 2482.75 eV and scans were obtained between 2420.0 and 2625.0 eV. A small step size of 0.2 eV was used between 2460.0 and 2490.0 eV to capture spectral details in this region. For all scans, the aperture dimensions of adjustable slits were set to horizontal and vertical width of 300 μm and 50 μm, respectively. Each spectrum is the average of at least seven scans. Sulfur XANES spectrainterpretation was conducted using linear-least squares fitting to determine the ratio of sulfur species in soil samples outlined in Manceau and Nagy (2012).

Results

Characterization of Forest Soil

Soil organic matter, total sulfur, and mercury results from unheated soils and soil heated at 225°C for 2 h are presented in Table 3.1. Soil collected from the West (Area A) and East (Area B) sides of Vallecito Reservoir had similar mercury concentrations. In Area A, moderately burned soils contained greater amounts of mercury than unburned and severely burned soil. In Area B, moderately burned soil contained the same amount of mercury as unburned soil. Organic matter content in Area B soils were approximately twice that of Area A soils. Previous burning did not decrease organic matter content. Sulfur concentrations varied between the sample areas similar to organic matter content (Table 3.1). Due to greater organic matter and sulfur content, Area B soils were used for temperature and time series XANES analysis, and CLE experiments.

Table 3.1: Organic matter, sulfur, and mercury content of soils collected from the Vallecito Reservoir watershed for unheated (25°C) and soil heated at 225°C for 2 h. Soil A and B represent to two areas from which samples were collected. Standard deviation is presented for measurements made in triplicate. All organic matter and mercury measurements were made in duplicate and the average is presented.

	Soil Burn Classification	Heating Treatment (225°C)	Organic Matter (%)	Total Sulfur (%)	Total Mercury (ng g^{-1})
Area A	Unburned		13.2	0.03	46 ± 2.5
		Heated	8.7	0.03	5.0
	Moderate		14.4	0.04	52 ± 5.0
		Heated	13.0	0.04	12
	Severe		10.8	0.03	41 ± 2.5
		Heated	9.6	0.03	11
Area B	Unburned		27.7	0.08	45 ± 1.0
		Heated	18.6	0.07	5.0
	Moderate		19.5	0.05	55 ± 2.5
		Heated	12.9	0.04	7.1
	Severe		28.0	0.06	56 ± 4.5
		Heated	19.3	0.06	4.6

Following furnace heating at 225°C for 2 h, organic matter and mercury concentrations in soil decreased substantially (Table 3.1). The losses of organic matter following heating were minimal in Area A, while heating caused about one-third of organic matter to be lost in Area B soils. Similar to trends in organic matter loss, total sulfur in Area A was not changed by furnace heating and total sulfur area decreased slightly in Area B.

In soil heating experiments, soil mercury and organic matter losses from Area B decreased following 20 min heating at increasing temperatures (Figure 3.2). Decreases in mercury concentrations in the soil samples occurred at all temperatures relative to the unheated reference. There was a narrow threshold for total mercury release; temperatures below 225°C released a smaller fraction of mercury than soils heated to and above 250°C. Temperatures exceeding 275°C resulted in loss of mercury below detection. The threshold for organic matter loss was broader; decreases in organic matter content began to occur near 200°C and continued until 500°C.

Release of Soil Organic Matter and Mercury

Increased heating temperature, in the range of 100-200 °C for 20 min, increased the amount of organic matter released from the heated soil (Figure 3.3). Soils heated at temperatures above 200°C did not continue to release greater amounts of organic matter to solution. The plateau of organic matter release corresponds with the onset of observed organic matter loss from soil. Measurements of $SUVA_{254}$ values in leachate revealed that, in addition to increased organic matter release, heating increased the aromatic content of the water-soluble soil organic matter. Iron was measured in release experiments to assess whether it could be interfering with $SUVA_{254}$ measurements, and was found to be well below the threshold for interference (Poulin *et al*., 2013).

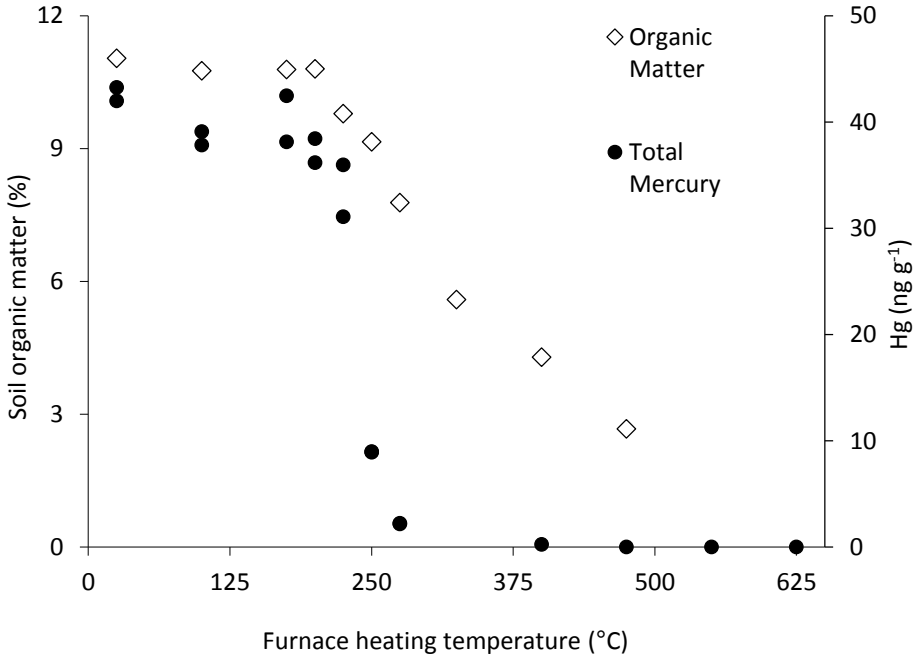

Figure 3.2: Temperature dependence of soil organic matter (left axis) and mercury (right axis) loss from unburned soil from area A over a range of temperatures for 2 h.

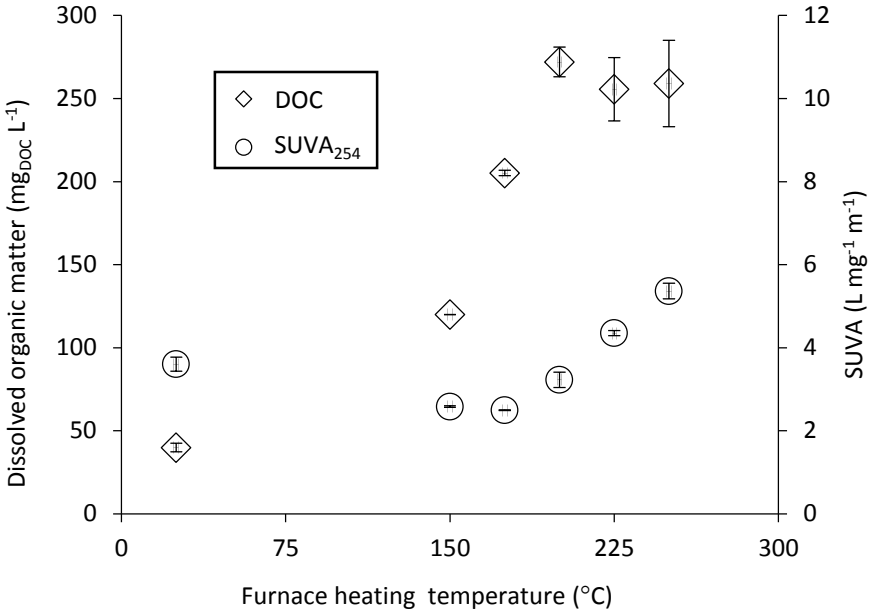

Figure 3.3: Dissolved organic matter measured as carbon (DOC; left axis) and specific ultraviolet absorption ($SUVA_{254}$; right axis) as a function of furnace heating of unburned soil from Area B. Error bars represent the standard deviation of triplicate experiments.

The results for soils heated at 225°C and 250°C for 2 h show that mercury release trends were similar to those for organic matter (Figure 3.4). Organic matter and mercury increased in aqueous leachate following heating. Soil subjected to heating released more mercury into solution than unheated soil due to the loss of soil-mercury during soil heating. Fractional release, determined by soil mercury concentrations following heating and total mercury in aqueous leachate, of both constituents increased with increasing temperature. At the temperature of 250°C, mercury was undetectable in leachate corresponding to the complete loss of mercury in soils.

Soil heated at 225°C for 2 h released greater major ion concentrations into solution than unheated soils (Figure 3.5). Based on a relative concentration basis, manganese appeared to be the constituent most affected by soil heating releasing (67-fold more manganese was released into solution following heating at 225°C). Sulfate release was consistently higher from heated soil, where concentrations increased up to 15-fold.

Sulfur Speciation and Transformation

Heating resulted in a shift of the absorption regions for sulfur in the XANES spectra (Figure 3.6). X-ray absorption by sulfur begins around 2,470 eV and extends to around 2,484 eV. Reduced sulfur species occupy the low energy absorption range near 2,471 to 2,475 eV. The lowest observable peak in the absorption spectra is near 2,473.0 eV; thus, we had no X-ray absorption by FeS (2,471.3 eV) or FeS_2 (2,472.6). The first peak is in the range of elemental sulfur (2,473.1) and di- and poly-sulfides (2,473.3 eV). This peak disappears through the heating series. The absorption region of a particular oxidation state of sulfur can vary depending on the specific arrangement of a sulfur moiety within organic matter (Vairavamurthy, 1998), which causes some ambiguity in species identification. For example, disulfide and polysulfide absorption extends into the elemental-sulfur absorption energy range, which makes the species indistinguishable. The low-energy peak that remains following heating

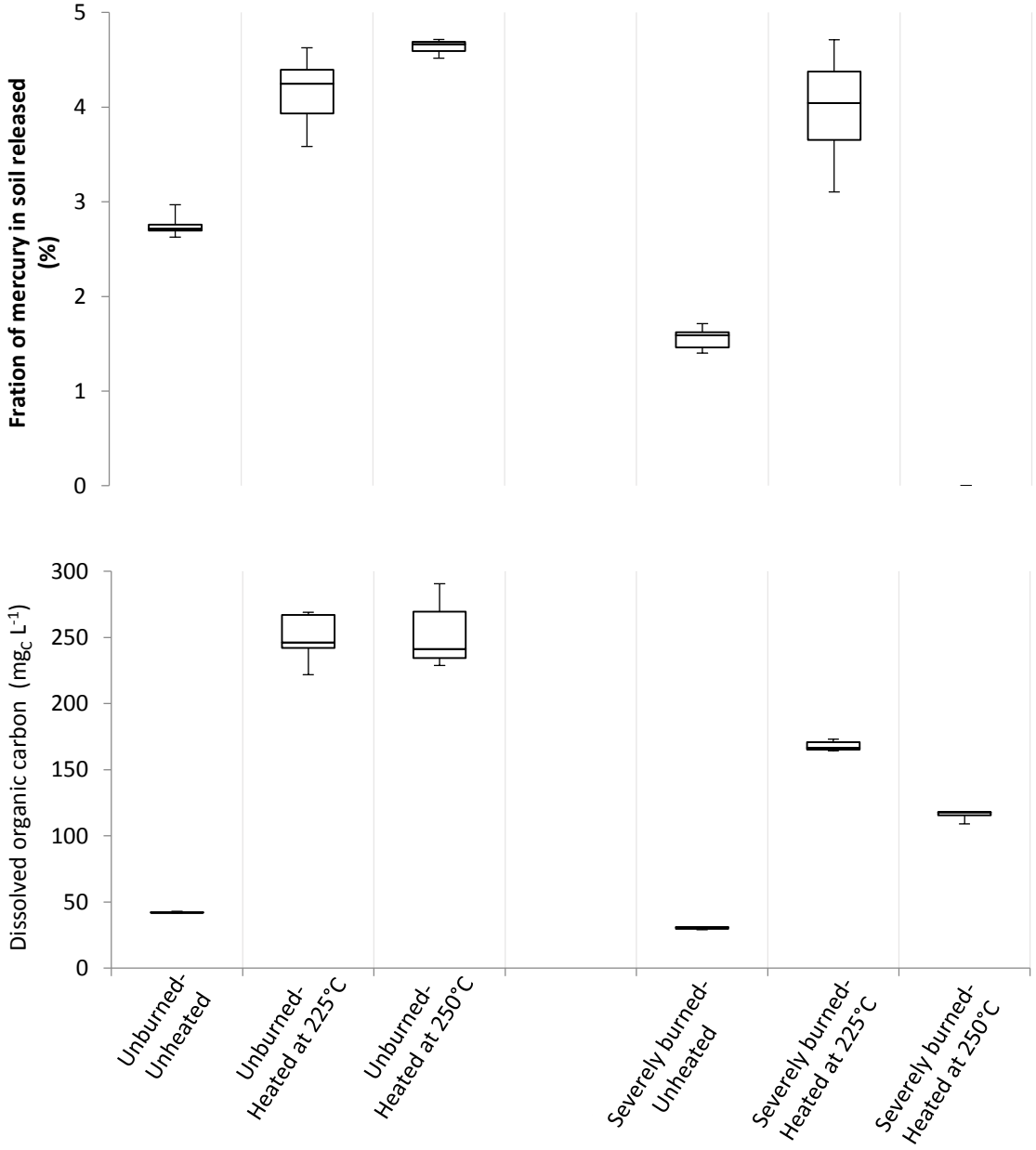

Figure 3.4: (top) Mercury released from soil expressed as a fraction of initial soil mercury and (bottom) organic matter released from soil measured as dissolved organic carbon as a function of heating.

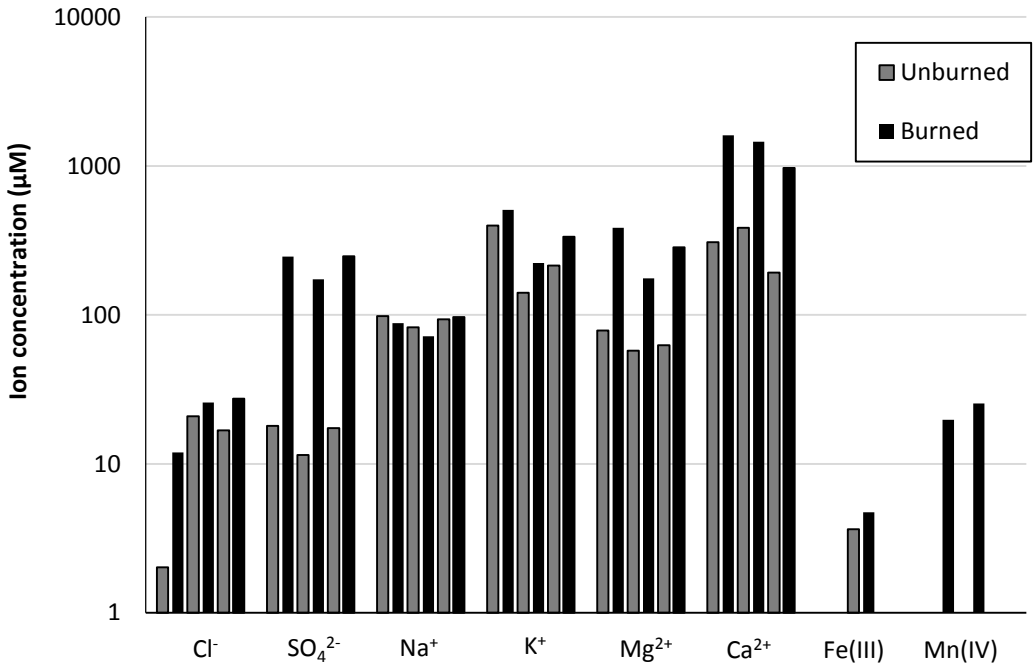

Figure 3.5: Measured ion release increased following heating of unburned soil collected from Area-B at 225°C. The greatest increase occurred for manganese (67-fold), the low initial value does not show up on a log scale.

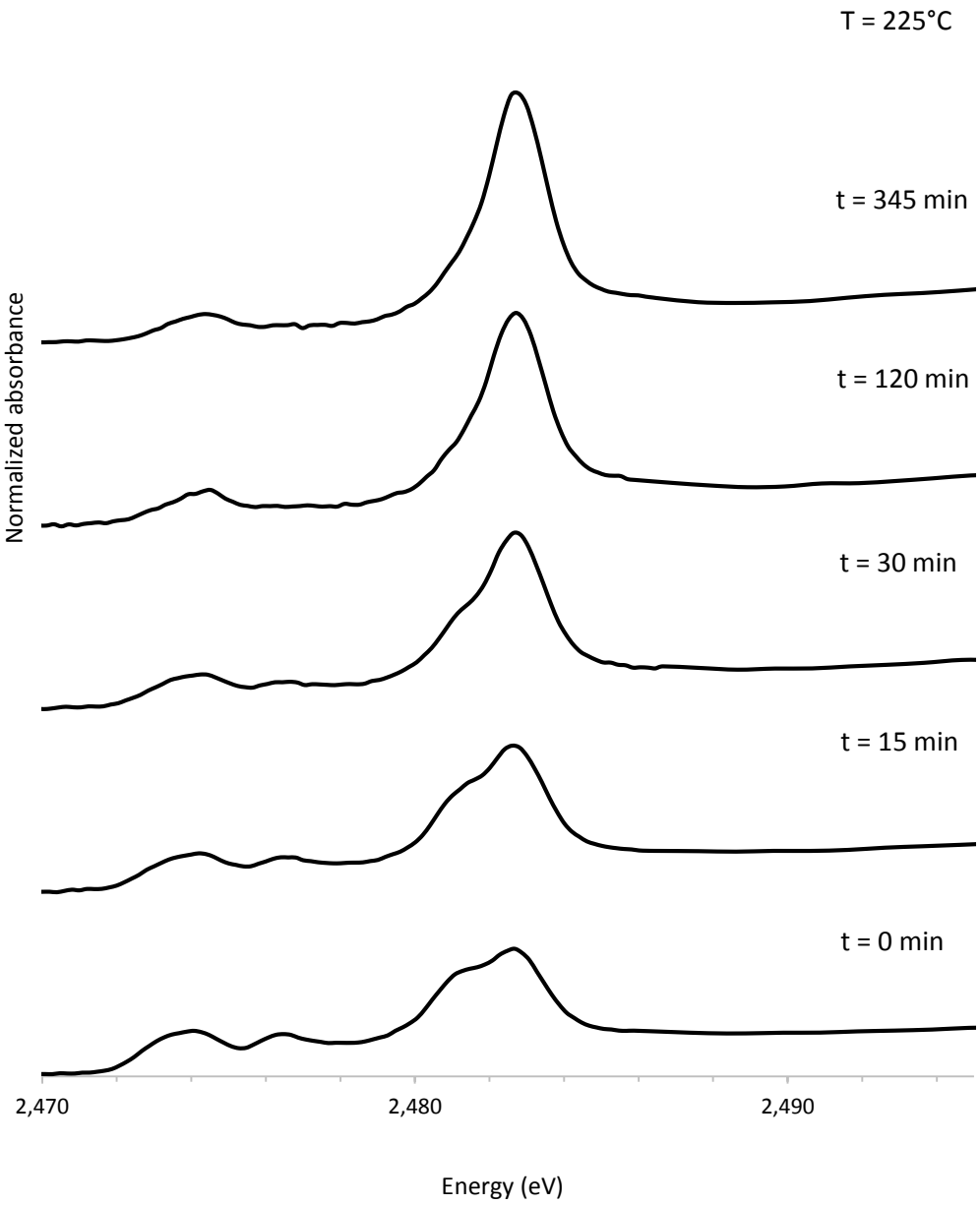

Figure 3.6: Sulfur XANES spectra in unburned soils (Area B) subjected to increasing duration of heating at 225°C reveals an increase in the oxidized sulfur peak above 2,480 eV and loss of reduced and intermediate oxidation states below 2,478 eV.

(2,473-2,475 eV) suggests the presence of sulfide- or thiol-like forms (exocyclic; 2,471.1 eV) and thiophene-like (heterocyclic) sulfur (2,474.7 eV). The extent of absorption region causes some overlap in absorption energy ranges for these species as well. A mid-range energy (2,475-2,478 eV) adsorption peak disappeared completely throughout the heating series signifying the loss of sulfoxide. Sulfoxide is an intermediately-oxidized sulfur species and has a peak between the prominent reduced and oxidized regions at 2,476.8 eV. Thinning of the high-energy peak and loss of the shoulder peak between 2,481 and 2,483 eV was a result of sulfone (2,480.4 eV; S(IV)) and sulfonate (2,481.7 eV; S(V)) loss and increases in sulfate (S(VI)). Organic sulfate esters (2,483.2 eV) and inorganic sulfate (2,483.1 eV) have overlapping absorbance ranges, making the two indistinguishable.

Soils exposed to constant heating at 225°C from 0-360 min show the greatest shifts in speciation occur at early time points (Figure 3.7). Sulfate increased throughout the duration of heating. Heterocyclic sulfur increased initially and remained elevated at 120 min. All other sulfur oxidation states decreased with heating duration. Minor changes in speciation, including slight decreases in heterocyclic sulfur and increases in sulfate, occurred between 120 and 345 min of heating.

In a second experiment, soils were heated for two hours at temperatures ranging from 150°C to 225°C (Figure 3.7). Minor changes to oxidation state occurred between 150°C and 175°C and moderate shifts in oxidation state were observed at and above 175°C (Figure 3.7). Highly-oxidized sulfur was generated when soil was heated at 225°C. A comparison of the fraction of sulfate identified by XANES spectroscopy at 225°C for 2 h was compared with sulfate concentration determined by ion chromatography in soil leachates. The mass balance revealed that 98 % of the oxidized sulfur was present as inorganic sulfate, and not retained as organic ester-bound sulfate.

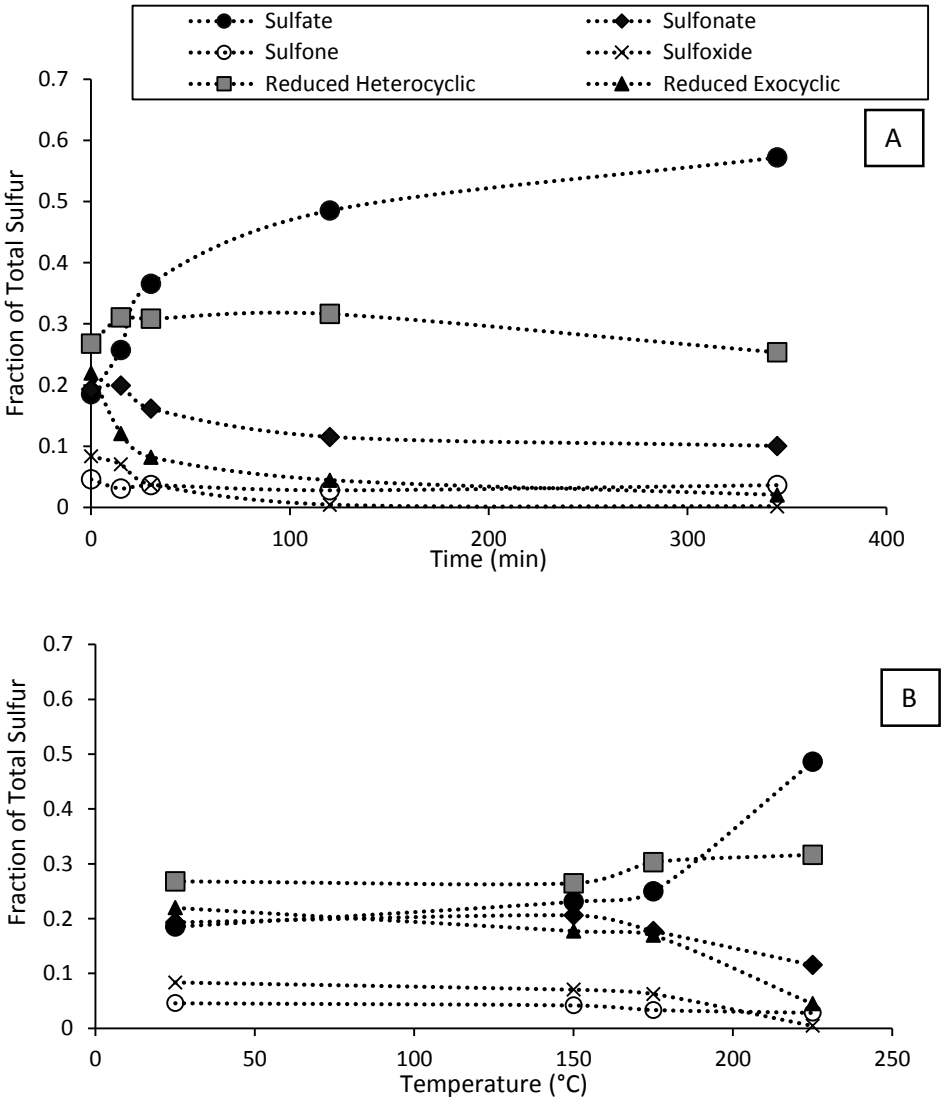

Figure 3.7: Sulfur speciation in unburned soil (Area B) as a function of (A) exposure to increasing temperature for 2 h intervals and (B) increasing duration of exposure to 225°C. The soil heated at 2 h for 225°C is shown in each series.

Competitive Ligand Exchange Experiments

To evaluate changes in the mercury binding capacity of soil following heating, unheated and heated soils were amended with mercury and equilibrated with DMSA to assess changes in phase distribution. Following soil heating at 225°C for 2 h, mercury equilibrated in the presence of DMSA tended to adsorb to soil to a greater degree than with unheated soil (Figure 3.8). In the absence of a competing ligand, 96-98 % of mercury was associated with the soil. Following addition of DMSA and a two-week equilibrium time, 30-45 % of mercury was associated with the solid phase. The fraction of mercury remaining in the solid phase following equilibrium varied positively with the soil heating treatments. Comparing two unheated soils (unburned and severely burned) following heating treatment revealed that heated soil retained 5 % more mercury on the soil in the presence of a ligand than unheated soil for unburned (p = 0.009) and severely burned (p = 0.03), respectively (SigmaPlot, version 11.1). The calculation using Eqn. 4 reveals that the shift in phase distribution following soil heating is the result of a 54 % increase in strong binding sites. Recoveries ranged between 72-107 % and had negligible mercury in blanks.

Discussion

Soil Heating Effects on Mercury and Organic Matter

Our results suggest that soil heated at low and moderate temperatures (100-250°C) are of most importance for mercury binding and transport. Soil heated beyond 250°C will lose nearly all of the initial mercury. In contrast, soils heated below 150°C are less likely to lose mercury and do not appear to undergo major changes to organic matter responsible for altering binding. In a forest soil column, surficial organic layers of soil will be consumed to some depth by fire and will lose all mercury to volatilization (Friedli *et al*., 2001).

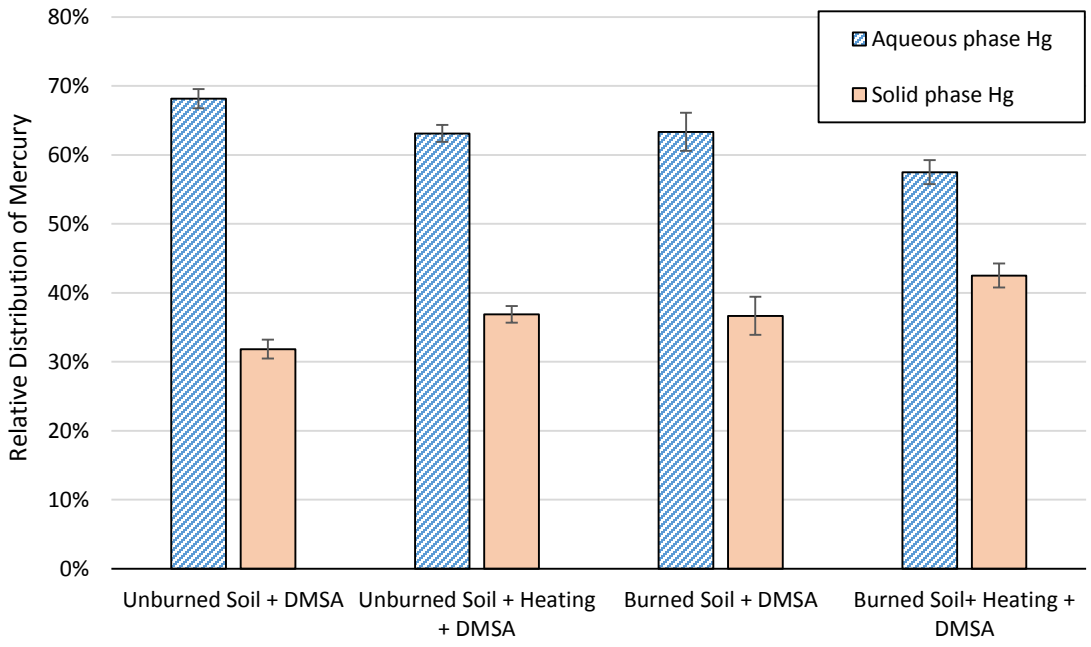

Figure 3.8: Mercury distribution following competitive ligand exchange with *meso*-2,3-dimercaptosuccinic acid (DMSA). Heated and unheated soils are confirmed to be statistically different (*t*-test, $p < 0.05$). The recovery of mercury in the vials accounted for native and added mercury mass and was 87 ± 10 % ($n = 12$).

During combustion, soil surface temperatures may be quite high (>850°C), but soil temperatures responsible for mercury loss do not extend beyond the first few centimeters (Gonzalez-Perez *et al*., 2004; Certini, 2005). Thus, the depth of soil we are concerned with in regard to mercury transport is limited to the first few centimeters.

Two stages of heating effects were observed in soil release experiments. First, the concentrations of leachable organic matter increased with increasing temperatures up to 200°C. Second, at temperatures between 200 and 250°C, there was an increase in organic matter aromaticity. Our results demonstrate significant increases in leachable organic matter at relatively low temperatures, and continued increased release as temperatures increased. Organic matter release reaches a maximum around 200°C (Figure 3.3). These observations may be explained by degradation of woody-plant macromolecules (Knicker, 2007; Knicker *et al*., 2008). For instance, hemicellulose degradation

through cleaving of glucose monomers may explain increased organic matter release at temperatures below 200°C (Knicker, 2007). We attribute the increase in fractional mercury release during batch experiment to the increased organic matter release from soil.

At temperatures above 200°C, organic matter release plateaued. The plateau in organic matter release may be caused by a combination of two processes: (1) soil organic matter vaporization due to heating, and (2) loss of oxygen moieties due to decarboxylation and dehydration near 200°C (Alemendros *et al*., 2003). A loss of oxygen moieties would lead to a less soluble organic material and would contribute to declines in soil organic matter release, occurring near 200°C. Decreases in fractional soil-mercury release are attributed to decreases in organic matter release from soils heated beyond 200°C.

Soil Heating Influence on Leachate Specific Ultra-Violet Light Absorption

Heating soils for 2 h at increasing temperatures resulted in increased specific ultra violet absorbance at 254 nm ($SUVA_{254}$; Figure 3.3). Correlation between aromaticity and $SUVA_{254}$ is due to sp^2-hybridized carbon bonds in aromatic moieties that have substantial UV absorption (Weishar *et al.*, 2003). Less UV_{254} absorbance in leachate from soils following low temperature heating is likely a result of cleaving of simple aliphatic molecules from larger parent compounds, such as cellulose and lignin (McGrath *et al.*, 2003, Knicker, 2007; Olefeldt *et al*., 2013). The progression of soil organic matter from aliphatic molecules and toward molecules that increasingly resemble polycyclic aromatic hydrocarbon has been demonstrated previously in soils using nuclear magnetic resonance techniques (Knicker, 2007; Knicker *et al*., 2008). The progression toward increasingly condensed structures would support $SUVA_{254}$ values of 5.4 L mg^{-1} m^{-1} (Figure 3.3). Notably, $SUVA_{254}$ values above 5 L mg^{-1} m^{-1} are considered high for typical surface waters (Spencer *et al*., 2012). Iron can cause an interference with UV absorption generally causing $SUVA_{254}$values greater than 5 L mg^{-1} m^{-1} (Poulin *et al*., 2013). We measured iron in leachates and confirmed there was no interference. We attribute the high $SUVA_{254}$to soil leachates containing increasingly aromatic molecules generated by soil heating.

Sulfur Transformations during Soil Heating

Sulfur-XANES spectroscopy analyses reveal that heating greatly increases sulfate in soil. This finding is consistent with our hypothesis that heating shifts sulfur speciation from lower to higher oxidation states. The shift in sulfur speciation to sulfate during heating aligns with previously reported observations of increases in sulfate release following wildfire (Smith *et al*., 2011) and could be one source of elevated sulfate exported from recently burned watersheds. The shift to sulfate is at the expense of all sulfur species excluding heterocyclic reduced sulfur, which was slightly increased in relative abundance. The slight increase in heterocyclic species is likely due to thermal alteration of sulfur-containing amino acids into aromatic or cyclic molecules, which occurs between 100 and 190°C (Cerny and Davideck, 2003; Wang *et al*., 2012). Losses of sulfur measured after heating at 225°C for 2 h is likely due to generation of volatile sulfur compounds. For instance, beyond 190°C cysteine and methionine are thermally degraded into gaseous products of mainly H_2S, CH_3SH, and CO_2 (Yablokov *et al.*, 2009). Additionally, the presence of H_2S may increase heterocyclic sulfur because H_2S reacts at unsaturated bonds (Mottram, 1998). Such a reaction would be favored in heated organic matter because the aromaticity of the organic matter would also increase the number of unsaturated sites for sulfide incorporation.

Mercury Association with Heated Soil

Sulfur oxidation and the increase in releasable sulfate did not decrease binding capacity. Instead, heated soils retained more mercury in the presence of a ligand than unheated soils. These results did not support our hypothesis that oxidation of sulfur would decrease soil binding capacity. This calculation accounts for differences in initial mercury in soils based on losses due to heating, and should account for newly available binding sites due to the vaporization of native mercury. The tendency for increased association with the soil following heating has been suggested by others (Burke *et al*., 2010).

However, previous explanations for increased binding were attributed to carboxyl functionality or other weak binding sites. The measurements made in the current CLE experiments are in the presence of excess strong-binding ligands that easily outcompete the adsorption of mercury by oxygen- and nitrogen-containing functional groups at equilibrium. Thus, the observed increase in binding should be attributed to strong binding (reduced sulfur) moieties. The increase in heterocyclic absorbance region points toward the addition of sulfur to aromatic functional groups. Addition of sulfur across the unsaturated aromatic bond produces terminal thiol-functional groups, which could lead to mercury binding (Figure 3.9; Mottram, 1998; Perlinger *et al*. 2002). Thus, our measurement of increased binding capacity within organic matter following heating is best explained by the addition of thiol-functional groups added across unsaturated aromatic groups during heating. Sulfur bound to an aromatic ring would likely have an absorption energy between those of thiophene and a terminal aliphatic thiol, and could be partially responsible for some of our modeled heterocyclic sulfur.

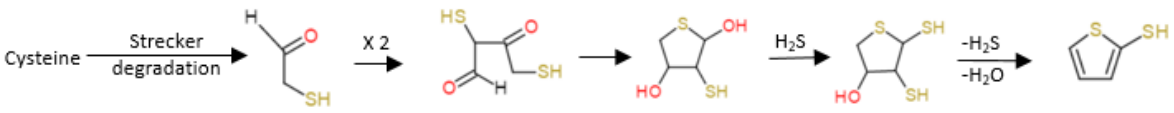

Figure 3.9: A mechanism for the formation of 2-thiophenethiol through a Maillard's reaction of cysteine. Figure adapted from Mottram (1998).

Summary

Following soil heating, a larger fraction of soil organic matter is released from soil and measurement of $SUVA_{254}$ revealed the formation of increasingly aromatic molecules throughout heating. The range of temperatures studied have two stages of heating effects observable in organic matter leachates. The first being a thermal production of soluble molecules, likely derived from larger polymers, and the second is an onset of apparent condensation reactions.

Shifts in sulfur speciation to higher oxidation states, mainly sulfate, are consistent with our hypothesis that wildfire oxidizes reduced organic sulfur. Comparison of predicted sulfate generation from the XANES spectra and the aqueous measurements indicate highly oxidized sulfur become soluble sulfate rather than ester-bound sulfate. The formation of sulfate was at the expense of nearly all of the other sulfur species, excluding those in the heterocyclic absorption region.

There was an increase in fractional release of mercury in batch experiments, however, we also measured an increase in mercury association with heated soils using competitive ligand exchange. The seemingly contradictory results are explained by the 6-fold increase in organic matter released from heated soils. This release of organic matter to solution likely increased the amount of dissolved organic matter complexing mercury in the aqueous phase. Measurement of the change in soil binding capacity using a competing ligand revealed increased mercury binding by heated soils consistent with a 54 % increase in strong binding capacity.

Chapter 4

Characterization of mercury, sulfur, and organic matter in ash-laden stream bank and reservoir sediments

Jackson P. Webster *[a], Jeffrey H. Writer [b], Katherin L. Nagy [c], David Vine[d], Alain Manceau [e]
George R. Aiken [f], Joseph N. Ryan [a]

[a] Department of Civil, Environmental, and Architectural Engineering, University of Colorado, Boulder

[c] Department of Earth and Environmental Sciences University of Illinois at Chicago

[d] Argonne National Laboratory

[e] ISTerre, CNRS Universite de Grenoble, Grenoble, France

[f] US Geological Survey, Boulder, Colorado

To be submitted to *Environmental Science & Technology*

Abstract

Deposition and accumulation of atmospheric mercury has led to the enrichment of this toxic metal in soils around the planet. Of particular concern is the organic form methylmercury, which is a potent neurotoxin that readily bioaccumulates. Wildfire runoff has been demonstrated to increase methylation in reservoir sediments and enhance trophic transfer of methylmercury. To investigate the geochemical processes leading to enhanced methylation, ash-laden sediments and native (underlying) reservoir sediments were collected from a watershed-reservoir system burned in the Hewlett Gulch Fire, 2012, near Fort Collins, Colorado, USA. The sediments were characterized for organic matter content, total mercury, methylmercury, and major elements. A single depth interval (2-3 cm), representing the deposited ash-laden sediments, was analyzed for total sulfur and sulfur oxidation state in summer, fall, and spring following the fire. The ash-laden sediment was found to contain 32 % organic matter and 68 % mineral material. The organic material was charred forest plant material and the mineral material was assumed to be derived from minerals present in the parent rocks of the watershed. The ash-laden sediment contained 51 ng g^{-1} total mercury. Methylmercury in recently deposited ash-laden sediments was 10 times higher (4.5 ng g^{-1}) than native sediments (0.4-0.6 ng g^{-1}) of the reservoir. Sulfur-XANES analyses revealed a major shift in the ash-laden sediments reduced inorganic sulfur before (2 %) and after deposition (35 %) into the reservoir. Each successive measurement revealed an increase in reduced organic sulfur in the deposited sediment on the reservoir bottom. Overall, the results of this study increase our understanding of how wildfire mobilizes mercury into surface waters. Furthermore, this study provides insight on underlying geochemical processes in ash-laden sediments that influence contaminant fate and transport in recently burned watersheds.

Introduction

Mercury is a globally-dispersed contaminant that poses ecological and human health risks (Poulin *et al*., 2008; Driscoll *et al.*, 2013). Of particular concern is methylmercury, due to its potent neurotoxicity and ability to bioaccumulate (Poulin *et al*., 2008; Selin, 2009; Driscoll *et al.*, 2013). Methylmercury is formed when mercury is transported into anoxic, primarily sulfate-reducing, environments, which enhances biotic conversion of mercury into this toxic form (Selin, 2009). In forested watersheds, mercury deposited from the atmosphere onto leaves, needles, and other forest materials is transferred into the soil, where strong association with soil organic matter causes retention and accumulation (Obrist *et al*., 2011). During wildfire, soil can release mercury into the atmosphere through heating and combustion (Friedli, 2001; Engle *et al*., 2006; Biswas *et al*., 2007); however, not all of the mercury is re-emitted into the atmosphere. Some of the mercury remains in the soil and can be mobilized into nearby surface waters by erosion (Caldwell *et al*., 2000; Kelly *et al*., 2006). The mobilization of mercury from recently-burned watersheds has been shown to be enhanced relative to unburned watersheds (Caldwell *et al*., 2000; Kelly *et al*., 2006). Increases in downstream methylmercury production and bioaccumulation have been observed following wildfire; however, there is relatively little information on the fate and transport of mercury in surface waters following wildfires (Caldwell *et al*., 2000; Krabbenhoft and Fink, 2001; Kelly *et al*., 2006).

Mercury transported from recently-burned watersheds is likely associated with soil components remaining on the forest floor after burning. Fire leaves behind ash and charred organic material. Ash is a combination of mineral and incompletely combusted organic material (Bodi *et al*., 2014). The charred organic material consists of the remnants of needles, leaves, and other plant components. Fully combusted materials lose all of their associated mercury to the atmosphere (Friedli, 2001). Soils below the combusted fuel layer release mercury to the atmosphere as a function of heat transfer (Engle *et al*. 2006; Biswas *et al*., 2007).

Wildfire increases the surface flow of water and sediment transport from watersheds (Moody and Martin, 2001; Ebel *et al*., 2012). The increase in flow is attributed to the loss of intercepting foliage and the development of a hydrophobic layer in the soil (DeBano, 2000; Moody and Martin, 2001; Ice *et al*., 2004; Smith *et al*., 2011). This combination leads to mobilization of ash-laden sediments (Neary *et al*., 2005). Increased surface flow allows relatively light precipitation to cause disproportionately heavy flooding (DeBano, 2000; Moody and Martin, 2001; Ice *et al*., 2004; Smith *et al*., 2011; Murphy *et al*., 2012; Ebel *et al*., 2012; Bodi *et al*., 2014). Erosional events result in the transport of ash-laden sediment in streams and deposition in lakes and reservoirs (Neary *et al*., 2005; Smith *et al*., 2011). There is no reported information regarding the early diagenesis of ash-laden sediments in lakes and reservoirs in regard to effects on the fate of associated mercury.

Mercury's fate and transport are greatly influenced by sulfur speciation in terrestrial and aquatic environments. Soft metals like mercury have a strong affinity for reduced sulfur ligands (Pearson, 1963). With regard to mercury binding to organic ligands, mercury is bound to reduced organic sulfur, primarily thiol moieties (Xia *et al*., 1999; Skyllberg *et al*., 2006). Reduced organic sulfur can range from 30 % to 80 % of the total organic sulfur in soils and sediment organic matter (Prietzel *et al*., 2007; Schroth *et al*., 2007; Prietzel *et al*., 2009) and the fraction of reduced sulfur available for mercury binding is approximately 3 % of the reduced sulfur (Haitzer *et al*., 2002). This strong ligand interaction may also be influenced by the ratio of mercury to sulfur, as increasing sulfur content likely leads to increased sulfur coordination (Nagy *et al*., 2011).

Under reducing conditions, ash-laden sediment may chemically change in a manner that influences mercury behavior in the sediments. Wildfire increases nitrogen and phosphorus export from watersheds, leading to downstream eutrophication (Neary *et al*. 2005; Smith *et al*., 2011). Under anoxic conditions that often develop in lakes and reservoirs receiving ash-laden sediment, sulfate can be microbially reduced to sulfide. Due to its strong nucleophilic tendency, sulfide produced in sediments

and anoxic waters can be incorporated into sediment organic matter to form reduced organic sulfur moieties, such as thiols and organic sulfides (Urban *et al*., 1999; van Dongen *et al*., 2003; Werne *et al.*, 2004; Heitmann and Blodau, 2006; Werne *et al*., 2008, Einsiedl *et al*., 2008). Sulfides can also form inorganic mineral phases. The formation of iron-sulfides, for instance, may impede sulfur incorporation by organic matter (Werne *et al*. 2004). Sulfide also reacts directly with iron(III), which oxidizes sulfide to elemental sulfur and polysulfides (Werne *et al*., 2004; Slowey and Brown, 2007). Polysulfides may also react with organic matter resulting in the incorporation of reduced sulfur groups into the organic matter (Vairavamurthy *et al*., 1997; Werne *et al*., 2004). Multiple sulfur atoms in close proximity can create bidentate reduced sulfur sites conducive to strong mercury binding (Xia *et al*., 1999; Skyllberg *et al*., 2006; Nagy *et al*., 2011). Furthermore, sulfide can react directly with mercury to form metacinnabar (β-HgS). The formation of colloidal metacinnabar has been shown to enhance methylation (Graham *et al*., 2012; Zhang *et al.*, 2012).

The transport of ash-laden sediments represents a great perturbation in burned watersheds; however, characterization of the deposited sediments is limited and the effects of early digenetic processes on the fate of mercury associated with these sediments is unknown. We hypothesized that (1) sediments transported from a recently-burned watershed would undergo sulfur incorporation into sediment organic matter following deposition into a sulfate-reducing environment. The formation of reduced organic sulfur functional groups in ash-laden sediments could enhance mercury binding, which could inhibit the formation of methylmercury or limit the mobilization of mercury from the recently deposited sediments. To test this hypotheses, we collected ash-laden sediment and underlying native sediment from the bottom of a reservoir. We also collected ash-laden sediment from the banks of a river draining the watershed, which was the origin of the sediments. We then measured sulfur speciation using sulfur X-ray absorbance near edge structure (XANES) spectroscopy, as well as mercury and methylmercury content.

Methods

Site Description

Sampling was conducted in Colorado's Front Range west of the city of Fort Collins, Colorado, USA (Figure 4.1). The samples were collected in an unnamed drainage that empties into Seaman Reservoir (starred on Figure 4.1). The watershed elevation ranges from 1600 m at the Reservoir to 2300 m. The terrain was mountainous with steep drainages forested with mixed pine and fir species that burned severely in 2012. The Hewlett Gulch Fire began on May 14, 2012, and burned 3100 ha before containment on May 22, 2012. A second fire, the High Park Fire, ignited June 9, 2012, and was declared out on July 2, 2012. The High Park Fire burned 35,000 ha including the area adjacent to the boundaries of the Hewlett Gulch Fire. The High Park Fire was primarily extinguished by a monsoonal rain event on June 28 that resulted in 35 mm of rain being recorded at the Hewlett Gulch rain gauge, which is located 9 km west of the Seaman Reservoir (Chris Lochra, City of Fort Collin's rain gauge network, personal communication).

The storm event caused major flooding and ash-laden soils were mobilized in the recently-burned drainage adjacent to Seaman Reservoir. This drainage enters the reservoir near the Poudre River inlet (starred on Figure 4.1). Following the June 28 rain event, we observed that ash, soil, and charred material had been transported into the reservoir from this drainage. At the mouth of the burned drainage, a depositional zone of ash-laden sediment was present (Figure 4.2). The unnamed drainage was determined to be the primary source of ash-laden sediment to the reservoir. The North Fork of the Cache la Poudre, upstream of Seaman Reservoir, appeared minimally affected by the fire.

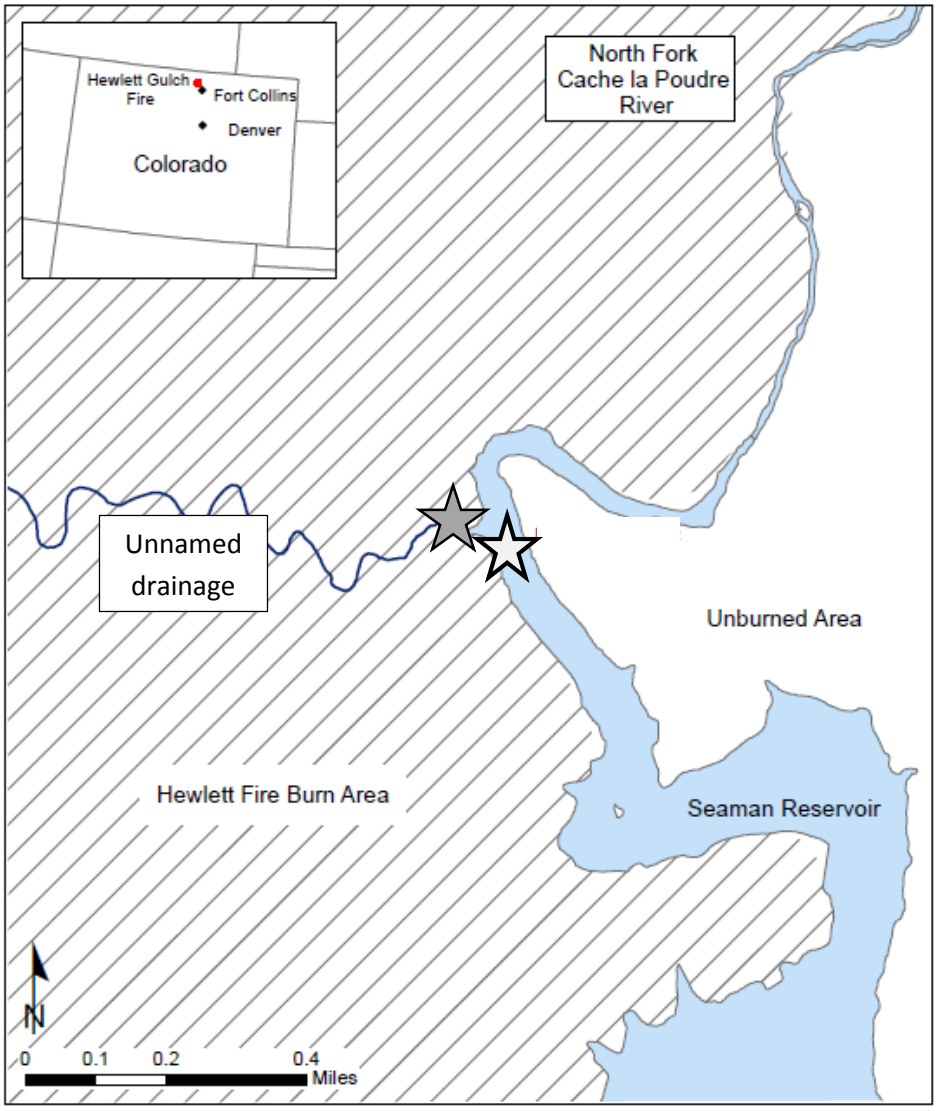

Figure 4.1: The Hewlett Gulch study area was at the mouth of an ephemeral drainage which flowed from the west to the east out of the Hewlett Fire burn area into Seaman Reservoir. Bank and reservoir sampling locations are starred of the map.

Water quality issues existed at Seaman Reservoir prior to the June 2012 ash-laden sediment deposition and are outlined in detail by Oropeza and Heath (2013). In short, there was low flow into the reservoir due to ongoing drought at the time of the fire. The low flow resulted in higher temperatures, higher levels of algal activity, and contributed to long periods of low dissolved oxygen in the reservoir, both in the time period immediately following the fire as well as the preceding four summers. Dissolved oxygen was completely consumed at the bottom and middle depths of the reservoir between late June and early September 2012.

Figure 4.2: Inlet of the study drainage at Seaman Reservoir looking west. Mobilized watershed debris are visible in the foreground in November 2012. This area is the filled grey star on the site map.

Sampling Procedures

A matrix of all samples collected and all analyses performed is presented in Table 4.1. Sediment samples were collected from Seaman Reservoir on August 12, 2012, November 1, 2012, and May 2, 2013, down the reservoir gradient from the unnamed drainage entrance to the reservoir (Location marked with open star on Figure 4.1). We employed a near-surface sediment-coring device (Universal Corer, Rickly Hydrological, Columbus, OH) to collect cores. Cores collected ranged from 15 -25 cm deep. During each sampling trip, at least two cores were collected from the same area of the reservoir. The exact locations varied depending on the ability to drive-in the core barrel and retrieve a quality core. The core barrels were capped on the bottom prior to removal from the water to avoid sediment exposure to air. Core barrels were cut above the sediment-water interface, capped, and sealed using electrical tape to

minimize atmospheric exposure. Cores were placed vertically in a cooler for transport back to the U.S. Geological Survey laboratory (Boulder, CO), where they were immediately frozen for future use.

Samples of ash-laden sediment transported from the watershed were collected on July 10 and November 1, 2012, from the unnamed drainage prior to entering Seaman Reservoir (Figure 4.1). The deposited sediment was collected from the banks of the drainage as a single bulk sample using a stainless steel scoop and placed in large re-sealable plastic bags for transport to the laboratory.

Table 4.1: Sampling and analyses matrix of this study at Seaman Reservoir following the Hewlett Gulch Fire. Analyses in bold were included in this paper unless noted in right-most column. Samples were collected from inlet mouth (Grey filled star, Reservoir bottom (open star), and watershed (not shown on map). Analysis of soil and sediment depth increments (inc.'s) included total mercury (Hg), methylmercury (CH_3Hg^+), organic matter, total sulfur, sulfur oxidation by X-ray absorption near edge structure (XANES) spectroscopy, major and trace elemental analyses by ion coupled plasma atomic emission spectroscopy (ICP-AES), and Ion coupled plasma mass spectrometry (ICP-MS).

Sample	Date	#	Processing	Hg	CH_3Hg^+	Organic matter	Sulfur	XANES	ICP-AES	ICP-MS	Samples Included
Bank sediment	Aug '12	1	Freeze dried, sieved, ground	**Yes**	No	**Yes**	No		**Yes**	**Yes**	No
Bank sediment	Nov '12	1	Air dried, sieved	**Yes**	**No**	**Yes**	**Yes**	**Not inc**	**Yes**	**Yes**	**Yes**
Reservoir core	Aug '12	4	Core # 1: Frozen, sectioned onto 1 cm increments, splits were freeze dried	**All inc.'s**	**2-3 cm, 10-11 cm**	**All inc.'s**	**2-3 cm**	**2-3 cm**	**0-4, 5, 8 cm**	0-4, 5, 8 cm	**Yes**
			Core #2: Frozen, sectioned in to 1 cm increments, freeze dried	**All inc.'s**	No	No	No	No	No	No	**Yes**
			Cores 3 and 4: Frozen	**No**	No	No	No	No	No	No	No
Reservoir core	Nov '12	3	Core 1: Frozen, sectioned onto 1 cm increments, splits were freeze dried	**All inc.'s**	**2-3 cm 19-20 cm**	**All inc.'s**	**2-3 cm**	**2-3 cm**	**0-4, 5, 8 cm**	0-4, 5, 8 cm	**Yes**
			Core 2: Frozen, sectioned onto 1 cm increments, splits were freeze dried	**All inc.'s**	No	No	No	No	No	No	**Yes**
			Core 3: Frozen	**No**	No	No	No	No	No	No	No
Reservoir core	May '13	3	Core1: Frozen, sectioned onto 1 cm increments, splits were freeze dried	**All inc.'s**	No	No	**2-3 cm**	**2-3 cm**	**0-4, 5, 8 cm**	0-4, 5, 8 cm	**Yes**
			Core 2: Same	**All inc.'s**	No	No	No	No	No	No	**Yes**
			Core : Frozen	**No**	No	No	No	No	No	No	No
Watershed soil-burned	Aug '12	3	frozen, sectioned into 1 cm, increments (10), composite sample made from triplicate cores, freeze dry	**All**	No	**Yes**	No	No	No	No	No
				All	No	**Yes**	No	No	No	No	No
Watershed soil unburned	Dec '12	1	Unburned reference: Same	**All**	No	**Yes**	No	No	No	No	No
				All	No	**Yes**	No	No	Yes	Yes	No

In the laboratory, frozen sediment cores were thawed, carefully extruded, and cut into 1 cm increments in a glove box with an argon atmosphere. The dried samples were placed in I-Chem™ jars (40 mL) with polytetraflouroethene (PTFE) lined caps sealed with electrical tape prior to removing the sample from the glove box. These I-Chem™ jars were tested and certified to contain negligible leachable mercury as shipped from the distributor (Fisher Scientific, USA). Split samples for analyses that were not redox sensitive were placed in I-Chem™ vials (40 mL) without tape.

The sediments were air-dried in a positive-pressure flow hood using high efficiency particulate arrestance (HEPA) filtered air and transferred into glass 1L I-Chem™ jars with PTFE-lined lids (Fisher Scientific, USA). The glass was cleaned (10 % HCL and 10% HNO_3 for 24 h) and rinsed three times with ultrapure water (18.2 MΩ cm, Millipore, Milli-Q®).

Analytical Procedures

The ash-laden sediments collected on the banks and reservoir bottom were characterized for organic matter content, total mercury, methylmercury, major elements, and trace elements (Table 4.1). We chose one core from each sampling time-point to analyze in detail. The second core, from the same vicinity, was sectioned and analyzed for total mercury only. The 2-3 cm depth in the reservoir cores containing the deposited ash-laden sediments were analyzed for total sulfur and sulfur oxidation state.

The organic matter content of each 1 cm increment was determined gravimetrically by loss on ignition (LOI) for 2 h at 550 °C. Approximately 1 g of a dried sample was weighed in ceramic boats, heated for 2 h, cooled in a desiccator, and re-weighed to determine mass loss.

Total mercury was measured using thermal decomposition / catalytic reduction / atomic absorption spectroscopy (DMA-80, Milestone, Shelton CT, USA). Approximately 0.1 g of dried sample was transferred to a pre-weighed sample boat using a stainless steel scoop. Total mercury measurements were calibrated using standards certified by the National Institute of Standards and

Technology (NIST) and the National Research Council of Canada (NRCC). Target concentrations of reference standards were confirmed to be within 5 % for each analytical run. Wet sediments were sent the U.S. Geological Survey Mercury Research Laboratory (Madison, Wisconsin) for methylmercury determination following protocols of DeWild *et al*. (2004).

Dried sediments were sent the Laboratory for Environmental and Geological Studies at the University of Colorado Boulder. Major elements were measured using inductively-coupled plasma atomic emission spectroscopy (ICP-AES). All sample runs were accompanied by external source certified QC samples, matrix blanks, digestion blanks, duplicates, matrix spikes, and sample spikes in accordance with good laboratory practice guidelines.

Total sulfur concentration in the soil samples was measured at Huffman Laboratories (Golden, Colorado) using perchlorate acid digestion and ICP-OES, following the methods of Huffman and Stuber (1985) for which the stated limit of detection was 0.01 % by sample weight.

The oxidation state of sulfur in samples of ash-laden sediment was determined by sulfur X-ray absorbance near-edge structure (XANES) spectroscopy. Samples were prepared for XANES analysis by drying sediment under an argon atmosphere in a glove box. Dried samples were powdered using a mortar and pestle and then placed in I-Chem™ jars (40 mL). The lids of the jars were sealed with electrical tape prior to removing them from the glove box. Just before analysis, samples were removed from the jars and mixed with methanol to allow transfer to the sample holder using a micro-pipet.

Sulfur XANES spectroscopy was conducted over two beamline sessions at the Advanced Photon Source at Argonne National Labs, (Chicago, IL) on beamline 2-ID-B. X-ray absorption was measured by fluorescence detection. A M1 spherical grating monochromator was used to focus X-rays into the sample chamber and fluorescence signals were recorded with a nine-element differential phase contrast detector. Energy was calibrated by setting the $CaSO_4$ peak to 2482.75 eV and scans were obtained between 2420 and 2625 eV. A step size of 0.2 eV was used throughout the energy range scanned. For

all scans, the aperture dimensions were set to 30 µm and 10 µm for the outer and inner beam slits, respectively. Sulfur XANES analyses were carried out on the ash-laden sediments, which had been deposited in the reservoir. The sediments used in the analyses were from the 2-3 cm increment (below the sediment water interface) of the reservoir cores to avoid interferences from algal deposition at the interface. Nordic aquatic humic acid and Elliot soil humic acid, obtained from the International Humic Substance Society, were analyzed for quality assurance by comparing our results with previously obtained speciation modeling sulfur XANES spectra. Interpretation was conducted using linear-least squares fitting to determine the ratio of sulfur oxidation state in the ash-laden sediments. Data was analyzed following the approach developed by Manceau and Nagy (2012).

Results

Reservoir Sediment Characterization

The sediment cores collected from Seaman Reservoir were of varying length due to density of the native sediments. All cores contained stratified materials of different thicknesses throughout the depth collected. The major layers of importance for this study were: (1) a dark grey layer of ash-laden sediment (upper) and (2) a light grey sediment (lower) below the ash-laden sediments (Figure 4.3). The light grey layer was assumed to represent the material present at the sediment water interface prior to the deposition of ash-laden sediment. In one core (November 2012), there was a distinct layer of gravel separating the deposited ash-laden sediments from reservoir sediment (Figure 4.3).

Organic matter content in the ash-laden sediment was variable with depth (Figure 4.3). Organic matter content was depleted in the in the first 2 cm of each core measured (August and November). It was unclear if the depletion was a result of disturbance of the sediment water interface during core collection, or present naturally.

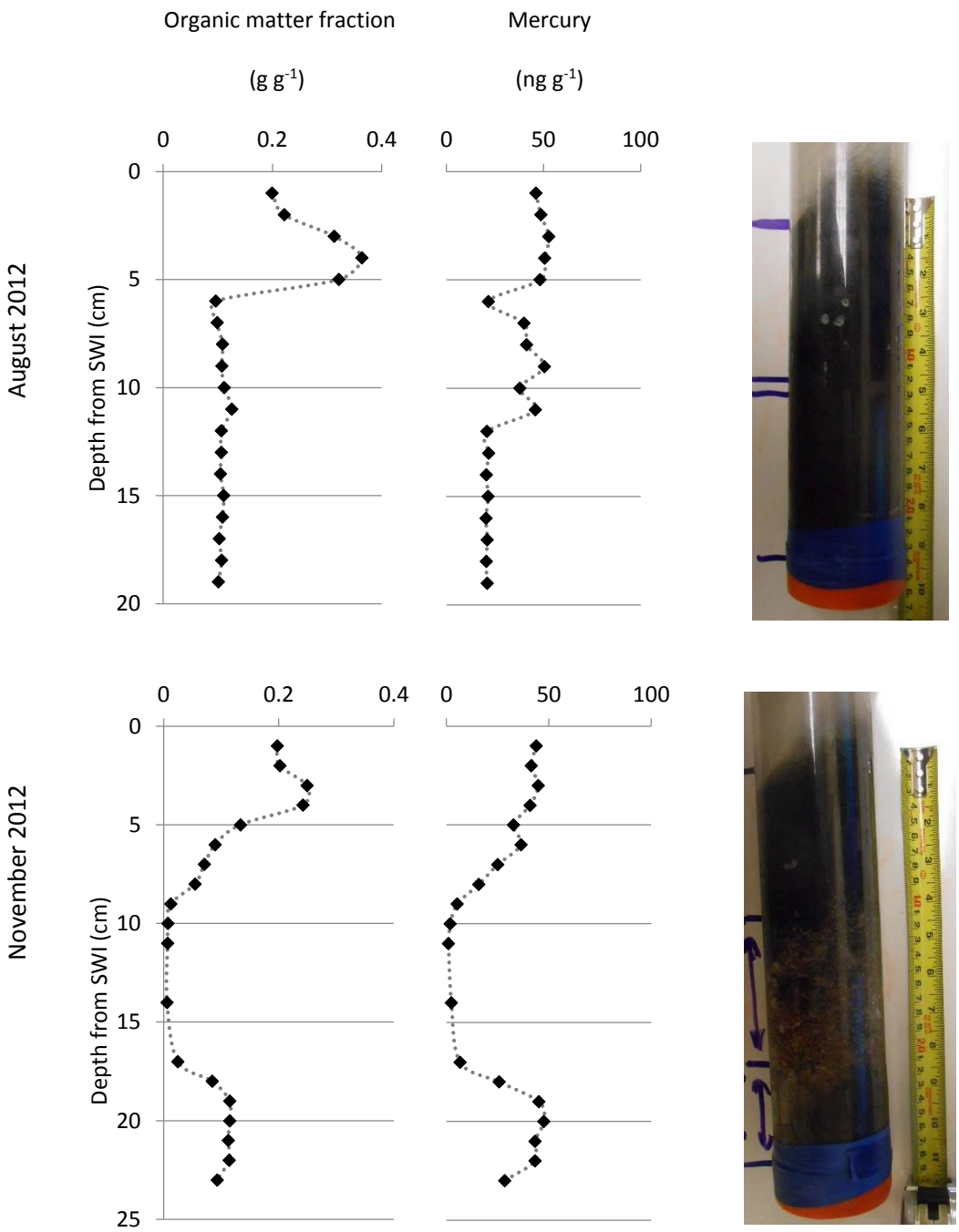

Figure 4.3: Organic matter and mercury profiles in reservoir cores collected in August and November 2012. Organic matter content was the best indicator of the deposited ash-laden sediments in the reservoir. In the November core, a gravel layer separated the ash-laden sediment and the native reservoir sediment.

In the August 2012 core, deposited ash-laden sediment contained an average of 33 ± 3 % organic matter in the 3-5 cm depth. In the November 2012 core, organic matter content was 25 % in the 2-3 cm and 3-4 cm increments and below 4 cm the ash-laden material was mixed with gravel. Organic-matter in the native sediments of the reservoir contained 11 ± 0.1 % (n=31) organic matter in both the August and November cores.

The concentration of total mercury in the native sediment varied depending on material that was present at specific depths and was markedly different for each reservoir core we collected. For instance, the presence of gravel in a November 2012 core caused total mercury to be undetectable between 10 and 15 cm depth (Figure 4.3). In general, the native sediment contained the same concentration of total mercury as the ash-laden sediment, where the average and standard deviations were 43 ± 5 ng g^{-1} (*n* = 4) and 45 ± 2 ng g^{-1} (*n* = 4) for August and November cores, respectively.

The ash-laden sediments deposited in the reservoir contain an average of 47 ± 5.2 ng g^{-1} total mercury in the 0-5 cm depth for all time points collected (Figure 4.4). There were no differences in concentration with depth that were consistent at each seasonal coring and there was not a trend in concentration in the ash-laden material with time.

Methylmercury concentrations were compared between the ash-laden reservoir sediment and the native reservoir sediment in the August 2012 and November 2012 cores (Table 4.2). Methylmercury in the ash-laden sediments, measured at 2-3 cm, was 4.5 ng g^{-1}, in both the August and November Core sediments. These were 12.2- and 7.5 -fold higher, respectively, compared to the native reservoir sediments collected at the same time (10-11 and 19-20 cm intervals, respectively). The ratio of methylmercury to total mercury (CH_3Hg^+:Hg_{tot}) was 0.08 in the August core and 0.1 in the November core.

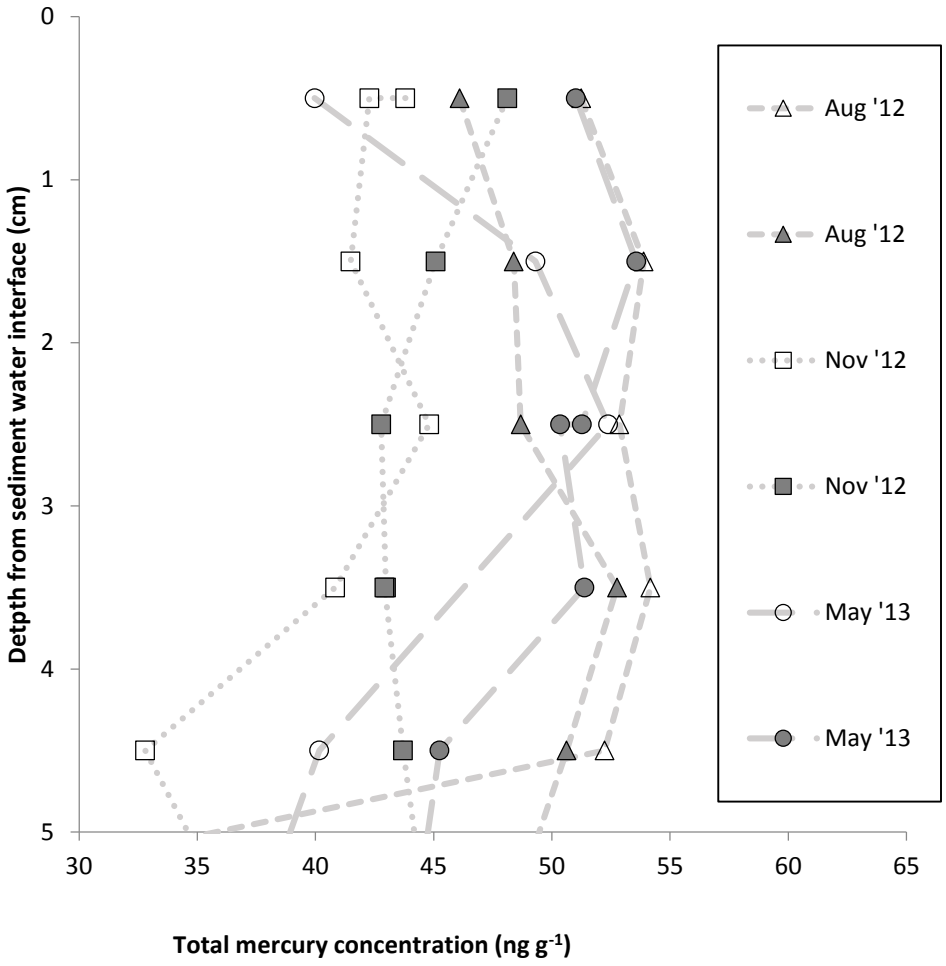

Figure 4.4: Mercury profiles of deposited ash laden sediments in cores collected in August 2012, November 2012, and May 2013.

Total sulfur was measured in samples being run for XANES analysis (Table 4.2). The ash-laden sediment contained sulfur concentrations that were not significantly different from the samples collected in the watershed or samples collected from the reservoir. The number of samples was small; therefore, we cannot attribute the differences reported to gains or losses in the material or sediment heterogeneity because we do not have an estimate of error in the measurement.

Elemental analyses were conducted on the first four 1-cm increments of ash-laden sediments from the reservoir cores and the concentrations were averaged to obtain a bulk value for each time point (Table 4.3). The analyses reveal that the material was primarily composed of silicon, aluminum, and iron. We did not conduct a mineralogical analysis, but the elemental composition was consistent with the visual observation of abundant mica (an aluminum silicate mineral often containing iron) in the ash-laden sediment and throughout the watershed. There were no increases or decreases in iron or manganese observed in the samples between sampling points.

Sulfur Characterization of Ash-Laden Sediment

Sulfur XANES analyses were conducted on ash-laden sediments collected from the unnamed drainage in November and from the reservoir bottom collected in August, November, and May (Figure 4.5). Due to the difficulty in obtaining sulfur XANES spectra, we have few data on the sediments, which limits our ability to delineate error or heterogeneity in the sulfur oxidation state. While there appears to be general trends among oxidations states, there was inherent uncertainty in the in the species distribution. For instance, sulfate appears to be a relatively small fraction of the total sulfur (6.2 %) in the November sample compared to the rest of the samples (13-17 % of total sulfur). Uncertainties were also apparent in the analyses of reference compounds, which yielded discrepancies in the reduced sulfur absorption region (Table 4.4). Specifically, we could not always correctly identify the percentage of reduced sulfur species in Nordic aquatic humic acid and Elliot soil humic acid.

Table 4.2: Comparison of sediment from stream bank and from the reservoir. Sulfur and methylmercury were measured in a single 1 cm increment.

Sample	Inorganic material	Organic matter	Sulfur	Hg	CH_3Hg^+	CH_3Hg^+:Hg
Ash-laden sediment	(%)	(%)	(%)	(ng g^{-1})	(ng g^{-1})	
November, River bank	64	32	0.11	51		
August, Reservoir	76	28	0.07	49	4.5	0.09
November Reservoir	68	22	0.07	43	4.5	0.11
May, Reservoir	80	-	0.1	52	-	-
Native sediment						
Reservoir, August	83	11	-	44	0.4	0.01
Reservoir, November	85	11	-	45	0.6	0.01

Table 4.3: Elemental analyses of ash-laden sediment collected from the river bank and the reservoir bottom. Sediments collected from the river bank were analyzed as a single sample, data for the reservoir ash-laden sediments were the average concentrations of the 0-1, 1-2, 2-3, and 3-4 cm depth intervals.

	Percent of total mass (standard deviation) (%)									
Ash-laden sediment	**Si**	**Al**	**Fe**	**K**	**Ca**	**Mg**	**Na**	**Ti**	**P**	**Mn**
Streambank	40	10	5.1	2.5	2.6	1.7	0.9	0.6	0.3	0.1
August, Reservoir	49(0.2)	13(0.1)	5.4(0.1)	2.8(0.0)	2.8(0.3)	1.7(0.0)	1.0(0.0)	0.7(0.0)	0.3 (0.0)	0.1(0.0)
November Reservoir	44(4.5)	11(0.9)	5.3(0.3)	2.5(0.1)	2.4(0.1)	1.7(0.1)	1.0(0.1)	0.6(0.1)	0.2(0.1)	0.1(0.0)
May, Reservoir	52(0.7)	13(0.2)	5.6(0.1)	2.8(0.1)	2.5(0.3	1.7(0.1)	1.1(0.1)	0.7(0.0)	0.2(0.1)	0.1(0.0)

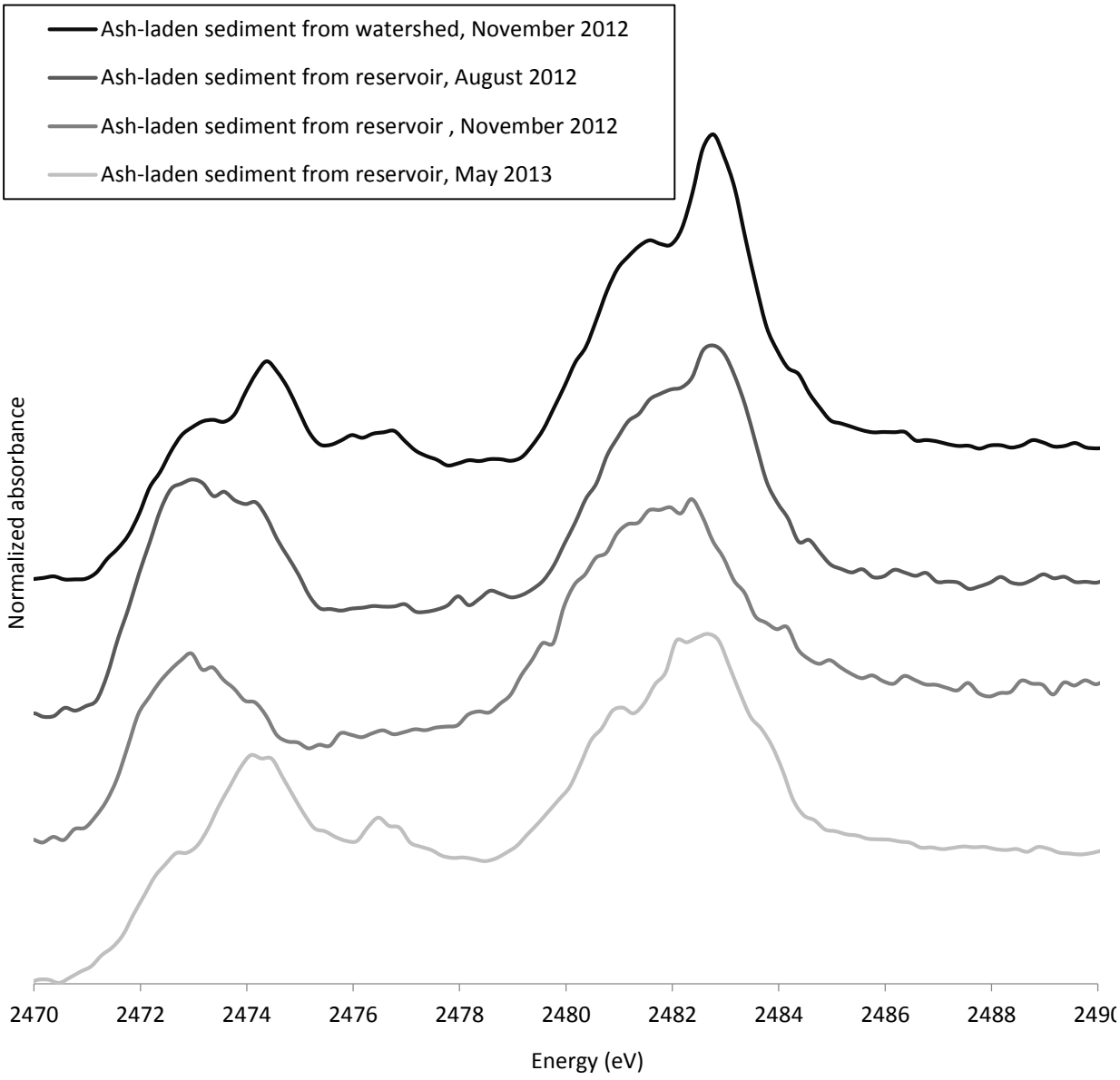

Figure 4.5: Sulfur XANES spectra collected from river bank and reservoir sediments at three time points after deposition.

Table 4.4: Linear combination fitting of sulfur species for two reference samples are compared with the database values and sulfur speciation in ash-laden sediments.

	(%)						
Ash-laden sediment	Sulfate	Sulfonate	Sulfone	Sulfoxide	Heterocyclic	Exocyclic	Inorganic reduced
Riverbank	17	15	1	0	9	0	21
Reservoir - August	14	13	0	0	4	0	10
Reservoir - November	6	16	11	0	7	1	11
Reservoir - May	12	11	1	0	10	0	33
Reference samples							
Nordic aquatic HA (ALS database)	4.9	13	6.4	3.6	37	24	12
Nordic aquatic HA	4.7	17	0.0	4.2	36	39	0.0
Elliot soil HA (ALS database)	18	26	4.9	6.4	29	15	0.6
Elliot soil HA	20	17	4.6	6.2	43	4.3	5.1

The discrepancies indicate that caution needs to be taken in reduced sulfur species interpretation, as there were likely some over and underestimations of the specific reduced sulfur species. To simplify and identify bulk sulfur oxidation state trends over the sampling times, these data were grouped into bulk oxidized, intermediate, reduced organic, and reduced inorganic categories (Figure 4.6). Ash-laden sediment collected from the reservoir in August 2012 contained a greater percentage of reduced inorganic sulfur than other sediment samples. Each successive coring (November and May) contained a greater fraction of reduced organic sulfur. Ash-laden sediments collected from the stream banks contained the lowest fraction of reduced inorganic sulfur species.

Discussion

The storm that followed the Hewlett Gulch and High Park Fires resulted in the transport of ash-laden sediment throughout the watershed, clearly affecting the watershed-reservoir system. Our characterization of the sediment revealed that the sediment matrix was composed of burned forest materials and mineral material from the parent rocks of the watershed. Large amounts of ash and other soil materials were eroded throughout the watershed, generating a substantial depositional zone at the north end of Seaman Reservoir. This material was markedly different from the previously deposited sediments at the sediment-water-interface of the reservoir. Our elemental analyses of the ash-laden sediment in the reservoir suggests that there were not substantial losses of iron and manganese to the overlaying water column. Although the ash-laden sediment had a high iron content, we assumed that most was bound in silicate minerals.

Mercury in Ash-Laden Sediments

The mobilization of ash-laden sediments from the recently burned watershed resulted in the transport of total mercury through the watershed and into Seaman Reservoir. Total mercury content in

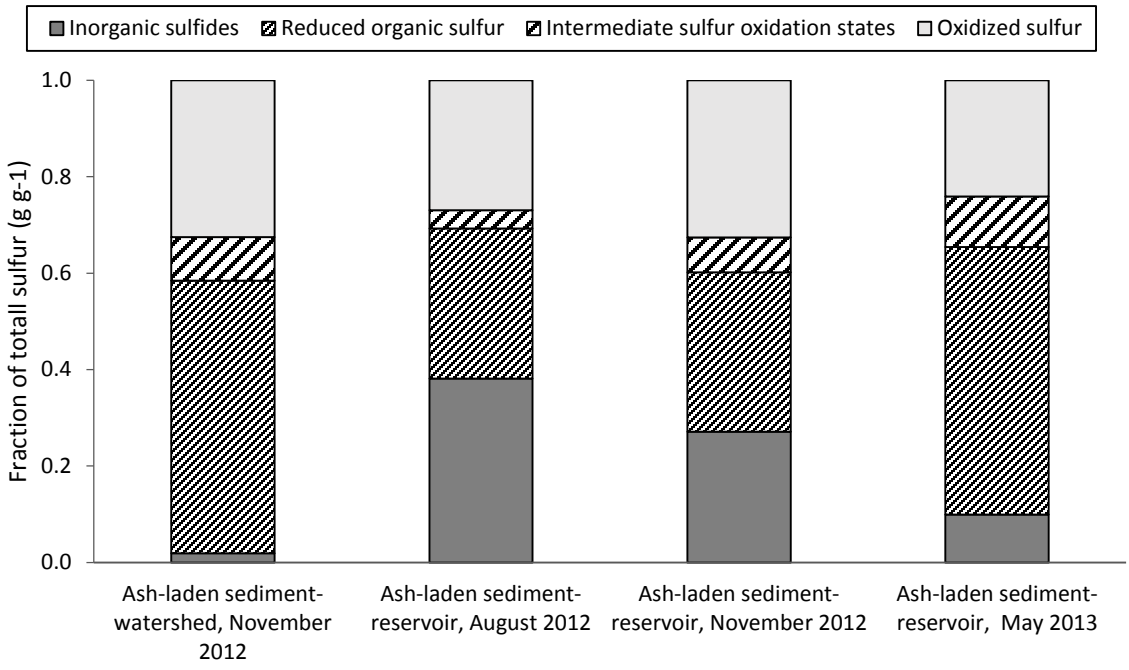

Figure 4.6: Fractional sulfur oxidation states in ash-laden sediment collected from stream banks and the reservoir bottom are grouped into absorption regions.

the ash-laden sediments collected from the stream bank was 51 ng g^{-1} and sediments deposited into the reservoir contained from 40 to 58 ng g^{-1}. This comparison reveals that mercury content of the material did not change dramatically during the transition from the watershed to the bottom of the reservoir. Because the bank material had prior contact with water during transport, mercury would have been previously released to the aqueous phase.

Mercury concentration profiles in the deposited ash-laden sediments revealed no measureable increase or decrease in mercury content over the time period studied. The average concentration of total mercury in ash-laden sediments (47 ± 5.2 ng g^{-1}) was similar to the average reported by Caldwell *et al*. (2000; 46 ng g^{-1}), sampled from the Caballo Reservoir in New Mexico after it received runoff from a recently burned watershed. Sulfate reduction could increase mercury binding in sediments through sulfide incorporation. Conversely, the reduction of iron oxides and manganese oxides could release organic matter in the dissolved phase, co-mobilizing mercury bound in dissolved organic matter

complexes. However, we did not find evidence supporting enhanced mobilization or enhanced mercury binding.

Methylmercury concentrations in ash-laden sediments collected 1.5 and 4.5 months following depostion in the reservoir were 4.5 ng g^{-1}, which indicates that conditions favorable for methylation were persitant in the reservoir sediments. In the ash-laden sediment, the ratio of the concentration of methylmercury to that of total mercury (CH_3Hg^+:Hg_{tot}) was 0.1. This ratio is on the high end of the molar ratio reported after methylation assays (Jonsson *et al*., 2012), which suggests a bio-labile form of mercury. The generation of these methylmercury concentrations were similar (though not as high) to the 12.5 ng g^{-1} reported in the Caballo Reservoir in ash-laden sediments (Caldwell *et al*. 2000). The methylmercury concentrations were 10-fold higher in the ash-laden sediment than native sediment. Clearly, ash-laden sediment and the redox transition associated with the deposition of fire derived sediments engender methylation potentials greater than the native sediments.

Sulfur Characterization of Ash-Laden Sediment

Sulfur in the river bank sediment was 57 % reduced-organic, 9 % intermediately-oxidized, and 33 % highly-oxidized (Figure 4.6), which was similar to the distributions reported from sulfur XANES studies of unburned forest soil (Schroth *et al*., 2007; Prietzel *et al*., 2007; Solomon *et al*., 2011). It was likely that the oxidized sulfur was organic, because unbound sulfate would be leached during mobilization and transport. In fact, the water quality data reported unprecedented summer-time sulfate concentrations in the reservoir following the wildfire, indicating enhanced release from burned material (Oropeza and Heath, 2013).

Ash-laden sediment collected from the reservoir bottom contains a greater fraction of reduced inorganic sulfur than that collected from the river bank, suggesting ongoing sulfate reduction (Figure 4.6). We found that in the reservoir material (August 2012), 35 % of the sulfur was in a reduced

inorganic form, compared to 2 % in the stream bank sediments. The percentage of reduced inorganic sulfur was similar to previous reports for relative abundance of reduced inorganic sulfur in waterlogged histosols (40 %) (Prietzel *et al*., 2009). Our results reveal the presence of reduced inorganic sulfur in the ash-laden sediment following deposition in the reservoir, which was consistent with our hypothesis. There was a fractional increase reduced inorganic sulfuring deposited sediment, but there was not an increase in total sulfur in ash-laden sediment collected in the reservoir when compared to sediment from the river bank (Figure 4.6). We hypothesized that sulfide would be generated from the microbial reduction of sulfate in the sediment pores and react with the ash-laden sediments organic matter; however, the lack of evidence for increased sulfur content makes us consider that sulfide in the ash-laden sediment might be formed from other forms already present in the matrix, such as organically bound sulfate.

The measured reduced inorganic sulfide likely contains multiple species of sulfur. The proximity of polysulfides, elemental sulfur, FeS, and FeS_2 absorption energies requires cautious analysis, as demonstrated by the modeling results from the lower absorption energy ranges of Elliot soil and Nordic aquatic humic acids. It is likely that each of these forms was present in the ash-laden sediment collected in August, November, and May. Sulfide was likely formed during the reduction of sulfate, but these sulfides can be oxidized by manganese(IV) and iron(III) to form elemental sulfur (Werne *et al*., 2004; Zopfi *et al*., 2004; Slowey and Brown 2007); thus, the presence of elemental sulfur was possible, assuming that deposited sediment contained some reducible ferric iron. Dissolved iron and manganese concentrations were reported to be elevated throughout the summer and fall of 2012, suggesting that iron and manganese reduction was occurring (Oropeza and Heath, 2013). The presence of dissolved iron in the water column suggests that it was present in sediments during sulfate reduction, which could also lead to iron sulfide formation.

Sulfur oxidation state in ash-laden sediment changed throughout the August, November, and May sampling times with increasing relative amounts of organic sulfur fractions (relative to inorganic forms) at each successive time point (Figure 4.6). Ash-laden sediment collected in November 2012 was modelled to contain 25 % reduced inorganic sulfur, while sediment collected in May 2013 contains only 10 % reduced inorganic sulfur. The formation of organic sulfur may be enhanced by redox transitions occurring during reservoir turnover (Werne *et al*., 2004). Specifically, sulfide and iron sulfides can react with oxygen, nitrate, manganese (III,IV) oxides, or ferric iron oxides to oxidize sulfur into elemental sulfur, which can catenate into polysulfides (Zopfi *et al*., 2004). The formation of polysulfides has been proposed as pathway for sulfur incorporation into organic matter (Vairavamurthy *et al*., 1997; Werne *et al*., 2004). Thus, it is possible that reservoir-turnover contributed to the incorporation of sulfur into sediment organic matter. The formation of polysulfide moieties, in particular, could be important for mercury binding as the interaction between mercury and a sulfur-rich site would produce an increasingly favorable binding location (Nagy *et al*., 2011).

Summary

We investigated the chemistry of ash-laden sediments transported from a recently burned watershed into a reservoir. Ash-laden sediments contained 32% organic material and an inorganic fraction of mainly silicon, aluminum, and iron, assumed to be aluminum-silicate minerals. Total sulfur was approximately 0.1 % by total mass in the ash-laden sediment.

Following deposition in the reservoir, the sulfur oxidation state changes continually through the seasons sampled. Sulfur in August 2012 was mainly reduced inorganic sulfur, but in May 2013 sulfur was predominantly in a reduced organic form. The speciation transition provides evidence that one effect of early diagenesis of ash-laden sediments deposited following wildfire was the formation of reduced sulfur.

Total mercury in the ash-laden sediment was found to be 51 ng g^{-1}. The concentration of mercury in the sediments did not appear to change during deposition into the reservoir, nor did the onset of early diagenesis appear to cause gains or losses of mercury content. The reservoir sediments had much higher methylmercury concentrations (4.5 ng g^{-1}) compared to the native sediment (0.4-0.6 ng g^{-1}), and these concentrations were observed to remain elevated at the last point we measured methylmercury (4.5 months following deposition).

Overall, the results of this study increase our understanding of how wildfire mobilizes mercury into surface waters. We have characterized the behavior of sulfur during the deposition of ash-laden sediments in a reservoir. Additionally, we have documented some of the elemental behavior and underlying geochemical processes in ash-laden sediment that will influence contaminant fate and transport in recently burned watersheds. The presented data were points representing fleeting conditions in watershed, but may have lasting effects on watershed health.

Chapter 5

Mercury affinity for ash-laden sediment increases following simulated reservoir deposition

Jackson P. Webster *[a], Brett A. Poulin [a,b], Erika Callagon [b], David Vine [c], Katheryn Nagy [b], Alain Manceau [d], George R. Aiken [e], and Joseph N. Ryan [a]

[a] Department of Civil, Environmental, and Architectural Engineering, University of Colorado, Boulder

[b] Department of Earth and Environmental Sciences University of Illinois at Chicago

[c] Argonne National Laboratory

[d] ISTerre, CNRS Universite de Grenoble, Grenoble, France

[e] US Geological Survey

To be submitted to *Environmental Science & Technology*

Abstract

Global increases in wildfire severity and occurrence contribute to mercury mobilization and transport into aquatic environments. Wildfire commonly leads to erosion of ash-laden sediment from watersheds during rain events and mobilizes associated mercury. Little information is reported on the fate of mercury associated with ash-laden sediment deposited in lakes and reservoirs. We attempted to simulate the conditions present at the bottom of a reservoir to investigate the influence of reducing conditions on ash-laden sediment mercury binding capacity. Ash-laden sediment was incubated in an argon-filled glove box and pore water was sampled from 0 d to 33 d to monitor mercury, dissolved organic matter, and major ions throughout the redox transition. Sediments representing initial conditions, pre- and post-sulfate reduction, and final conditions were analyzed using sulfur X-ray absorption near-edge structure spectroscopy to characterize changes in sulfur oxidation states throughout microcosm incubation. Competitive ligand exchange experiments were employed to quantify changes in mercury binding capacity at four time points in the incubation. Reducing conditions decreased highly-oxidized sulfur from 32 % to 23 % total sulfur and increased reduced organic sulfur from 56 % to 66 % total sulfur. The increase in reduced organic sulfur suggests that sulfide converted to organic sulfur in sediments. Aging under reducing conditions was found to increase mercury binding sites by 10-fold and this was attributed to increases in reduced organic sulfur.

Introduction

Transport and deposition of mercury from natural and anthropogenic sources has led to its global enrichment in surficial soils. In arid climates, such as the western U.S., the common occurrence of wildfire acts as a source of re-emission of accumulated mercury (Wiedinmyer and Friedli, 2007). In addition to atmospheric re-emission, wildfire enhances the transport of mercury from forest soils to the sediments of lakes and reservoirs where there is increased mercury methylation and transfer into food-webs (Caldwell *et al*., 2000; Kelly *et al.*, 2006). There are few studies investigating the fate and transport of mercury following wildfire and mechanistic explanations are needed to assess the potential for human and ecological health risks associated with increased post-wildfire mercury methylation.

Wildfire commonly results in increased surface flow and sediment transport resulting from rainfall events (Martin and Moody 2000; Ice *et al*., 2004; Nearly, 2005). In burned watersheds, storms with frequent return intervals can result in disproportionate flood events (Moody and Martin, 2001; Ice *et al*., 2004). Increased surface flow is due to loss of intercepting foliage and development of a hydrophobic layer in the soil (Martin and Moody, 2000; Ice, 2004). Large increases in overland flow in burned areas can mobilize and transport sediment, and these erosional events can result in the deposition of ash-laden sediment in downstream rivers, lakes, and reservoirs (Moody and Martin, 2001; Ice *et al*., 2004; Neary *et al*., 2005; Bodi *et al.* 2014). In addition to ash-laden sediment, wildfire mobilizes nutrients and dissolved constituents, which can affect water quality (Smith *et al*., 2011). Information regarding the post-depositional early diagenesis of ash-laden sediment in lakes and reservoirs in regard to mercury fate and transport is currently lacking.

In forest soils and sediments, mercury is bound by organic matter through coordination with reduced organic sulfur moieties (Xia *et al*., 1999; Skyllberg *et al*., 2000; Hesterberg *et al*., 2001; Wolfenden *et al.*, 2005; Khwaja *et al*., 2006;, Skyllberg *et al*., 2006; Nagy *et al*., 2011). Although reduced organic sulfur is responsible for strong binding capacity, not all reduced organic sulfur participates in

binding (Haitzer *et al*., 2002). The number of available strong mercury binding sites is defined as the strong binding capacity of the soil or sediment. The strong interactions between reduced organic sulfur and mercury are retained as soluble organic matter mobilizes into waterways, making reduced organic sulfur functional groups important for the transport of mercury in surface water (Ravichandran, 2004). Furthermore, under sulfidic conditions, interactions between dissolved organic matter and mercury can inhibit the formation of metacinnabar by stabilizing colloids and inhibiting aggregation (Aiken *et al*., 2011; Graham *et al*., 2012; Zhang *et al*., 2012). Recently-formed nanoparticulate metacinnabar has been shown to be methylatable (Graham *et al*., 2012; Zhang *et al.*, 2012; Pham *et al*., 2014).

Sulfur in sediment is mainly derived from the overlying water column, primarily in the form of sulfate (Holmer and Storkholm, 2001). Under anoxic conditions, sulfate may be microbially reduced to inorganic sulfide. Sulfide produced in sediments and anoxic waters can be incorporated into sediment organic matter (Urban *et al*., 1999; van Dongen *et al*., 2003; Werne *et al.*, 2004; Heitmann and Blodau, 2006; Werne *et al*., 2008, Einsiedl *et al*., 2008). Incorporation of sulfur into organic matter is the result of strong nucleophilic tendencies of sulfide reacting with organic matter moieties (Werne *et al*., 2004). Sulfide incorporation occurs at specific moieties such as unsaturated bonds, ketones, alcohols, and quinones (Kok *et al*., 2000; Perlinger *et al.,* 2002, Werne *et al*., 2004). The incorporation of sulfide in organic matter engenders strong binding sites for metals (Hoffman *et al*., 2012).

In addition to interactions with organic matter, sulfides can form inorganic mineral phases. The formation of iron-sulfides, for instance, may somewhat impede sulfurization by reacting with sulfide. However, iron-sulfide formation has also been shown to occur concomitantly with sulfurization (Werne *et al*., 2004). Sulfide may also react directly with ferric iron resulting in the oxidation of sulfide to elemental sulfur and polysulfides, and the reduction of ferric iron (Werne *et al*., 2004). The formation of polysulfides could lead to polysulfide-organic matter incorporation and create bidentate reduced sulfur sites conducive to strong mercury binding (Vairavamurthy *et al*., 1997; Xia *et al*., 1999; Drexel *et al*.,

2002; Haitzer *et al*., 2003; Khwaja *et al*., 2006; Skyllberg *et al*., 2006). Furthermore, inorganic sulfides can react directly with mercury to form metacinnabar (β-HgS). Formation of colloidal metacinnabar or mixed metal-mercury sulfide colloids can enhance mercury transport from sediments (Hofacker *et al.*, 2013). The precipitation of iron sulfide in sediments could also limit the transport of mercury because mercury can bind on the surface of iron sulfide precipitates (Skyllberg and Drott, 2010).

Transport and deposition of ash-laden sediment mobilizes mercury in streams, lakes, and reservoirs following wildfire. Early diagenesis of sediment, particularly sulfur incorporation, following wildfire could be an important control on the fate and bioavailability of mercury. Incorporation of sulfur within sediment organic matter can make a preferred site for soft metal binding. Conversely, sulfur interactions with other metals and formation of metal-sulfide could potentially mobilize or immobilize mercury. We hypothesized that following deposition and burial, ash-laden sediment under sulfate reducing conditions will undergo sulfur incorporation due to high organic matter content. As a result of sulfur incorporation, there will be an increase in the number of strong mercury binding sites in deposited ash-laden sediments. To test this, we simulated reducing conditions present at the bottom reservoir following ash-laden sediment deposition by adding this material to glass vessels and incubating the sediments from 0-33 d. We tracked the behavior of total mercury in pore waters and the dynamics of redox-sensitive constituents, including sulfate. We used X-ray absorbance near-edge structure (XANES) spectroscopy to measure sulfur oxidation state during redox transitions. Following incubation, changes to mercury-binding capacity of the sediments were measured using a competitive ligand exchange method.

Methods

Sampling Location

The Hewlett Gulch Fire ignited on May 14, 2012, in Larimer County, Colorado, USA, and burned 3110 ha before being extinguished on May 22, 2012. The fire burned pine and fir forests on steep hillslopes with ephemeral drainages that empty into the North Fork of the Cache la Poudre. Seaman Reservoir is located on the North Fork of the Cache la Poudre, adjacent to the burned area (Figure 5.1). Following the May 2012 fire, a flood event in early July 2012 transported large amounts of ash-laden sediment into the Cache la Poudre River system and Seaman Reservoir.

Sample Collection and Preparation

Ash-laden sediment was collected on November 11, 2012, from the banks of an ephemeral stream near its inlet at Seaman Reservoir (Figure 5.1). The samples were collected using a stainless steel scoop pre-cleaned with ultrapure water (18.2 MΩ cm, Millipore, MilliQ®), were placed in re-sealable plastic bags, sealed, and placed in a cooler for transport. Once in the laboratory (within 4 h of sampling), they were frozen immediately. Frozen ash-laden sediments were thawed and air-dried in a positive-pressure flow hood a high-efficiency particulate arrestance (HEPA) filter for approximately two weeks being stirred regularly. Dried samples were sieved (stainless steel, 25 mesh) to remove large pieces of burnt wood, needles, leaves, and stones.

Microcosm Experiments

To attempt to simulate the conditions at the bottom of a reservoir, ash-laden sediments were added to a glass vessels and kept in a glove box with an argon atmosphere to generate reducing conditions. The environment within each glass vessel was a microcosm of the conditions at the bottom of the reservoir.

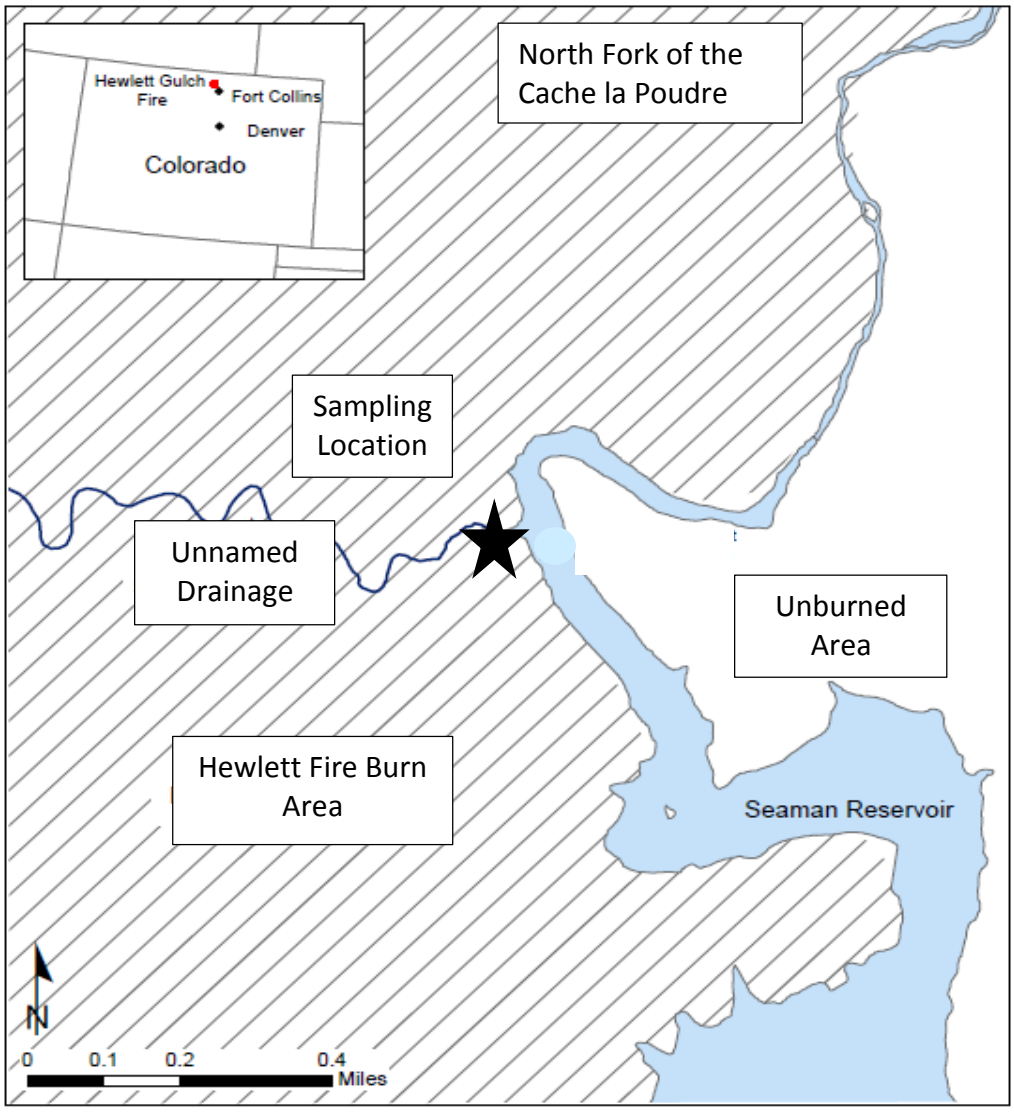

Figure 5.1: The Hewlett Gulch study area was at the mouth of an ephemeral drainage (starred on map) which flowed west to east out of the Hewlett Fire burn area into Seaman Reservoir.

The microcosms were prepared in glass jars with polytetrafluoroethene (PTFE)-lined caps (125 mL; I-Chem, Fisher, USA) which were pre-cleaned by a 24 h rinse with 10 % HCl and 10 % HNO_3 solution. Following the acid wash, jars were rinsed three times with ultrapure (18.2 MΩ cm, Millipore, MilliQ®) water. Sediments and ultrapure water, de-aired with nitrogen by bubbling for 30 min, were added to the vessels to a ratio of 50 g sample to 125 mL water. A total of 24 microcosm vessels were prepared. Microcosm vessels were wrapped in aluminum foil to exclude light and incubated for 1-33 d. One set of duplicate microcosms was prepared under an ambient atmosphere and sampled following settling of sediment (2 h) to represent the initial conditions.

Pore water was extracted at a rate of 0.6 mL min^{-1} from the microcosms using a lysimeter with pore size cutoff of 10-16 μm. Once pore water was collected, the sediments were immediately frozen for future experiments and analysis. Sediments were briefly thawed in a glove box with an argon atmosphere and 5-10 g of sediment were removed from the vessel. Sediments were then dried under an argon atmosphere for one week. Dried samples were placed in clean vials and the lids were sealed with electrical tape to prevent atmospheric exposure and stored for future use. These argon-dried samples were analyzed for sulfur oxidations state using X-ray absorbance near-edge structure (XANES) spectroscopy and used in competitive ligand exchange (CLE) experiments. The samples used for sulfur XANES were taken at times (1) before sulfate reduction (0 d), (2) at the onset of sulfate reduction (5 d), (3) following sulfate reduction (14 d), and (4) at the end of the full incubation (33 d), as identified by the concentration of sulfate in the microcosm pore waters.

Competitive Ligand Exchange Experiments

Mercury exchange between sediment and a competing ligand was used to determine the change in sediment binding capacity throughout the microcosm incubation. Ash-laden sediments from the microcosm vessels were ground using a mortar and pestle. Stock solutions were made in an argon

filled glove box. A 0.01 M stock solution of *meso*-2,3-dimercaptosuccinic acid (DMSA; Sigma Aldrich, 98 % purity) was made prior to each experiment. Ultrapure water was de-oxygentated by purging a 1 L vessel with high-purity nitrogen for 30 min prior to use to minimize the potential for oxidation of DMSA. DMSA is sparingly soluble, so 2 mL of 0.1 M NaOH was added to the stock solution to raise the pH to circumneutral values and promote dissolution. Stock solutions were allowed to sit for 24 h and used immediately. Stock solution of acetate buffer was made with glacial acetic acid (Fisher Scientific, USA) and sodium acetate (Fisher Scientific, USA) to 1 M.

Mercury addition to the dried and ground sediment was carried out in an argon head filled glove box where 0.1 g solid, 5 mL of de-oxygenated ultrapure water, and 40 µL of stock solution containing 1 mg L^{-1} $Hg(NO_3)_2$ in 1% nitric acid solution were combined in glass vials (40 mL, I-chem™, Fisher Scientific, USA). We added 0.03 M sodium azide to the vessels to inhibit microbial activity in the experiments. Aqueous suspensions were gently mixed at 10 rpm for 7 d on an end-over-end mixer to allow mercury to associate with strong binding sites in the solids (Khwaja *et al*., 2006). Following mixing, DMSA (2 mL of the 0.01 M stock solution) was added to the vials to achieve 0.5 mM DMSA. Acetate buffer was added to the vials in the amount of 0.4 mL of 1 M to achieve a 0.01 M buffer, and 1.33 mL of 3 M sodium perchlorate was added to achieve 0.1 M electrolyte. Vials were brought to 40 mL total volume with ultrapure water and mixed at 10 rpm on an end-over-end mixer for 14 d. After mixing, samples were transferred into PTFE centrifuge tubes (50 mL, Nalgene, Oak Ridge, cleaned using a solution of 10 % hydrochloric acid and 10 % nitric acid), centrifuged for 15 min at 24,000 relative centrifugal force (RCF), decanted into disposable syringes (BD Luer-Lok®), and filtered through a 32 mm Acrodisc® filter cartridge containing a 0.45 µm polyethersulfone Supor® membrane (Pall Corporation, USA). Syringes and filter cartridges were rinsed with ultrapure water using three syringe volumes prior to use. Sample filtrate was collected in the original glass vials. A volume of 5 mL filtrate was pipetted into 40 mL amber glass vials (I-Chem™) and diluted 8-fold using ultrapure water for dissolved organic

carbon measurements. The remaining filtrate was preserved for future mercury analysis by adding BrCl at 3 % of the sample weight (Telliard and Gomez-Taylor, 2002). Sediment remaining in the centrifuge tube following decanting was rinsed using 20 mL of 0.1 M sodium perchlorate in the PTFE centrifuge tube, shaken, and centrifuged for 15 min at 24,000 RCF to remove any remaining ligand-bound mercury from the solid. Ultrapure water in the amount of 5 mL was added to sediment, which was then poured into polystyrene weigh boats and air-dried in a HEPA-filter positive-pressure flow hood prior to mercury analysis.

The competitive ligand exchange experiments were conducted in triplicate and were accompanied by experimental blanks to evaluate mercury and carbon losses and recovery in the vials. Blanks were treated as competitive ligand exchange (CLE) samples and run with chemical additions identical to those with solids and mercury. Mercury spikes were conducted without solids to evaluate recovery. Recoveries were calculated for each of the individual CLE vials based on mercury addition and native mercury. Dissolved organic matter blanks were prepared to verify recovery of ligand and buffer additions. Blanks were also used to determine the release of dissolved organic carbon from the ash-laden sediment by measuring and comparing independent samples containing buffer, ligand, and no ash-laden sediments.

Analytical Procedures

The ash-laden sediments were characterized for organic matter content gravimetrically by loss on ignition (LOI) for 2 h at 550 °C. Air-dried ash-laden sediment samples were weighed out to 1 g in pre-weighed and cleaned ceramic boats. Samples were heated for 2 h, cooled in a desiccator, and re-weighed to determine mass loss. Ash-laden sediments were digested following the methods of Farrell *et al*. (1980). Following digestion, major elements were measured using inductively-coupled plasma-optical emission spectroscopy (ICP-OES) and trace elements were measured using inductively-

coupled plasma-mass spectrometry (ICP-MS). Total sulfur was measured using a perchloric acid digestion and measurement by ICP-OES. All analyses were accompanied by external source-certified quality control samples, matrix blanks, digestion blanks, duplicates, matrix spikes and sample spikes in accordance with good laboratory practice guidelines. Total mercury concentrations were measured using thermal decomposition / catalytic reduction / atomic absorption spectroscopy (DMA-80 analyzer, Milestone, Shelton CT, USA). All solid-phase mercury measurements were quantified using National Institute of Standards and Technology (NIST) and National Research Council of Canada (NRCC) certified standards. Target concentrations of reference standards were confirmed to be within 10 % for each set of samples analyzed.

Dissolved Constituents

In microcosm pore water and CLE filtrate, total mercury was measured by cold vapor atomic fluorescence spectroscopy (Tekran 2600 mercury analyzer) using stannous chloride reduction (Telliard and Gomez-Taylor, 2002). In microcosm pore water, the difference between filter-passing mercury (< 0.2 µm, polyethersulfone) and total mercury was defined as colloidal mercury. Calibration standards were made using the National Institute of Standards and Technology (NIST) 3133 mercury standard. Dissolved organic carbon (DOC) was measured with a total organic carbon analyzer using persulfate oxidation (OI Corporation, model 700; Aiken, 1992). All DOC measurements were made within two weeks of the experiments. Ultraviolet absorption at a wavelength of 254 nm (UVA_{254}) was measured using an ultraviolet-visible spectrophotometer (Agilent, model UV-Vis 8453) with a 1-cm path length. Iron absorption interference was avoided during UVA_{254} measurements by preparing samples for UV absorbance measurements in a glove box under an argon head (Poulin *et al*., 2013). Specific ultraviolet absorbance at 254 nm was calculated as the ratio of UVA_{254} to DOC concentration and adjusted for the

absorbance path length (SUVA, L mg_C^{-1} m^{-1}). Major ions were quantified by ion chromatography (IC; Dionex IonPac® AS14A column).

Sulfur Oxidation State Measurements

Sulfur oxidation state in the ash-laden sediment was determined by sulfur XANES spectroscopy. Sulfur XANES spectroscopy was conducted on Beamline 2-ID-B at the Advanced Light Source, Argonne National Labs, Chicago, IL. X-ray absorption was measured by fluorescence detection. An M1 spherical grating monochromator was used to focus X-rays into the sample chamber. Fluorescence signals were recorded with a nine-element differential phase contrast detector. The estimated uncertainty in energy was 0.1 eV (Manceau and Nagy, 2012). Energy was calibrated by setting the $CaSO_4$ peak to 2482.75 eV and scans were obtained between 2420 and 2625 eV. The distribution of sulfur oxidation states were quantified using linear combination fitting of XANES spectra using the fitting program *Linear Fit w overabsorption* (Marcus, 2010). Each sample run was accompanied by two reference compounds obtained from the International Humic Substance Society, Nordic Aquatic humic acid, and Elliot Soil humic acid. Each of these humic acids have been characterized using the same component database we employed (Manceau and Nagy, 2012). The modeled fit of each of these reference compounds was compared to the data base fit for quality assurance.

Results

Ash-Laden Sediment Characterization

The ash-laden sediment was characterized prior to use in microcosm experiments (Table 5.1). The material contained 32 % organic matter and the major elemental components were silicon, aluminum, and iron. The remaining elements represented less than 3 % each (Table 5.1). The

concentration of total sulfur in the ash-laden sediment was 31 ± 4.4 μmol g^{-1} (*n* = 4). The concentration of total mercury in the ash-laden sediment was 51 ± 0.7 ng g^{-1} (*n* = 3).

The Effects of Redox Conditions on Pore Water Constituents

A redox transition toward increasingly reducing conditions occurred in in our microcosms (Figure 5.2). The depletion of nitrate occurred first (1 d), followed by the appearance of manganese (1 d) and iron (3 d). Sulfate was initially present at 0.55 mM and began to be depleted at 5 d, decreasing to less than 0.1 mM by 14 d. At the onset of sulfate reduction (5 d), accumulation of iron and manganese in pore water appears to slow (Figure 5.3). Following the depletion of sulfate at 14 d, iron and manganese concentrations increased again until 18 d. The microcosm constituents reached a steady state at 18 d. Pore water pH was 7.0 ± 0.1 in each microcosm sample.

Ash-laden sediment added to microcosm vessels (50 g into 125 mL) released approximately 100 mg L^{-1} of organic carbon (Figure 5.2). After 3 d, the DOC concentration increased from the initial concentration to 350 mg L^{-1}. Acetate was measured in one of the duplicate microcosms between 0 d and 3 d, then again from 10 d to 18 d and is reported as mg L^{-1} DOC. No other organic acids were detected in pore water. After correcting for acetate in pore water, SUVA was calculated (Figure 5.3).

Table 5.1. Characterization of ash-laden sediment prior to microcosm incubation.

Major elements	**SiO_2**	**Al_2O_3**	**Fe_2O_3**	**CaO**	**K_2O**	**Organic Matter**
(%)	40	10	5.1	2.6	2.5	32
Minor elements	**MgO**	**Na_2O**	**TiO_2**	**P_2O_5**	**MnO**	**S**
(%)	1.7	0.9	0.6	0.3	0.1	0.1
Trace elements	**As**	**Cu**	**Ni**	**Pb**	**Zn**	
($\mu g\ g^{-1}$)	37	33	35	50	140	

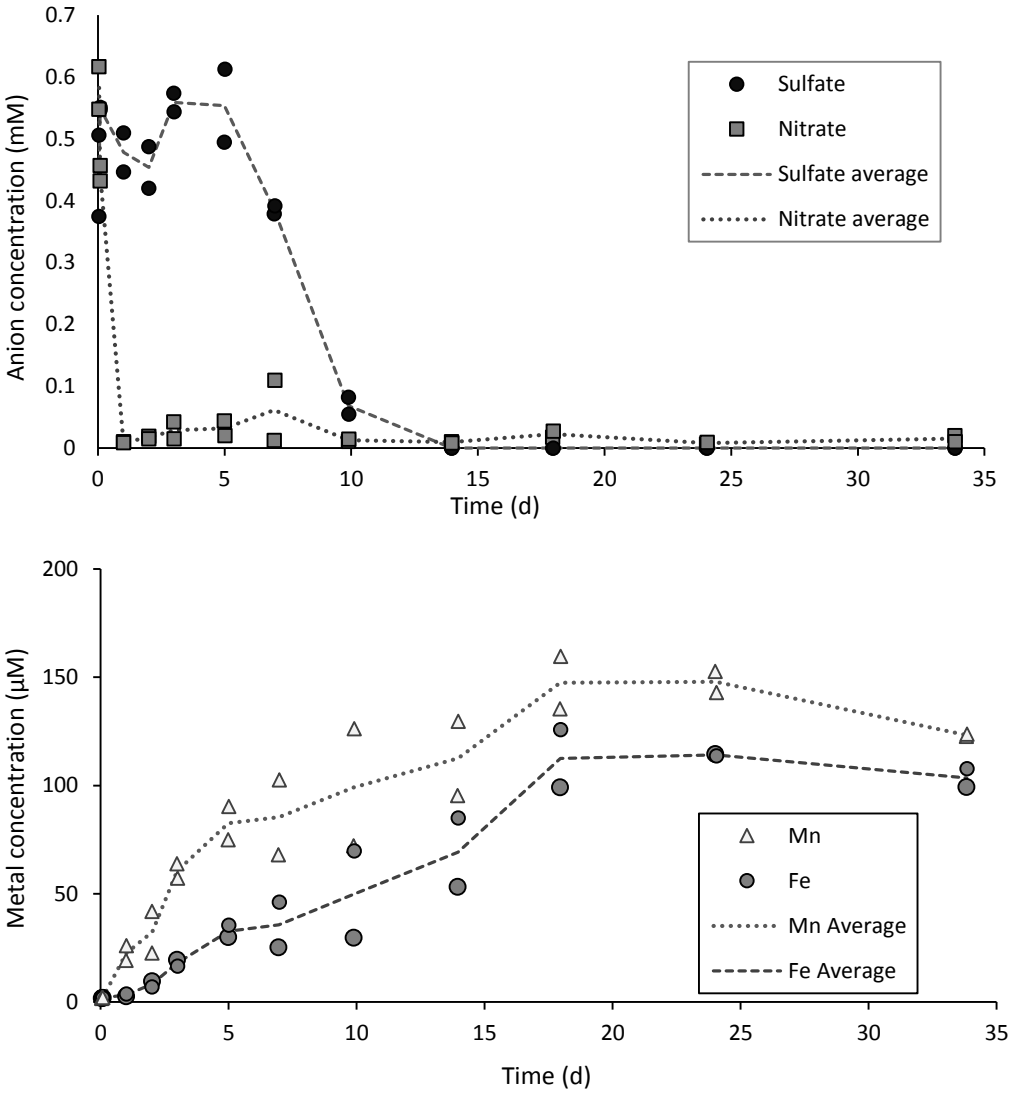

Figure 5.2: Concentrations of redox-sensitive anions and metals as a function of time in microcosms.

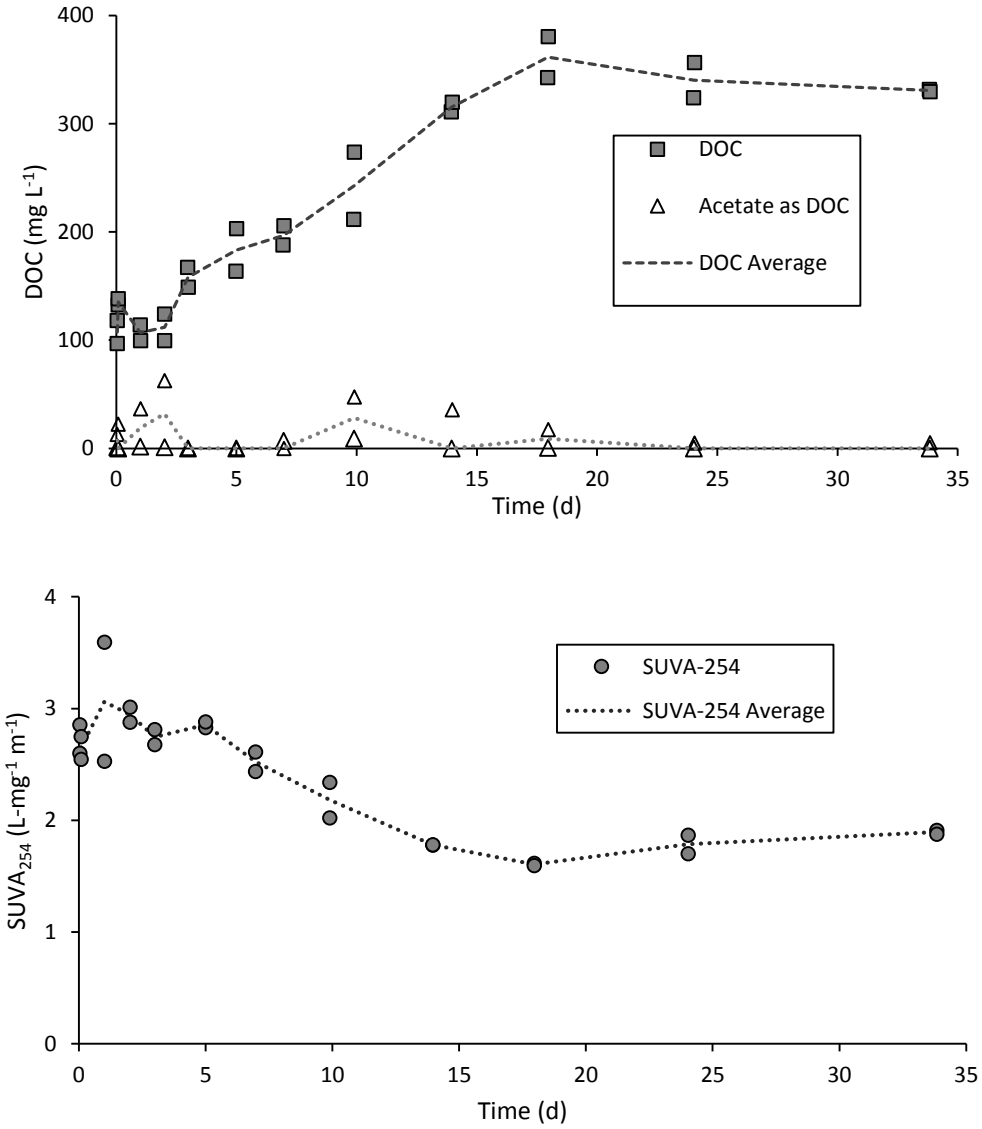

Figure 5.3: Dissolved organic carbon (DOC) and specific ultraviolet absorption ($SUVA_{254}$) of pore water as a function of time are shown in duplicate microcosms DOC and $SUVA_{254}$ are shown after correction for acetate. Acetate is shown as its DOC contribution.

Sulfur Speciation in Microcosm Sediments

Sulfur XANES spectra of ash-laden sediment revealed a shift from oxidized sulfur to reduced sulfur over the time in the microcosm (Figure 5.5). Linear combination fitting of the sulfur XANES spectra reveals a loss of highly-oxidized sulfur and an increase in reduced organic sulfur (Table 5.3). Organic sulfate esters (2,483.2 eV) and inorganic sulfate (2,483.1 eV) have overlapping absorbance ranges, making the two indistinguishable. Sulfate initially accounted for 17 % of the total sulfur, but was measured to be 13 % at 5 d and remained relatively constant throughout the remainder of the incubation. Two other sulfur types of different oxidation state, sulfonate and sulfone, both peaked in relative abundance at 5 d, just prior to sulfate reduction. The fraction of reduced organic sulfur increased by 17 % over the incubation period. Heterocyclic species increased between 5 d and 14 d, but decreased at 33 d. Conversely, exocyclic sulfur steadily decreased between 5 d and 14 d and increased at 33 d. The amount of reduced inorganic sulfur was highest at 14 d, but was measured to be 40 % of the peak value at 33 d.

Due to the analytical burden of obtaining sulfur XANES spectra, we have few data on the sediments, which limits our ability to delineate error or heterogeneity in the sediment sulfur. While there appears to be general trends among modeled oxidation states, there is inherent uncertainty in the in the distribution of species based on modeling of the oxidations state. The analyses of reference compounds yielded discrepancy in the reduced sulfur absorption region (Table 5.2). Specifically, we could not always correctly identify reduced sulfur oxidation states in Nordic aquatic humic acid and Elliot soil humic acid. The discrepancies indicate that caution needs to be taken in the interpretation of reduced sulfur oxidation states.

Mercury Behavior in Microcosms

Total mercury measurement of both colloidal and filter-passing mercury decreased throughout the incubation (Figure 5.4). Colloidal mercury concentrations decreased more rapidly than filter-passing mercury until 10 d. The colloidal mercury concentration declines until 18 d and appears to become steady, while filter-passing mercury continued to decrease throughout the incubation. Filter-passing and colloidal mercury concentrations at 33 d were 25 % and 28 % of the initial concentration, respectively.

Competing ligand experiments resulted in a consistent increase in mercury association with the ash-laden sediment over time (Figure 5.5). The binding of mercury by the ash-laden sediment increased by 25 % from 0 d to 33 d. Applying Eqn. 4, and assuming that binding of mercury to the sediment was reversible, revealed that the shift in mercury distribution is the result of 5-fold, 7- fold, and 10-fold increases in strong binding site abundance at 7 d, 24 d, and 33 d, respectively (Table 5.2).

Discussion

Sulfate Oxidation State and Evidence for Incorporation into Organic Matter

The sulfur XANES spectra obtained from the microcosm sediments revealed a shift in sulfur speciation through the redox transition consistent with our hypothesis that ash-laden sediment would undergo sulfur incorporation. There was a loss of highly-oxidized sulfur between 0 d and 33 d and an increase in energy absorbance in the ranges representing oxidations states associated with reduced organic sulfur (Figure 5.6). Initially, sulfur XANES spectra revealed a decrease of sulfate from 17 % to 13 % of total sulfur from 0 d to 5 d. Measured sulfate concentrations of 0.55 mM in pore water correspond to 4 % of the 12.4 mM of total sulfur calculated from soil mass, soil sulfur, and vessel volume, which validates the sulfur measurements.

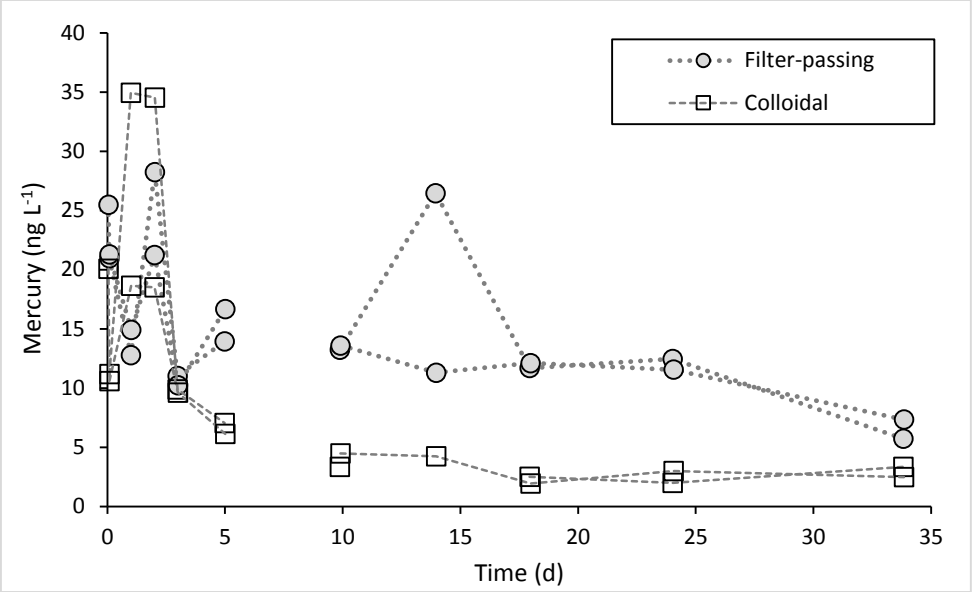

Figure 5.4: Filter-passing and colloidal mercury in microcosm pore water as a function of time in duplicate microcosms. We lost the 7 d samples.

Table 5.2: Competitive ligand exchange data for each triplicate set of vials. In the table, $Hg(NO_3)_2$ is the amount of total Hg measured in spikes. $[Hg_2DMSA^{4-}]$ is the aqueous mercury measured in the vessel and $[RSHg^+]$ is the solid phase mercury in the vessel. Using the definition of $\Delta[RS^-]$ provided in the text (Eqn 4) we calculated the percent change in strong biding sites ($\Delta[RS^-]$).

Sample	Sediment mass (g)	Sediment Hg (nM)	$Hg(NO_3)_2$ added (nM)	Ligand added (mM)	Reduced organic sulfur (mM)	$[Hg_2DMSA^{4-}]$ (nM)	$[RSHg^+]$ (nM)	$\Delta [RS^{-1}]$ (%)	Recovered Hg %
0 d	0.100 ± 0.003	0.64 ± 0.01	5.3 ± 0.7		7.0 (0 d)		5.6 ± 0.1		91.9 ± 1
	0.102 ± 0.007	0.64 ± 0.01	5.3 ± 0.7	0.5		1.8 ± 0.1	2.7 ± 0.1		103 ± 1
7 d	0.102 ± 0.003	0.64 ± 0.01	5.3 ± 0.7		6.8 (5 d)		6.7 ± 0.1		112 ± 2
	0.101 ± 0.007	0.64 ± 0.01	5.3 ± 0.7	0.5		1.5 ± 0.3	3.2 ± 0.1	540	102 ± 9
24 d	0.104 ± 0.005	0.64 ± 0.01	5.3 ± 0.7		7.3 (14 d)		5.8 ± 0.1		100 ± 12
	0.099 ± 0.003	0.64 ± 0.01	5.3 ± 0.7	0.5		1.4 ± 0.1	3.4 ± 0.1	720	101 ± 5
33 d	0.102 ± 0.005	0.64 ± 0.01	5.3 ± 0.7		8.2 (33 d)		6.3 ± 0.1		106 ± 17
	0.100 ± 0.002	0.64 ± 0.01	5.3 ± 0.7	0.5		1.3 ± 0.1	4.0 ± 0.1	1000	107 ± 2

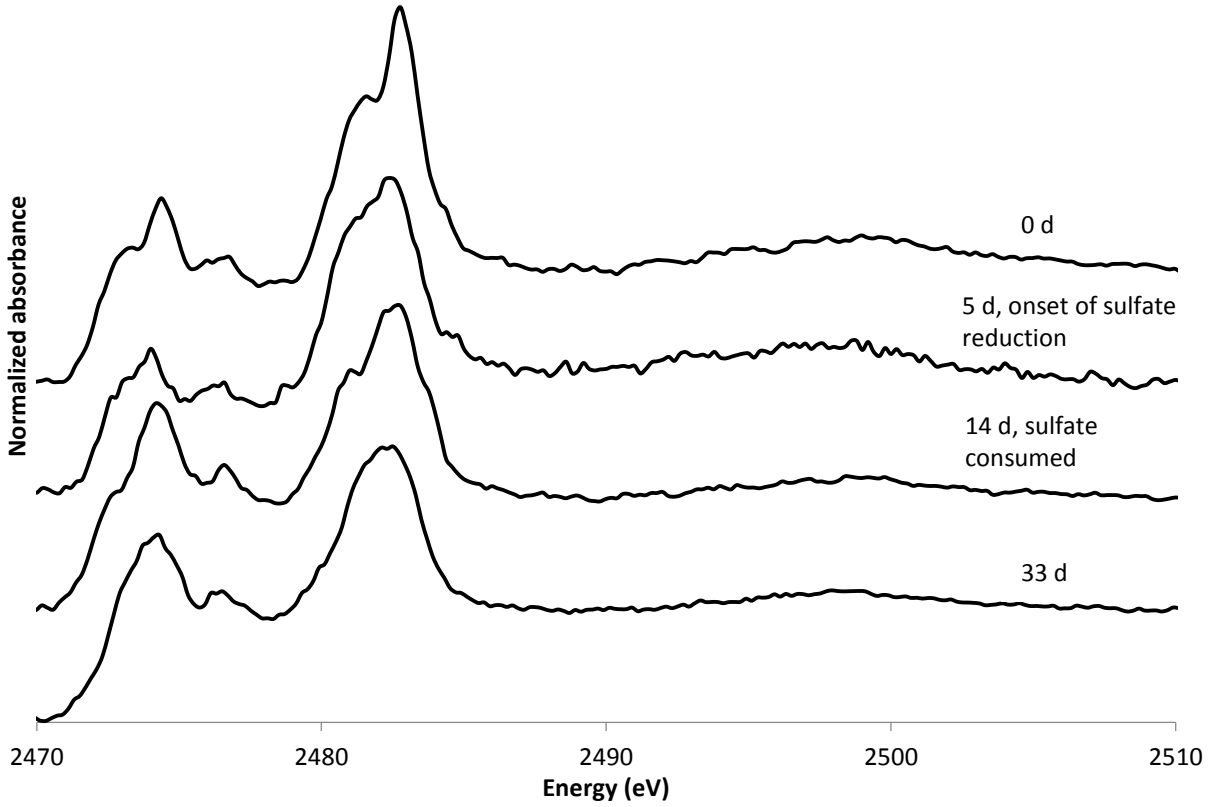

Figure 5.5. Sulfur XANES absorbance spectra obtained from ash-laden sediments for four times during the redox transition in the microcosms.

Table 5.3: Linear combination fitting of sulfur oxidation state for two reference compounds are compared with the database values (italics) and sulfur speciation in ash-laden sediment at four times and redox conditions in the microcosm incubation.

	Sulfur species of different oxidation states (%)						
	---------- oxidized ----------				---------- reduced ----------		
	sulfate	sulfonate	sulfone	sulfoxide	heterocyclic	exocyclic	inorganic reduced
Ash-laden sediment							
0 d	17	15	0.8	9.0	21	35	1.9
5 d, beginning of sulfate reduction	13	17	6.3	6.7	25	30	1.2
14 d, sulfate consumed	13	11	0.0	10	34	25	7.1
33 d	11	12	0.0	7.6	21	45	3.0
Reference compounds							
Nordic Aquatic HA (ALS database)	*4.9*	*13*	*6.4*	*3.6*	*37*	*24*	*12*
Nordic Aquatic HA (measured)	4.7	17	0.0	4.2	36	39	0.0
Elliot Soil HA (ALS database)	*18*	*26*	*4.9*	*6.4*	*29*	*15*	*0.6*
Elliot Soil HA (measured)	20	17	4.6	6.2	43	4.3	5.1

*HA is humic acid, ALS is the Advanced Light Source.

Reduced sulfur in the microcosm sediments increased from 7.0 to 8.2 mM, suggesting that some of the newly-formed reduced organic sulfur was generated in the sediment. Assuming that all of the sulfate became incorporated, this would only account for 0.55 mM of the1.2 mM estimated increase of reduced organic sulfur. Sulfide was not directly measured in pore water; however, S-XANES spectra contain a peak attributed to reduced inorganic sulfur at 14 d corresponding with the loss of sulfate from microcosm pore water. Absorption attributed to reduced inorganic sulfur in the XANES spectra increased by 5 % of the total sulfur, which is near the 4 % of total sulfur assumed to be released from sediment as sulfate initially. There was less reduced inorganic sulfur at 33 d than at 14 d. The decrease in absorption in the reduced inorganic sulfur energy range and increase in absorption in the reduced organic sulfur range suggests that a conversion to organic sulfur occurred. The incubation period in our experiment was sufficient for sulfide incorporation into organic matter, as others have observed sulfide being incorporated into organic matter at a rate of 0.17 h^{-1} (Heitman and Blodau, 2006). Additionally, the presence of ferrous iron in solution does not preclude sulfur incorporation into sediment organic matter (Werne *et al*., 2004). The amount of carbon in the microcosm vessel was 5.3 M (assuming carbon is 50 % of the sediment organic matter), which is much greater than the maximum concentration of ferrous iron (125 μM).

We can only speculate about the exact speciation of sulfur responsible for absorption in the reduced inorganic sulfur energy ranges. The ambiguity is due to overlap of energy absorption in sulfur of similar oxidation state. Specifically, pyrite, the outer sulfur atom of thiosulfate, elemental sulfur, di- and poly-sulfides, and the lower-energy range of thiols and organic sulfides all share the energy region of 2472.2 to 2474.0, the shoulder of the low energy absorption peak (Vairavamurthy, 1998; Figure 5.6). It is possible that many of these constituents were present in the ash-laden sediment. The measured dissolved iron in the pore water is assumed to be ferrous due to the onset of reducing conditions and the increase in iron concentration.

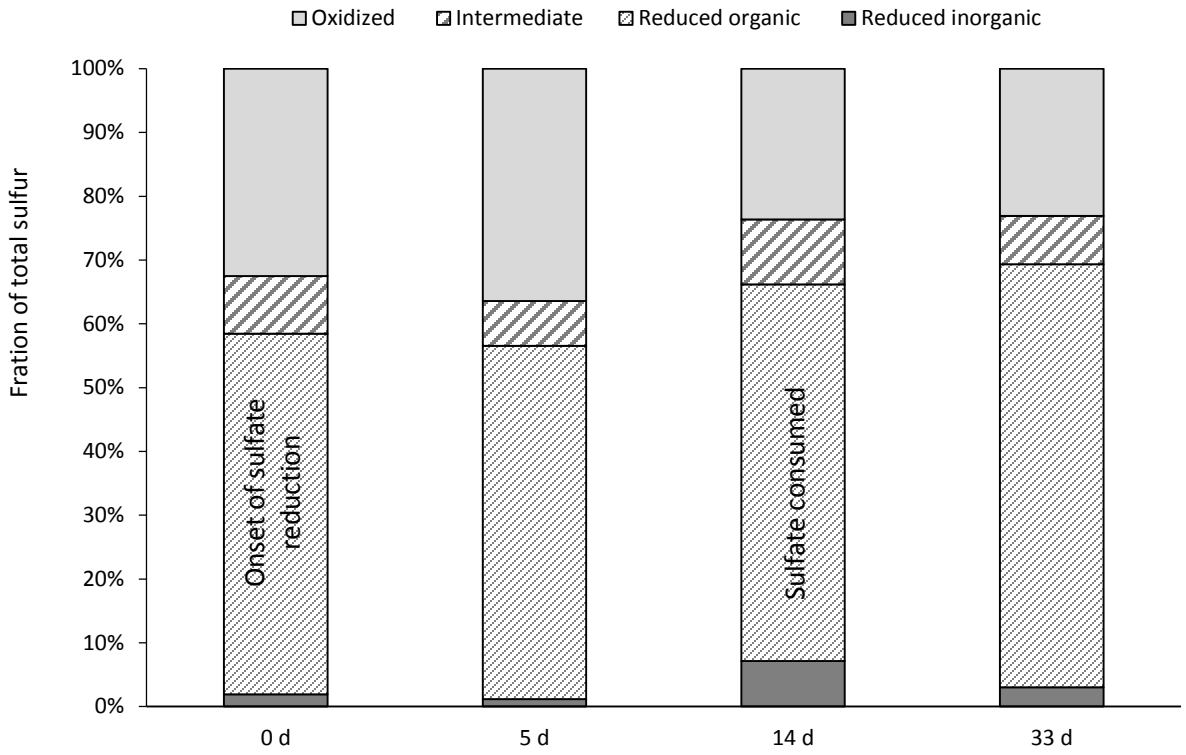

Figure 5.6: Fractional sulfur oxidation states of microcosm sediments are grouped into absorption regions.

Ferrous iron reacts with sulfide to form FeS (mackinawite), which is the form of most iron sulfide precipitates in the environment (Rickard and Luther, 2007). The absorption energy of FeS is 1 eV lower than that of FeS_2 (pyrite) suggests that the presence of mackinawite would be distinguishable in the absorption spectra if it were forming. Instead, absorption peaks in the reduced sulfur region are suggestive of elemental sulfur or polysulfides. Thiosulfate is formed through reactions of sulfide and organic matter, possibly quinone moieties, but it is likely a small component of total sulfur (Heitmann and Blodau, 2006).

Our observations of increased dissolved iron in the pore water during sulfate reduction suggest that newly-formed sulfide did not precipitate the ferrous iron present in the microcosm pore water at the onset of sulfate reduction (5 d; Figure 5.2). At the onset of sulfate reduction (5 d), the measured ferrous iron concentrations was 33 µM, and sulfate was 0.55 mM. The difference between these two concentrations suggests that the assumed production of sulfide from sulfate would have been sufficient for scavenging the relatively little ferrous iron present if FeS was precipitating. It is unknown if FeS could be responsible for the majority of the reduced inorganic sulfur absorption peak measured at 14 d, as it might be too stable to explain the diminished reduced inorganic sulfur content at 33 d.

Mercury Behavior in Microcosms

Mercury concentrations declined throughout the microcosm incubation. This decrease suggests that mercury in pore water was not controlled by the presence of dissolved organic matter or newly formed sulfides. If mercury release from sediment is controlled by organic matter complexation in the aqueous phase, the 3.5-fold increase in DOM (Figure 5.3) would be predicted to cause an increase in filter-passing mercury. Additionally, sulfate reduction, which we assume produced sulfide, did not appear to influence mercury in the pore water. If mercury and sulfide were reacting and forming metacinnabar, precipitation would lead to a decrease in pore water mercury concentrations between

5 d and 14 d. A similar decrease in pore water mercury would occur if co-precipitation with newly-formed FeS were occurring. The lack of precipitation could be due to high DOM concentrations stabilizing mercuric sulfide colloids to prevent continued growth of particles (Aiken *et al*., 2011; Gerbig *et al*., 2011). Over the course of the incubations, simultaneous declines in both filter-passing and colloidal mercury, and an overall 3.5-fold increase in DOM, suggests that mercury had an increased affinity for the ash-laden sediments. This increase in sediment association was likely driven by the measured increase in reduced organic sulfur in the sediments.

The competitive ligand exchange experiments revealed a 10-fold increase in strong binding sites between 0 d and 33 d. The increase in mercury binding capacity of the ash-laden sediment during the microcosm incubation was attributed to measured increases in reduced organic sulfur. Reduced organic sulfur was the most prevalent mercury binding component of the sediment, accounting for 66 % of the total sulfur at 33 d; however, we also have to acknowledge that mercury interactions with reduced inorganic sulfur could contribute to the distribution of added mercury between the ligand and the sediment. Precipitated iron-sulfide, for instance, could be providing a site for mercury binding in the sediment (Skyllberg and Drott, 2010), causing our distribution to favor the solid phase. Additionally, mercury could react with free sulfide and precipitate as metacinnabar in the sediment.

Summary

This study reveals the behavior of mercury and sulfur during a redox transition that attempted to simulate the deposition of ash-laden sediment in oxygen limited environments. Sulfur XANES analysis of sediment collected throughout the microcosm incubation revealed that sulfur underwent oxidation state shifts throughout the transitioning redox conditions. Sulfur oxidation state transitions are mainly observed as a loss of highly oxidized sulfur from 32 % to 23 % total sulfur, and an increase from 56 % to 66 % reduced organic sulfur over the 33 d incubation. The formation of reduced inorganic sulfur was

identified by sulfur XANES at the point of sulfate depletion (7 %, 14 d), but this was followed by a decline to only 3% of total sulfur at 33 d. We can only speculate on the species responsible for this absorption peak in the XANES spectra.

We observed an increase in mercury association with ash-laden sediments throughout the incubation. While a fraction of mercury was initially released as a pulse, the transition through increasingly reducing conditions resulted in an increase in binding of mercury by the ash-laden sediment. Increased mercury affinity for the ash-laden sediment was characterized by a decrease in the filter-passing and colloidal mercury concentration in the pore water over time and decreasing exchange of mercury from the sediments in the presence strong mercury binding ligand. Over the course of a 33 d incubation, mercury binding capacity of ash-laden sediment increased by 10-fold based on mercury distribution and basic equilibrium calculations. The increase in mercury binding was attributed to the increase in reduced organic sulfur in the ash-laden sediment.

Chapter 6

Summary and Future Work

Summary

Studies measuring the release of mercury during wildfire are usually limited by a paucity of pre-fire data because it is difficult to predict where a forest fire will occur. The use of an adjacent unburned area is typically used as a control from which to measure the effects of fire. This can be problematic as the effects of forest fire vary locally and forest soils can be heterogeneous. Therefore, studies limited to a few locations might not truly represent changes in soil mercury caused by fire. To circumvent the problem of under-sampling and reduce the potential for mischaracterizing soil mercury losses from a particular forest type, we evaluated soils on a large scale, using average soil mercury values from nearly 100 sites in our comparison of mercury losses from pinion-juniper forest of southwestern Colorado.

Many previous studies examining the effects of wildfire on water quality are strictly from a hydrologic (increases in flow, soil infiltration), or morphological (erosional processes, sediment transport) perspective. There are far fewer studies characterizing geochemical effects of wildfire on downstream waterbodies (Smith *et al*., 2011; Bodi *et al.*, 2014). Also noted by Smith *et al*. (2011), there are only a few studies which have measured the concentrations of dissolved trace metals exported from recently burned watersheds. Furthermore, studies of the geochemical processes taking place in ash-laden sediments appear to be non-existent.

Effects of Wildfire on Soil Mercury and Organic Matter

In pinion-juniper forests of southwestern Colorado, wildfire was found to consistently cause a 60 % loss of Hg in the first 4 cm of soil. We compared soil mercury content among two historical fires, occurring in 1934 and 2000, and determined an average accumulation rate of 0.06 g ha^{-1} y^{-1}. This deposition rate was similar to wet deposition rates measured in the Park over the previous decade

(0.063 g ha^{-1} y^{-1}) reported by the Mercury Deposition Network. Using the estimated deposition rate, we were able to adjust our mercury release estimates, which ranged from 9.5 ± 1.8 g ha^{-1} to 22 ± 7.9 g ha^{-1} depending on initial mercury content. In addition to atmospheric emissions, we found that unburned soils tended to release a greater total amount of organic matter and mercury into aqueous solution compared to the burned soil; however, burned and unburned soils release the same fractional percentage of soil mercury into solution. These results apply to historical burns only and runoff could have already mobilized readily releasable organic matter and mercury.

The results of this study suggest substantial atmospheric mercury is released from arid soils during wildfire if all of the mercury is vaporized during heating in gaseous form.. These release estimates contribute to the relatively few studies providing such information. These data will be very useful for constraining estimates of atmospheric mercury re-emission during wildfire and predicting mercury retention in burned soils.

Soil Heating Effects on Mercury, Organic Matter, and Sulfur

Soil heating at low and intermediate temperatures (100-250°C) are of most interest for mercury binding and transport. Soil heated beyond 250°C will lose nearly all of the initial mercury, whereas soils heated to less than 150°C are unlikely to lose much mercury and will undergo only minor changes to organic matter and organic sulfur.

In contrast to soils collected from historical burns from Mesa Verde National Park, soil subjected to furnace heating resulted in a 5-fold increase in releasable organic matter. Heating produced increases in leachable organic matter below 200°C, which we attributed to the thermal breakdown of larger polymers in the soil matrix. Once temperatures surpassed a threshold near 200°C, onset of condensation reactions and the formation of increasingly aromatic and less soluble molecules was

observed as a simultaneous increase in specific ultraviolet absorption ($SUVA_{254}$) and decrease in dissolved organic matter release.

The fractional release of mercury from soil to water increased with heating treatment, similar to organic matter release. However, the total amount of mercury released into solution was consistently lower in heated soils due to losses of mercury from the soils during heating. The increase in fractional mercury release was attributed the presence of much greater amounts of organic matter in solution.

Sulfur X-ray absorbance near edge structure spectroscopy (S-XANES) analyses revealed that heating greatly increased highly oxidized sulfur in soil. Confirming this, soils heated for 2 h and 225°C released 14-fold more sulfate into solution than unheated soils. Comparison of highly-oxidized sulfur in XANES spectra with measurements of aqueous sulfate revealed that nearly all of the highly-oxidized sulfur in heated soils was soluble inorganic sulfate. The shift to sulfate is at the expense of all sulfur species excluding heterocyclic reduced organic sulfur, which was increased in relative abundance after heating. The increase in heterocyclic oxidation states pointed toward the addition of sulfur to aromatic functional groups during heating. This functionality, likely similar to thiophenes, was attributed to thermally degraded amino acids generated through Maillard's reactions.

The conversion of sulfur to highly-oxidized oxidation states during heating did not decrease binding capacity. Instead, heated soils retained more mercury in the presence of a ligand than unheated soils. These results did not support our hypothesis that oxidation of sulfur would decrease soil binding capacity. We attributed the increase in binding capacity to the addition of thermogenic sulfide across the unsaturated bonds in organic matter, resulting in terminal thiol-functional groups.

The results of this study provide the first characterization of sulfur transformation in heated soils and provides a likely contributing factor to reports of elevated sulfate in burned watersheds (Smith *et al*., 2011). The finding that mercury binding capacity was increase by heating suggest that mercury is

likely to be associated with sediment particles during transport from recently burned watersheds rather than in a dissolved phase.

Characterization of Mercury, Organic Matter, and Sulfur in Ash-Laden Sediment

In mobilized ash-laden sediments, total mercury in ash-laden sediment was found to be 51 ng g^{-1}. The concentration of mercury in the sediment did not appear to change during deposition into a reservoir, nor did the onset of early diagenesis appear to cause gains or losses of mercury content in the ash-laden sediment. Ash-laden sediment at the bottom of the reservoir had much higher methylmercury concentrations (4.5 ng g^{-1}) than the native sediment (0.4 - 0.6 ng g^{-1}), and these concentrations were observed to remain elevated at the last point we measured methylmercury (20 weeks following deposition).

Following transport of ash-laden sediment though a watershed, we found that sulfur oxidation state shifted in the ash-laden sediment. In bank sediments, sulfur was primarily measured as organic forms, but deposition into a reservoir resulted in greater reduced inorganic sulfur. Ash-laden bank sediments contained 2 % reduced inorganic, 57 % reduced organic, 9 % moderately oxidized organic, and 33 % highly-oxidized sulfur. We found that the ash laden sediment collected from a reservoir in August 2012 (deposited in July 2012) contained 35 % reduced inorganic sulfur, compared to 2 % reduced inorganic sulfur in the bank sediment. However, sulfur oxidation states were dynamic and aging throughout a reservoir turnover cycle, resulting in a shift toward reduced organic sulfur species. Ash-laden sediment collected in November 2012 was modelled to contain 25 % reduced inorganic sulfur and ash-laden sediment collected in May 2013 contained only 1 % reduced inorganic sulfur. The formation of organic sulfur may be enhanced by redox transitions occurring during reservoir turnover.

The results of this study demonstrate that sulfur in ash-laden sediment undergoes a reductive transformation, which leads to reduced organic sulfur formation. While the occurrence of

methylmercury was high, the presence of reduced organic sulfur in reservoir sediments could be a control on fate and transport of trace-metals in ash-laden sediment.

The Effects of Reducing Conditions on Mercury, Organic Matter, and Sulfur in Ash-Laden Sediment

Over the course of a 33 d incubation simulating deposition of ash laden sediment in a reservoir, there was an overall 3.5 fold increase in pore water DOM. The release of DOM into pore water did not correspond to an increase in pore water mercury predicted by the complexation of mercury by DOM. Instead, we measured decreases in both filter-passing and colloidal mercury over the course of the incubation. The observed transfer of mercury from the aqueous phase to the sediment phase suggests that mercury has an increased affinity for the ash-laden sediments. Confirming this, there was a 15 % shift in mercury distribution favoring sediment in the presence of a competing ligand. This observation corresponds to an approximate 10-fold increase in strong binding capacity as a result of reducing conditions. We attributed the increase in strong binding to increased reduced organic sulfur content in the sediments. Ash-laden sediments in reducing conditions undergo a shift in sulfur speciation consistent with sulfide incorporation. Highly-oxidized sulfur decreased from 33 % to 23 % while reduced organic sulfur increased from 56 % to 66 % of total sulfur. The presence of reduced inorganic sulfur was identified by sulfur XANES at the point of sulfate depletion, but this was followed by a decline to only 3 % of total sulfur at the end of our incubation. This detection of transient reduced inorganic sulfur is of interest due to its reactivity with the organic matter; however, we could only speculate on the species responsible for this absorption peak in the XANES spectra. Specifically, pyrite, the outer sulfur atom of thiosulfate, elemental sulfur, di- and poly-sulfides, and the lower energy range of thiols and organic sulfides all share the energy region of 2472.2 to 2474.0 eV in the XANES spectra.

The results of this study demonstrate an increase in mercury binding by ash laden sediments during a simulated deposition in a reservoir. The increase in mercury binding reveals that mercury

introduced into a waterbody under these conditions was likely sequestered by the sediment due to the formation of strong binding sites.

Future Work

Ash-laden sediments have previously been shown to increase sediment methylmercury (Caldewell *et al*. 2000, Kelly *et al*., 2006); however, the mechanism for increased methylation is still not entirely known. As shown in Chapter 3, wildfire increases sulfate and releasable organic matter, both of which could enhance sulfate reduction and methylation by sulfate reducing bacteria. There is also a possibility that the mercury associated with ash-laden sediment (possibly the ash and charcoal components not specifically examined in this study) is more favorable to methylation than typical watershed sediments. Future studies could benefit from characterization of mercury using tin-reducible mercury assays on ash laden sediments (Krabbenhoft *et al*., 1998). The use of tin-reducible assays have been demonstrated to correlate with the methylmercury production rates in a variety of sediments (Marvin-DiPasqauale *et al*., 2009). This assay would be of interest for forest floor materials prior to precipitation and mobilization. Additionally, applying this assay on sediments following transport, deposition, and early diagenesis could identify changes in mercury lability and methylation potential. Based on the increase in binding potential in sediments, it is hypothesized that there will be a decrease in methylation potential throughout early diagenesis.

Similar to experiments conducted on whole soils in this study, the use of competing ligands may be a valuable tool for characterizing changes in mercury binding capacity of dissolved organic matter originating from recently burned watersheds. It would be interesting to characterize changes in DOM-metal reactivity due to wildfire by applying the competitive ligand exchange-solid phase extraction (CLE-SPE) method (Hsu-Kim and Sedlak, 2003; Gasper *et al*., 2007). This could be a novel application of the method, as it has not been used to quantify changes to dissolved organic matter (DOM) binding

capacity, only to measure conditional stability constants. This experiment might also set the stage for identifying changes to strong binding ligand abundance in a variety of environments where DOM could undergo reductive and oxidative changes influencing its ability to strongly bind metals.

One of the current difficulties in describing metal behavior in surface water is obtaining appropriate stability constants. Ligands can be an effective, and one of the only available, means of measuring stability constants at low metal concentrations. However, there is also uncertainty in some of the values reported for metal-ligand stability constants. One example of such uncertainty is revealed by extended X-ray absorbance fine structure (EXAFS) spectroscopy of mercury complexes with *meso*-2,3-dimercaptosuccinc acid (George *et al*., 2004). These EXAFS studies revealed that complexes previously assumed to contain 1:1 complex stoichiometry are instead 2:2 or 3:3 complexes. The stability of such complexes are unreported and are likely many orders of magnitude greater than that of a true 1:1 complex. This is just one example of the uncertainties involved in using competing ligands as a tool for measuring stability constants. It would be exceedingly beneficial to produce a review that (1) identified data gaps in stability constants, (2) identified potential interferences for specific ligands, (3) matched particular ligands with appropriate measurements, and (4) provided a complete review on past uses of ligands for environmental measurements.

Concluding Statement

Overall, this study has investigated the geochemistry influencing trace metals following wildfire. The study attempts characterize atmospheric losses, aqueous release, sediment transport, and deposition effects on the fate and transport of mercury in recently burned watershed. This characterization is important for understanding environmental behavior of trace metals and adds to the limited body of work addressing the fate and transport of trace metals exported from recently burned watersheds.

References

Aiken, G. R., 1992. Chloride interference in the analysis of dissolved organic carbon by the wet oxidation method. *Environmental Science &Technology* **26**, 2435-2439.

Aiken, G. R., Hsu-Kim, H., Ryan, J. N., 2011. Influence of dissolved organic matter on the environmental fate of metals, nanoparticles, and colloids. *Environmental Science & Technology* **45**, 3196-3201.

Almendros, G., Knicker, H., Gonzalez-Vila, F. J., 2003. Rearrangement of carbon and nitrogen forms in peat after progressive thermal oxidation as determined by solid-state C-13 and N-15-NMR spectroscopy. *Organic Geochemistry* **34**, 1559-1568.

Amirbahman, A., Ruck, P. L., Fernandez, I. J., Haines, T. A., Kahl, J. S., 2004. The effect of fire on mercury cycling in the soils of forested watersheds: Acadia National Park, Maine, USA. *Water, Air, and Soil Pollution* **152**, 315-331.

Amos, H. M., Jacob, D. J., Holmes, C. D., Fisher, J. A., Wang, Q., Yantosca, R. M., Corbitt, E. S., Galarneau, E., Rutter, A. P., Gustin, M. S., Steffen, A., Schauer, J. J., Graydon, J. A., St. Louis, V. L., Talbot, R. W., Edgerton, E. S., Zhang, Y., Sunderland, E. M., 2012. Gas-particle partitioning of atmospheric Hg (II) and its effect on global mercury deposition. *Atmospheric Chemistry and Physics* **12**, 591-603.

Benoit, J. M., Gilmour, C. C., Heyes, A., Mason, R. P., Miller, C. L., 2003. Geochemical and biological controls over methylmercury production and degradation in aquatic ecosystems. In Cai, Y., Olin, B. C., (eds.) *Biogeochemistry of important trace elements*. *ACS Symposium Series* **835**, 262-297.

Benoit, J. M., Mason, R. P., Gilmour, C. C., Aiken, G. R., 2001. Constants for mercury binding by dissolved organic matter isolates from the Florida Everglades. *Geochimica et Cosmochimica Acta* **65**, 4445-4451.

Biester, H., Scholz, C., 1996. Determination of mercury binding forms in contaminated soils: Mercury pyrolysis versus sequential extractions. *Environmental Science & Technology* **31**, 233-239.

Biswas, A., Blum, J. D., Keeler, G. J., 2008. Mercury storage in surface soils in a central Washington forest and estimated release during the 2001 Rex Creek Fire. *Science of the Total Environment* **404**, 129-138.

Biswas, A., Blum, J. D., Klaue, B., Keeler, G. J., 2007. Release of mercury from Rocky Mountain forest fires. *Global Biogeochemical Cycles* **21,** 1-13.

Bloom, N. S., Preus, E., Katon, J., Hiltner, M., 2003. Selective extractions to assess the biogeochemically relevant fractionation of inorganic mercury in sediments and soils. *Analytica Chimica Acta* **479**, 233-248.

Bodi, M. B., Martin, D. A., Balfour, V. N., Santín, C., Doerr, S. H., Pereira, P., Cerdà, A., Mataix-Solera, J., 2014. Wildland fire ash: Production, composition and eco-hydro-geomorphic effects. *Earth-Science Reviews* **130**, 103-127.

Burke, M. P., Hogue, T. S., Ferreira, M., Mendez, C. B., Navarro, B., Lopez, S., Jay, J. A., 2010. The effect of wildfire on soil mercury concentrations in Southern California watersheds. *Water Air and Soil Pollution* **212**, 369-385.

Caldwell, C. A., Canavan, C. M., Bloom, N. S., 2000. Potential effects of forest fire and storm flow on total mercury and methylmercury in sediments of an arid-lands reservoir. *Science of the Total Environment* **260**, 125-133.

Carrara, P.E., 2012. Surficial geologic map of Mesa Verde National Park, Montezuma County, Colorado: U.S. Geological Survey Scientific Investigations Map 3224, 22 p.

CDPHE, 2015. Fish consumption site-specific guidelines. https://www.colorado.gov/pacific/cdphe/wq-fish-consumption-site-specific-guidelines. Colorado Department of Public Health and Environment, State of Colorado. Accesses 6-01-2015.

Cerny, C., Davideck, T., 2003. Formation of aroma compounds from ribose and cysteine during the Maillard reaction. *Journal of Agricultural and Food Chemistry* **51**, 2714-2712.

Certini, G., 2005. Effects of fire on properties of forest soils: A review. *Oecologia* **143,** 1-10.

Czimczik, C. I., Preston, C. M., Schmidt, M. W. I., Schulze, E. D., 2003. How surface fire in Siberian Scots pine forests affects soil organic carbon in the forest floor: Stocks, molecular structure, and conversion to black carbon (charcoal). *Global Biogeochemical Cycles* **17**, 1020, doi:10.1029/2002GB001956

DeBano, L. F., 2000. The role of fire and soil heating on water repellency in wildland environments: A review. *Journal of Hydrology* **231**, 195-206.

Demers, J. D., Blum, J. D., Zak, D. R., 2013. Mercury isotopes in a forested ecosystem: Implications for air-surface exchange dynamics and the global mercury cycle. *Global Biogeochemical Cycles* **27**, 222-238.

Demers, J. D., Driscoll, C. T., Fahey, T. J., Yavitt, J. B., 2007. Mercury cycling in litter and soil in different forest types in the Adirondack region, New York, USA. *Ecological Applications* **17**, 1341-1351.

DeWild, J. F., Olund, S. D., Olson, M. L., Tate, M. T., 2004. Methods for the preparation and analysis of solids and suspended solids for methylmercury. *U.S. Geological Survey Techniques and Methods*, Chapter A7, Book 5, 21.

Di Toro, D. M., Mahony, J. D., Hansen, D. J., Scott, K. J., Hicks, M. B., Mayr, S. M., Redmond, M. S., 1990. Toxicity of cadmium in sediments -the role of acid volatile sulfide. *Environmental Toxicology and Chemistry* **9**, 1487-1502.

Dornblaser, M., Giblin, A. E., Fry, B., Peterson, B. J., 1994. Effects of sulfate concentration in the overlying water on sulfate reduction and sulfur storage in lake sediments. *Biogeochemistry* **24**, 129-144.

Drexel, R. T., Haitzer, M., Ryan, J. N., Aiken, G. R., Nagy, K. L., 2002. Mercury(II) sorption to two Florida Everglades peats: Evidence for strong and weak binding and competition by dissolved organic matter released from the peat. *Environmental Science & Technology* **36**, 4058-4064.

Driscoll, C. T., Mason, R. P., Chan, H. M., Jacob, D. J., Pirrone, N., 2013. Mercury as a global pollutant: Sources, pathways, and effects. *Environmental Science & Technology* **47**, 4967-4983.

Ebel, B. A., Moody, J. A., Martin, D. A., 2012. Hydrologic conditions controlling runoff generation immediately after wildfire. *Water Resources Research* **48**, W03529, doi:10.1029/2011WR011470.

Einsiedl, F., Mayer, B., Schäfer, T., 2008. Evidence for incorporation of H2S in groundwater fulvic acids from stable isotope ratios and sulfur K-edge X-ray absorption near edge structure spectroscopy. *Environmental Science & Technology* **42**, 2439-2444.

Engle, M. A., Gustin, M. S., Johnson, D. W., Murphy, J. F., Miller, W. W., Walker, R. F., Wright, J. W., Markee, M., 2006. Mercury distribution in two Sierran forest and one desert sagebrush steppe ecosystems and the effects of fire. *Science of the Total Environment* **367**, 222-233.

Environmental Protection Agency (2015). National summary of impaired waters and TMDL information. Accessed at: http://iaspub.epa.gov/waters10/attains_nation_cy.control?p_report_type=T on 6-01-2015.

Fang, X., Hua, F., Fernando, Q., 1996. Comparison of *rac*- and *meso*-2,3-dimercaptosuccinic acids for chelation of mercury and cadmium using chemical speciation models. *Chemistry Research in Toxicolgy* **9**, 284-290.

Farrell R. F., Matthes S. A., Mackie A. J., 1980. A simple, low-cost method for the dissolution of metal and mineral samples in plastic pressure vessels, Report of investigations - Bureau of Mines 8480, 19 pages.

Fernandez, I., Cabaneiro, A., Carballas, T., 1997. Organic matter changes immediately after a wildfire in an Atlantic forest soil and comparison with laboratory soil heating. *Soil Biology & Biochemistry* **29**, 1-11.

Filley, T. R., Freeman, K. H., Wilkin, R. T., Hatcher, P. G., 2002. Biogeochemical controls on reaction of sedimentary organic matter and aqueous sulfides in Holocene sediments of Mud Lake, Florida. *Geochimica et Cosmochimica Acta* **66**, 937-954.

Floyd, M. L., Hanna, D. D., Romme, W. H., 2004. Historical and recent fire regimes in Pinon-Juniper woodlands on Mesa Verde, Colorado, USA. *Forest Ecology and Management* **198**, 269-289.

Friedli, H. R., Arellano, A. F., Cinnirella, S., Pirrone, N., 2009. Initial Estimates of Mercury emissions to the atmosphere from global biomass burning. *Environmental Science & Technology* **43**, 3507-3513.

Friedli, H. R., Radke, L. F., Lu, J. Y., 2001. Mercury in smoke from biomass fires. *Geophysical Research Letters* **28**, 3223-3226.

Friedli, H. R., Radke, L. F., Prescott, R., Hobbs, P. V., Sinha, P., 2003. Mercury emissions from the August 2001 wildfires in Washington State and an agricultural waste fire in Oregon and atmospheric mercury budget estimates. *Global Biogeochemical Cycles* **17**, 1039, doi:10.1029/2002GB001972.

Gasper, J. D., Aiken, G. R., Ryan, J. N., 2007. A critical review of three methods used for the measurement of mercury (Hg^{2+})-dissolved organic matter stability constants. *Applied Geochemistry* **22,** 1583-1597.

George, G. N., Prince, R. C., Gailer, J., Buttigieg, G. A., Denton, M. B., Harris, H. H., Pickering, I. J., 2004. Mercury binding to the chelation therapy agents DMSA and DPMS and the rational design of custom chelators for mercury. *Chemical Research in Toxicology* **17**, 999-106.

Gerbig, C. A., Kim, C. S., Stegemeier, J. P., Ryan, J. N., Aiken, G. R., 2011. Formation of nanocolloidal metacinnabar in mercury-DOM-sulfide systems. *Environmental Science & Technology* **45**, 9180-9187.

Gert-Jan De Maagd, J., Hulscher, D., Van Den Heuval, H., Opperhuizen A., Sijm, D.T.H.M., 1998. Physiochemical properties of polycyclic aromatic hydrocarbons: Aqueous solubilities, *n*-octanol/water partition coefficients, and Henry's law constants. *Environmental Toxicology and Chemistry* **17**, 251-257.

Gilmour, C. C., Elias, D. A. , Kucken, A. M., Brown, S. D., Palumbo, A. V., Schadt, C. W., Wall, J. D., 2011. Sulfate-reducing bacterium *Desulfovibrio desulfuricans* ND132 as a model for understanding bacterial mercury methylation. *Applied and Environmental Microbiology* **77**, 3938-3951.

Gilmour, C. C., Podar, M., Bullock, A. L., Graham, A. M., Brown, S. D., Somenahally, A. C., Johs, A., Hurt, R.A., Bailey, K.L., Elias, D. A., 2013. Mercury methylation by novel microorganisms from new environments. *Environmental Science & Technology* **47**, 11810-11820.

Gilmour, C. C., Krabbenhoft, D., Orem, W., Aiken, G. R., 2004. Influence of drying and rewetting on mercury and sulfur cycling in Everglades and STA soils. South Florida Water Management District, West Palm Beach, FL. Everglades Consolidated Report. Available at http://mytest.sfwmd.gov/portal/page/portal/pg_grp_sfwmd_sfer/portlet_prevreport/final/appendices/app2b-1.pdf accessed 601-2015.

Gonzalez-Perez, J. A., Gonzalez-Vila, F. J., Almendros, G., Knicker, H., 2004. The effect of fire on soil organic matter: A review. *Environment International* **30**, 855-870.

Graham, A. M., Aiken, G. R., Gilmour, C. C., 2012. Dissolved organic matter enhances microbial mercury methylation under sulfidic conditions. *Environmental Science & Technology* **46**, 2715-2723.

Gray, J. E., Fey, D. L., Holmes, C. W., Lasorsa, B. K., 2005. Historical deposition and fluxes of mercury in Narraguinnep Reservoir, southwestern Colorado, USA. *Applied Geochemistry* **20**, 207-220.

Gray, J. E., Hines, M. E., Goldstein, H. L., Reynolds, R. L., 2014. Mercury deposition and methylmercury formation in Narraguinnep Reservoir, southwestern Colorado, USA. *Applied Geochemistry*, ***50*** 82-90.

Grigal, D. F., 2003. Mercury sequestration in forests and peatlands. *Journal of Environmental Quality* **32**, 393-405.

Haitzer, M., Aiken, G. R., Ryan, J. N., 2002. Binding of mercury(II) to dissolved organic matter: The role of the mercury-to-DOM concentration ratio. *Environmental Science & Technology* **36**, 3564-3570.

Haitzer, M., Aiken, G. R., Ryan, J. N.,2003. Binding of mercury(II) to aquatic humic substances: Influence of pH and source of humic substances. *Environmental Science & Technology* **37**, 2436-2441.

Heitmann, T., Blodau, C., 2006. Oxidation and incorporation of hydrogen sulfide by dissolved organic matter. *Chemical Geology* **235**, 12-20.

Hesterberg, D., Chou, J. W., Hutchison, K. J., Sayers, D. E., 2001. Bonding of Hg(II) to reduced organic, sulfur in humic acid as affected by S/Hg ratio. *Environmental Science & Technology* **35**, 2741-2745.

Hofacker, A. F., Voegelin, A., Kaegi, R., Kretzschmar, R., 2013. Mercury mobilization in a flooded soil by incorporation into metallic copper and metal sulfide nanoparticles. *Environmental Science & Technology* **47**, 7739-7746.

Hofacker, A. F., Voegelin, A., Kaegi, R., Weber, F. A., Kretzschmar, R., 2013. Temperature-dependent formation of metallic copper and metal sulfide nanoparticles during flooding of a contaminated soil. *Geochimica et Cosmochimica Acta* **103**, 316-332.

Hoffmann, M., Mikutta, C., Kretzschmar, R., 2012. Bisulfide reaction with natural organic matter enhances arsenite sorption: Insights from X-ray absorption spectroscopy. *Environmental Science & Technology* **46**, 11788-11797.

Holmer, M., Storkholm, P., 2001. Sulphate reduction and sulphur cycling in lake sediments: A review. *Freshwater Biology* **46**, 431-451.

Hsu-Kim, H., Kucharzyk, K. H., Zhang, T., Deshusses, M. A., 2013. Mechanisms regulating mercury bioavailability for methylating microorganisms in the aquatic environment: A critical review. *Environmental Science &Technology* **47**, 2441-2456.

Hsu-Kim, H., Sedlak, D. L., 2003. Strong Hg(II) complexation in municipal wastewater effluent and surface waters. *Environmental Science & Technology* **37**, 2743-2749.

Hsu-Kim, H., Sedlak, D. L., 2005. Similarities between inorganic sulfide and the strong Hg(II) - Complexing ligands in municipal wastewater effluent. *Environmental Science & Technology* **39**, 4035-4041.

Huffman, E. W D., Stuber, H. A., 1985. Analytical methodology for elemental analysis of humic substance. In Aiken, G., R., McKnight, D. M., MacCarthy, P. (eds.), *Humic Substances in Soil, Sediment, and Water*. Wiley, New York, pp. 433-455.

Hynes, A. J., Donohoue, D. L., Goodsite, M. E., Hedgecock, I. M., 2009. Our current understanding of major chemical and physical processes affecting mercury dynamics in the atmosphere and at the air-water/terrestrial interfaces. In Pirrone, N., Mason, R.P. (eds.), *Mercury Fate and Transport in the Global Atmosphere*. Springer, USA, pp. 427-457.

Ice, G. G., Neary, D. G., Adams, P. W., 2004. Effects of wildfire on soils and watershed processes. *Journal of Forestry* **102**, 16-20.

Jonsson, S., Skyllberg, U., Nilsson, M. B., Westlund, P. O., Shchukarev, A., Lundberg, E., Björn, E., 2012. Mercury methylation rates for geochemically relevant Hg(II) species in sediments. *Environmental Science & Technology* **46**, 11653-11659.

Karlsson, T., Skyllberg, U., 2003. Bonding of ppb levels of methyl mercury to reduced sulfur groups in soil organic matter. *Environmental Science & Technology* **37**, 4912-4918.

Kasischke, E. S., Verbyla, D. L., Rupp, T. S., McGuire, A. D., Murphy, K. A., Jandt, R., Barnes, J. L., Hoy, E. E., Duffy, P. A., Calef, M.,Turetsky, M. R., 2010. Alaska's changing fire regime-implications for the vulnerability of its boreal forests. *Canadian Journal of Forest Research* **40**, 1313-1324.

Kelly, E. N., Schindler, D. W., St Louis, V. L., Donald, D. B., Vlaclicka, K. E., 2006. Forest fire increases mercury accumulation by fishes via food web restructuring and increased mercury inputs. *Proceedings of the National Academy of Sciences of the United States of America* **103**, 19380-19385.

Khwaja, A. R., Bloom, P. R., Brezonik, P. L., 2006. Binding constants of divalent mercury (Hg^{2+}) in soil humic acids and soil organic matter. *Environmental Science & Technology* **40**, 844-849.

Knicker, H., 2007. How does fire affect the nature and stability of soil organic nitrogen and carbon? A review. *Biogeochemistry* **85**, 91-118.

Knicker, H., Almendros, G., Gonzalez-Vila, F. J., Gonzalez-Perez, J. A., Polvillo, O., 2006. Characteristic alterations of quantity and quality of soil organic matter caused by forest fires in continental Mediterranean ecosystems: A solid-state ^{13}C NMR study. *European Journal of Soil Science* **57**, 558-569.

Knicker, H., Hilscher, A., Gonzalez-Vila, F. J., Almendros, G., 2008. A new conceptual model for the structural properties of char produced during vegetation fires. *Organic Geochemistry* **39**, 935-939.

Kok, M. D., Schouten, S., Damsté, J. S. S., 2000. Formation of insoluble, nonhydrolyzable, sulfur-rich macromolecules via incorporation of inorganic sulfur species into algal carbohydrates. *Geochimica et Cosmochimica Acta* **64**, 2689-2699.

Krabbenhoft, D. P., Fink, L. E., 2001. Appendix 7-8, The effect of dry down and natural fires on mercury methylation in the Florida Everglades. In: 2001 Everglades Consolidated Report. South Florida Water Management District, West Palm Beach, FL, 2001.14 pp

Krabbenhoft, D. P., Hurley, J. P., Olson, M. L., Cleckner, L. B., 1998. Diel variability of mercury phase and species distributions in the Florida Everglades. *Biogeochemistry* **40**, 311-325.

Lee, B. G., Griscom, S. B., Lee, J. S., Choi, H. J., Koh, C. H., Luoma, S. N., Fisher, N. S., 2000. Influences of dietary uptake and reactive sulfides on metal bioavailability from aquatic sediments. *Science* **287**, 282-284.

Littell, J. S., McKenzie, D., Peterson, D. L., Westerling, A. L., 2009. Climate and ecoprovince fire area burned in western U.S. ecoprovinces, 1916-2003. *Ecological Applications* **19**, 1003-1021.

Mack, M. C., Bret-Harte, M. S., Hollingsworth, T. N., Jandt, R. R., Schuur, E. A. G., Shaver, G. R., Verbyla, D. L., 2011. Carbon loss from an unprecedented Arctic tundra wildfire. *Nature* **475**, 489-492.

Madsen, M. D., Zvirzdin D. L., Peterson, S. L., Hopkins, B. G., Roundy, B. A., Chandler, D. G., 2011. Soil Water repellency within a burned pinon-juniper woodland: Spatial distribution, severity, and ecohydrological implications. *Forest, Range & Wildland Soils* **75**, 1543-1553.

Manceau, A., Nagy, K. L., 2012. Quantitative analysis of sulfur functional groups in natural organic matter by XANES spectroscopy. *Geochimica et Cosmochimica Acta* **99**, 206-223.

Marcus, M.A., 2010. Linear Fit w overabsorption. In-house XANES fitting software. Available at https://sites.google.com/a/lbl.gov/microxas-lbl-gov/software

Martinez, C. E., McBride, M. B., Kandianis, M. T., Duxbury, J. M., Yoon, S. J., Bleam, W. F., 2002. Zinc-sulfur and cadmium-sulfur association in metalliferous peats evidence from spectroscopy, distribution coefficients, and phytoavailability. *Environmental Science & Technology* **36**, 3683-3689.

Marvin-DiPasquale, M., Lutz, M. A., Brigham, M. E., Krabbenhoft, D. P., Aiken, G. R., Orem, W. H., Hall, B. D., 2009. Mercury cycling in stream ecosystems. 2. Benthic methylmercury production and bed sediment− pore water partitioning. *Environmental Science & Technology* **43**, 2726-2732.

McCoy, V. M., Burn, C. R., 2005. Potential alteration by climate change of the forest-fire regime in the Boreal forest of central Yukon Territory. *Arctic* **58**, 276-285.

McGrath , T. E., Chan, W. G., Hajaligol, M. R., 2003. Low temperature mechanism for the formation of polycyclic aromatic hydrocarbons from the pyrolysis of cellulose. *Journal of Analytical and Applied Pyrolysis* **66**, 51-70.

Mierle, G., Ingram, R., 1991. The role of humic substances in the mobilization of mercury from watersheds. *Water, Air, and Soil Pollution* **56**, 349-357.

Mitchell, C. P., Kolka, R. K., Fraver, S., 2012. Singular and combined effects of blowdown, salvage logging, and wildfire on forest floor and soil mercury pools. *Environmental Science & Technology* **46**, 7963-7970.

Moody, J. A., Martin, D. A., 2001. Initial hydrologic and geomorphic response following wildfire in the Colorado Front Range. *Earth Surface Processes and Landforms* **26**, 1049-1070.

Mottram D.D., 1998. Flavour formation in meat and meat products: A review. *Food chemistry* **62,** 415-424.

Nagy, K. L., Manceau, A., Gasper, J. D., Ryan, J. N., Aiken, G. R., 2011. Metallothionein-Like Multinuclear Clusters of Mercury(II) and Sulfur in Peat. *Environmental Science & Technology* **45**, 7298-7306.

National Atmospheric Deposition Program*,* Mercury Deposition Network (MDN): A NADP Network*,http://nadp.sws.uiuc.edu/mdn/, NADP Program Office, Ill. State Water Surv.,* Champaign*.* Mercury deposition data accesses on 5-30-15.

National Park Service, 2009. Mesa Verde National Park, Colorado, Fire History: 1933-2008, http://www.nps.gov/meve/learn/management/upload/fire_map_2008.pdf. Department of the Interior. Accessed on 7-13-2015.

Neary, D. G., Ryan, K. C., DeBano, L. F., 2005. Wildland fire in ecosystems: Effects of fire on soils and water. *General Technical Report,* RMRS-GTR-42-vol, 4, Ogden, UT: USDA Forest Service, Rocky Mountain Research Station. 250 p.

Obrist, D., 2012. Mercury distribution across 14 US forests. Part II: Patterns of methyl mercury concentrations and areal mass of total and methyl mercury. *Environmental Science & Technology* **46**, 5921-5930.

Obrist, D., Johnson, D. W., Lindberg, S. E., Luo, Y., Hararuk, O., Bracho, R., Battles, J. J., Dail, D. B., Edmonds, R. L., Monson, R. K., Ollinger, S. V., Pallardy, S. G., Pregitzer, K. S., Todd, D. E., 2011. Mercury distribution across 14 US forests. Part I: Spatial patterns of concentrations in biomass, litter, and soils. *Environmental Science & Technology* **45**, 3974-3981.

Obrist, D., Moosmüller, H., Schürmann, R., Chen, L. W. A., Kreidenweis, S. M., 2007. Particulate-phase and gaseous elemental mercury emissions during biomass combustion: Controlling factors and correlation with particulate matter emissions. *Environmental Science & Technology* **42**, 721-727.

Obrist, D., Pokharel, A. K., Moore, C., 2014. Vertical profile measurements of soil air suggest immobilization of gaseous elemental mercury in mineral soil. *Environmental Science & Technology* **48**, 2242-2252.

Olefeldt, D., Turetsky, M. R., Blodau, C., 2013. Altered Composition and microbial versus UV-mediated degradation of dissolved organic matter in boreal soils following wildfire. *Ecosystems* **16**, 1396-1412.

Oropeza, J., Heath, J., 2013. Five Year Summary Report (2008- 2012). *Upper Cache la Poudre River Collaborative Water Quality Monitoring Program Report*. City of Fort Collins. Accessed at http://www.fcgov.com/utilities/img/site_specific/uploads/2012_Five_Year_Summary_Report_Upper_CLP.pdf on 5-24-2015

Parsons, A., 2003. Burned area emergency rehabilitation (BAER) soil burn severity definitions and mapping guidelines. USDA Forest Service, Rocky Mountain Research Station. (Missoula, MT) Available at http://www.fws.gov/fire/ifcc/esr/Remote%20Sensing/soil_burnsev_summary_guide042203.pdf [Accesses 6-01-15].

Pearson, R. G., 1963. Hard and soft acids and bases. *Journal of the American Chemical Society* **85**, 3533-3539.

Perlinger, J. A., Kalluri, V. M., Venkatapathy, R., Angst, W., 2002. Addition of hydrogen sulfide to juglone. *Environmental Science & Technology* **36**, 2663-2669.

Pham, A. L. T., Morris, A., Zhang, T., Ticknor, J., Levard, C., Hsu-Kim, H., 2014. Precipitation of nanoscale mercuric sulfides in the presence of natural organic matter: Structural properties, aggregation, and biotransformation. *Geochimica et Cosmochimica Acta*, **133**, 204-215.

Pirrone, N., Cinnirella, S., Feng, X., Finkelman, R. B., Friedli, H. R., Leaner, J., Mason, R., Mukherjee, A. B., Stracher, G. B., Streets D. G., Telmer, K., 2010. Global mercury emissions to the atmosphere from anthropogenic and natural sources. *Atmospheric Chemistry and Physics* **10**, 5951-5964.

Pokharel, A. K., Obrist, D., 2011. Fate of mercury in tree litter during decomposition. *Biogeosciences* **8**, 2507-2521.

Poulin, B. A., Ryan, J. N., Aiken, G. R., 2014. Effects of iron on optical properties of dissolved organic matter. *Environmental Science & Technology* ***48***, 10098-10106.

Poulin J., Gibb, H., 2008. Mercury: Assessing the environmental burden of disease at national and local levels. Editor, Prüss-Üstün A. WHO Environmental Burden of Disease Series No. 16. World Health Organization, Geneva. Accessed at http://whqlibdoc.who.int/publications/2008/9789241596572_eng.pdf. Accessed on 6-01-15.

Prietzel, J., Thieme, J., Neuhausler, U., Susini, J., Kogel-Knabner, I., 2003. Speciation of sulphur in soils and soil particles by X-ray spectromicroscopy. *European Journal of Soil Science* **54**, 423-433.

Prietzel, J., Thieme, J., Salome, M., Knicker, H., 2007. Sulfur K-edge XANES spectroscopy reveals differences in sulfur speciation of bulk soils, humic acid, fulvic acid, and particle size separates. *Soil Biology & Biochemistry* **39**, 877-890.

Prietzel, J., Thieme, J., Tyufekchieva, N., Paterson, D., McNulty, I., Kogel-Knabner, I., 2009. Sulfur speciation in well-aerated and wetland soils in a forested catchment assessed by sulfur K-edge X-ray absorption near-edge spectroscopy (XANES). *Journal of Plant Nutrition and Soil Science* **172**, 393-403

Qian, J., Skyllberg, U., Frech, W., Bleam, W. F., Bloom, P. R., Petit, P. E., 2002. Bonding of methylmercury to reduced sulfur groups in soil and stream organic matter as determined by X-ray absorption spectroscopy and binding affinity studies. *Geochimica et Cosmochimica Acta* **66**, 3873-3885.

Ranchou-Peyruse, M., Monperrus, M., Bridou, R., Duran, R., Amouroux, D., Salvado, J. C., Guyoneaud, R., 2009. Overview of mercury methylation capacities among anaerobic bacteria including representatives of the sulphate-reducers: Implications for environmental studies. *Geomicrobiology Journal* **26**, 1-8.

Ravichandran, M. 2004. Interactions between mercury and dissolved organic matter – A review. *Chemosphere* ***55,*** 319-331.

Rea, A. W., Lindberg, S. E., Keeler, G. J., 2000. Assessment of dry deposition and foliar leaching of mercury and selected trace elements based on washed foliar and surrogate surfaces. *Environmental Science & Technology* **34**, 2418-2425.

Rea, A. W., Lindberg, S. E., Keeler, G. J., 2001. Dry deposition and foliar leaching of mercury and selected trace elements in deciduous forest throughfall. *Atmospheric Environment* **35**, 3453-3462.

Rea, A. W., Lindberg, S. E., Scherbatskoy, T., Keeler, G. J., 2002. Mercury accumulation in foliage over time in two northern mixed-hardwood forests. *Water, Air, and Soil Pollution* **133**, 49-67.

Reinhardt, E. D., Dickinson, M. B., 2010. First-order fire effects models for land management: overview and issues. *Fire Ecology* **6**, 131-142.

Rickard, D., & Luther, G. W. (2007). Chemistry of iron sulfides. *Chemical Reviews* ***107***, 514-562.

Riscassi, A. L., Scanlon, T. M., 2011. Controls on stream water dissolved mercury in three mid-Appalachian forested headwater catchments. *Water Resources Research* **47**, 1-16.

Rutter, A. P., Schauer, J. J., Shafer, M. M., Creswell, J. E., Olson, M. R., Robinson, M., Collins, R. M., Parman, A. M., Katzman, T. L., Mallek, J. L., 2011. Dry deposition of gaseous elemental mercury to plants and soils using mercury stable isotopes in a controlled environment. *Atmospheric Environment* **45**, 848-855.

San Miguel, G., 2011. Natural Resource Manager at Mesa Verde National Park. Corresponded through face-to-face meetings and email correspondence.

Schelker, J., Burns, D. A., Weiler, M., Laudon, H., 2011. Hydrological mobilization of mercury and dissolved organic carbon in a snow-dominated, forested watershed: Conceptualization and modeling. *Journal of Geophysical Research: Biogeosciences* **116,** 1-17.

Schroth, A. W., Bostick, B. C., Graham, M., Kaste, J. M., Mitchell, M. J., Friedland, A. J., 2007. Sulfur species behavior in soil organic matter during decomposition. *Biogeosciences* **112**, 1-10.

Schuster, P. F., Striegl, R. G., Aiken, G. R., Krabbenhoft, D. P., DeWild, J. F., Butler, K., Kamark, B., Dornblaser, M., 2011. Mercury export from the Yukon River Basin and potential response to a changing climate. *Environmental Science & Technology* **45**, 9262-9267.

Selin, N. E., 2009. Global biogeochemical cycling of mercury: A review. *Annual Review of Environment and Resources* **34**, 43-63.

Selin, N. E., Jacob, D. J., Park, R. J., Yantosca, R. M., Strode, S., Jaeglé, L., Jaffe, D., 2007. Chemical cycling and deposition of atmospheric mercury: Global constraints from observations. *Journal of Geophysical Research: Atmospheres* **112**, 1-14.

Sherman, L. S., Blum, J. D., Keeler, G. J., Demers, J. D., Dvonch, J. T., 2012. Investigation of local mercury deposition from a coal-fired power plant using mercury isotopes. *Environmental Science & Technology* **46**, 382-390.

Skyllberg, U., Bloom, P. R., Qian, J., Lin, C. M., Bleam, W. F., 2006. Complexation of mercury (II) in soil organic matter: EXAFS evidence for linear two-coordination with reduced sulfur groups. *Environmental Science & Technology* **40**, 4174-4180.

Skyllberg, U. 2008. Competition among thiols and inorganic sulfides and polysulfides for Hg and MeHg in wetland soils and sediments under suboxic conditions: Illumination of controversies and implications for MeHg net production. *Journal of Geophysical Research: Biogeosciences* **113**, 2005-2012.

Skyllberg, U., Drott, A., 2010. Competition between disordered iron sulfide and natural organic matter associated thiols for mercury(II) - An EXAFS study. *Environmental Science & Technology* **44**, 1254-1259.

Skyllberg, U., Xia, K., Bloom, P. R., Nater, E. A., Bleam, W. F., 2000. Binding of mercury (II) to reduced sulfur in soil organic matter along upland-peat soil transects. *Journal of Environmental Quality* **29**, 855-865.

Slowey, A. J., Brown, G. E., 2007. Transformations of mercury, iron, and sulfur during the reductive dissolution of iron oxyhydroxide by sulfide. *Geochimica et Cosmochimica Acta* **71**, 877-894.

Smith-Downey, N. V., Sunderland, E. M., Jacob, D. J., 2010. Anthropogenic impacts on global storage and emissions of mercury from terrestrial soils: Insights from a new global model. *Journal of Geophysical Research: Biogeosciences* **115**, 1-11.

Smith, D. S., Bell, R. A., Kramer, J. R., 2002. Metal speciation in natural waters with emphasis on reduced sulfur groups as strong metal binding sites. *Comparative Biochemistry and Physiology C-Toxicology & Pharmacology* **133**, 65-74.

Smith, H. G., Sheridan, G. J., Lane, P. N. J., Nyman, P., Haydon, S., 2011. Wildfire effects on water quality in forest catchments: A review with implications for water supply. *Journal of Hydrology* **396**, 170-192.

Solomon, D., Lehmann, J., de Zarruk, K. K., Dathe, J., Kinyangi, J., Liang, B., Machado, S., 2011. Speciation and long-and short-term molecular-level dynamics of soil organic sulfur studied by X-ray absorption near-edge structure spectroscopy. *Journal of Environmental Quality* **40**, 704-718.

Solomon, D., Lehmann, J., Martinez, C. E., 2003. Sulfur K-edge XANES spectroscopy as a tool for understanding sulfur dynamics in soil organic matter. *Soil Science Society of America Journal* **67**, 1721-1731.

Spencer, R. G. M., Butler, K. D., Aiken, G. R., 2012. Dissolved organic carbon and chromophoric dissolved organic matter properties of rivers in the USA. *Journal of Geophysical Research: Biogeosciences* **117**, 1-14.

St. Louis, V. L., Rudd, J. W., Kelly, C. A., Hall, B. D., Rolfhus, K. R., Scott, K. J., Lindberg, S. E., Dong, W., 2001. Importance of the forest canopy to fluxes of methyl mercury and total mercury to boreal ecosystems. *Environmental Science & Technology* **35**, 3089-3098.

Stoof, C. R., Moore, D., Fernandes, P. M., Stoorvogel, J. J., Fernandes, R. E., Ferreira, A. J., Ritsema, C. J., 2013. Hot fire, cool soil. *Geophysical Research Letters* **40**, 1534-1539.

Streets, D. G., Devane, M. K., Lu, Z. F., Bond, T. C., Sunderland, E. M., Jacob, D. J., 2011. All-time releases of mercury to the atmosphere from human activities. *Environmental Science & Technology* **45**, 10485-10491.

Telliard, W., Gomez-Taylor, M., 2002. *Method 1631, Revision E: Mercury in Water by Oxidation, Purge and Trap, and Cold Vapor Atomic Fluorescence Spectrometry. United States Environmental Protection Agency, Office of Water, 4303* (p. 38). EPA-821-R-02-019.

Thomas, K. A., McTeague, M. L., Ogden, L., Floyd, M. L., Schulz, K., Friesen, B., Fancher, T., Waltermire, R., Cully, A., 2009. Vegetation classification and distribution mapping report: Mesa Verde National Park. Natural Resource Report NPS/SCPN/NRR—2009/112. National Park Service, Fort Collins, Colorado.

Turetsky, M. R., Harden, J. W., Friedli, H. R., Flannigan, M., Payne, N., Crock, J., Radke, L., 2006. Wildfires threaten mercury stocks in northern soils. *Geophysical Research Letters* **33**, 1-6.

Turetsky, M. R., Kane, E. S., Harden, J. W., Ottmar, R. D., Manies, K. L., Hoy, E., Kasischke, E. S., 2011. Recent acceleration of biomass burning and carbon losses in Alaskan forests and peatlands. *Nature Geoscience* **4**, 27-31.

Urban, N. R., Ernst, K., Bernasconi, S., 1999. Addition of sulfur to organic matter during early diagenesis of lake sediments. *Geochimica et Cosmochimica Acta* **63**, 837-853

Vairavamurthy, A., 1998. Using X-ray absorption to probe sulfur oxidation states in complex molecules. *Spectrochimica Acta Part A: Molecular and Biomolecular Spectroscopy***54**, 2009-2017.

Vairavamurthy, M. A., Maletic, D., Wang, S. K., Manowitz, B., Eglinton, T., Lyons, T., 1997. Characterization of sulfur-containing functional groups in sedimentary humic substances by X-ray absorption near-edge structure spectroscopy. *Energy & Fuels* **11**, 546-553.

Van Dongen, B. E., Schouten, S., Baas, M., Geenevasen, J. A., Damsté, J. S. S., 2003. An experimental study of the low-temperature sulfurization of carbohydrates. *Organic Geochemistry* **34**, 1129-1144.

Vergnoux, A., Di Rocco, R., Domeizel, M., Guiliano, M., Doumenq, P., Theraulaz, F., 2011. Effects of forest fires on water extractable organic matter and humic substances from Mediterranean soils: UV-vis and fluorescence spectroscopy approaches. *Geoderma* **160**, 434-443.

Wang, R., Yang, C., Song, H., 2012. Key meat flavor compounds formation mechanism in a glutathione-xylose Maillard reaction. *Food Chemistry* **131**, 280-285.

Weber, F. A., Voegelin, A., Kretzschmar, R., 2009. Multi-metal contaminant dynamics in temporarily flooded soil under sulfate limitation. *Geochimica et Cosmochimica Acta* **73**, 5513-5527.

Weishar, J. L., Aiken, G. N., Bergamaschi, B. A., Fram, M. S., Fuji, R., Mopper, K., 2003. Evaluation of specific ultraviolet absorbance composition and reactivity of dissolved organic carbon. *Environmental Science & Technology* **37**, 4702-4708.

Werne, J. P., Hollander, D. J., Lyons, T. W., Damsté, J. S. S., 2004. Organic sulfur biogeochemistry: recent advances and future research directions. *Geological Society of America Special Papers **379***, 135-150.

Werne, J. P., Lyons, T. W., Hollander, D. J., Schouten, S., Hopmans, E. C., Damsté, J. S. S., 2008. Investigating pathways of diagenetic organic matter sulfurization using compound-specific sulfur isotope analysis. *Geochimica et Cosmochimica Acta* **72**, 3489-3502.

Westerling, A. L., Hidalgo, H. G., Cayan, D. R., Swetnam, T. W., 2006. Warming and earlier spring increase western US forest wildfire activity. *Science* **313**, 940-943.

Westerling, A., Brown, T., Schoennagel, T., Swetnam, T., Turner, M., Veblen, T., 2014. Briefing: Climate and wildfire in western US forests, in: Sample, V. A, Bixler, R. P. (Eds.), Forest conservation and management in the Anthropocene: Conference proceedings. Proceedings. RMRS-P-71. Fort Collins, CO: US Department of Agriculture, Forest Service. Rocky Mountain Research Station. pp. 81-102.

Wiedinmyer, C., Friedli, H. 2007. Mercury emission estimates from fires: An initial inventory for the United States. *Environmental Science & Technology* **41**, 8092-8098.

Wolfenden, S., Charnock, J. M., Hilton, J., Livens, F. R., Vaughan, D. J., 2005. Sulfide species as a sink for mercury in lake sediments. *Environmental science & technology* **39**, 6644-6648.

Woodruff, L. G., Cannon, W. F., 2010. Immediate and long-term fire effects on total mercury in forests soils of northeastern Minnesota. *Environmental Science & Technology* **44**, 5371-5376.

Xia, K., Skyllberg, U. L., Bleam, W. F., Bloom, P. R., Nater, E. A., Helmke, P. A., 1999. X-ray absorption spectroscopic evidence for the complexation of Hg (II) by reduced sulfur in soil humic substances. *Environmental Science & Technology* **33**, 257-261.

Xia, K., Weesner, F., Bleam, W. F., Bloom, P. R., Skyllberg, U. L., Helmke, P. A., 1998. XANES studies of oxidation states of sulfur in aquatic and soil humic substances. *Soil Science Society of America Journal* **62**, 1240-1246.

Yablokov, V. A., Vasina, Y. A., Zelyeav, I. A., Mitrofanova, S. V., 2009. Kinetics of thermal decomposition of sulfur-containing amino acids. *Russian Journal of General Chemistry* **79,** 1141-1145.

Yoon, S. J., Diener, L. M., Bloom, P. R., Nater, E. A., Bleam, W. F., 2005. X-ray absorption studies of CH3Hg+-binding sites in humic substances. *Geochimica et Cosmochimica Acta* **69**, 1111-1121.

Yue, X., Mickley, L. J., Logan, J. A., Kaplan, J. O., 2013. Ensemble projections of wildfire activity and carbonaceous aerosol concentrations over the western United States in the mid-21st century. *Atmospheric Environment* **77**, 767-780.

Zhang, T., Kim, B., Leyard, C., Reinsch, B. C., Lowry, G. V., Deshusses, M. A., Hsu-Kim, H., 2012. Methylation of mercury by bacteria exposed to dissolved, nanoparticulate, and microparticulate mercuric sulfides. *Environmental Science & Technology* **46**, 6950-6958.

Zopfi, J., Ferdelman, T. G., Fossing, H., 2004. Distribution and fate of sulfur intermediates—sulfite, tetrathionate, thiosulfate, and elemental sulfur—in marine sediments. *Geological Society of America Special Papers* **379**, 97-116.

)